In vitro characterization of porous knitted titanium scaffold for the replacement of intervertebral disc nucleus pulposus

Thesis submitted as requirement to fulfill the degree
„Doctor of Philosophy“ (Ph.D.)

at the
Faculty of Medicine
Eberhard Karls University
Tübingen

by

Gauri, Tendulkar

from

Pune, India

2018

Dean: Professor Dr. I. B. Autenrieth

1. Reviewer: Professor Dr. Andreas K. Nüssler

2. Reviewer: Professor Dr. Dorothea Alexander-Friedrich

To my parents

Table of contents

Thesis outline

Chapter one reviews the literature pertaining to the intervertebral disc nucleus pulposus replacements and repair strategies with emphasis on the cell material interactions and the effect of various scaffold surface properties on the cell behavior. To start with the chapter, it reviewed basic structure of intervertebral disc, strategies to disc replacements, currently available biomaterials their application, and the surface modification techniques to improve scaffold surface properties.

Chapter two investigates the biocompatibility of knitted titanium scaffold that supports cell viability and adhesion.

Chapter three gives the insights on the effect of electro-polishing treatment on wear particle generation, wear particles characterization, effect of scaffold surface modification on overall cell response with a particular focus on the effect of surface roughness and surface energy. Furthermore, it also describes the effect of surface hydrophilisation using oxygen plasma treatment on scaffold surface wettability and thus effectively on the cell behavior.

Chapter four describes the *in vitro* generation of synthetic modified Link N mRNA and their effect on mesenchymal stromal cells and human primary chondrocytes *in vitro* in 2D and together with knitted titanium scaffold in augmenting chondrocytes specific gene expression and thus reparative response together with replacement.

Chapter five studies the cellular response to knitted titanium scaffold wear debris, describes the effect of electro-polishing treatment on the hemocompatibility of the knitted titanium scaffold and further provides the insights on the biochemical surface modification of the knitted titanium scaffold

Chapter six discusses the findings from this study and provides conclusion to direct a future research

Chapter seven provides the comprehensions on the current research in the form of summary.

Chapter eight compiles the references which are marked correspondingly

CHAPTER 1

1 Introduction

1.1 Chronic low back pain

Chronic low back pain is the most common condition among people aged 40-80 years, affecting men and women alike globally (Hoy *et al.*, 2012). It is one of the leading causes of disability that is associated with high socio- economic costs due to increased morbidity of afflicted individuals and hence correspondingly decreased productivity (Murray *et al.*, 2012; Waldrop *et al.*, 2015). Worldwide prevalence is approximately 84% in their lifetime, out of which 50% occurs at young (18–44 years) or middle (45–64 years) age (Murray *et al.*, 2014). In Germany, the annual costs of low back pain (LBP) were estimated over € 50 billion, as reported by Werber and Schiltenwolf (Werber and Schiltenwolf, 2016). Low back pain can fluctuates over the period of time with frequent recurrences and exacerbations, and moreover 10% of the patients develop chronic persistent or recurrent pain, thereby generating approximately 80% of health care costs. During initial period of low back pain, 26–37 % relapses of work absence and 44–78% pain relapse has been described (Suri *et al.*, 2016; Werber and Schiltenwolf, 2016).

Chronic low back pain has been described to be strongly associated with intervertebral disc degeneration, although the exact etiology still remains unclear (Luoma *et al.*, 2000; de Schepper *et al.*, 2010; De Palma *et al.*, 2011). Degenerative disc disease (DDD) is a condition known to result in chronic back pain due to the biomechanical instability caused by loss of disc height, disc dehydration and / or annular tears (Urban and Roberts, 2003; Adams and Dolan, 2012).

1.2 Intervertebral disc- structure and morphology

Human vertebral column is responsible for supporting the body balance thereby protecting nerve roots and the spinal cord. The spine is not just straight but has 4 curvatures; two kyphotic that concave posteriorly and two lordotic that convex anteriorly. This unique structure enables body flexibility and motion to perform all body functions simultaneously (Putz and Müller-Gerbl, 1996). The human spine comprised of 24 vertebrae (seven cervical, twelve thoracic and five lumbar vertebrae) which are connected to one another by fibrocartilage intervertebral discs which is normally surrounded by muscles and ligaments.

Therefore, the spinal column along with vertebral bodies and intervertebral discs helps to absorb the load applied to the spine which normally include different kind of movements *i.e.;* flexion, extension, lateral flexion, rotation and circumduction (Cramer Gregory *et al.*, 2014). So, the intervertebral discs are complex main joints of the vertebral column (Raj, 2008). Since the shape of spinal column is not the same throughout, varied vertebral bodies shape determines the different shape of intervertebral disc. Adult intervertebral disc is a largest avascular fibrocartilaginous structure situated between the two vertebral bodies, despite having rich vascular supply during fetal development and shortly after birth (Cramer Gregory *et al.*, 2014). Intervertebral disc mainly function as flexible pivots, by providing the flexibility and stability to the spinal column thereby absorbing and transmitting the mechanical load (Raj, 2008; Colombier *et al.*, 2014). It is a joint that mainly provides flexibility and elasticity with a wide range of movement to the spine as a whole and while doing so, it does allow limited mobility between adjacent vertebrae. The intervertebral discs strongly provides pressure and tension resistance while transmitting mechanical load through the spinal column (Pattappa *et al.*, 2012). Intervertebral disc (**figure 1**) comprised of gelatinous centre called Nucleus pulposus (NP), which is peripherally enclosed by annulus fibrous (AF) and cartilaginous endplate (CEP) that limits majorly the most peripheral rim of the disc superiorly and inferiorly (Walter *et al.*, 2015).

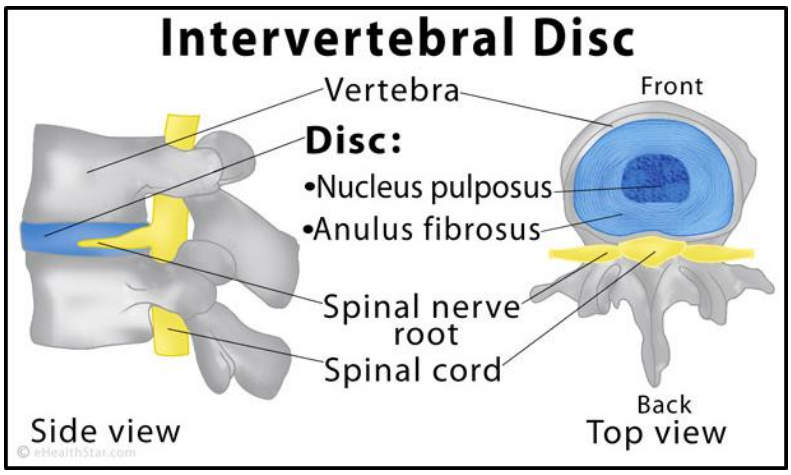

Figure 1: Anatomy of the intervertebral disc (source: wikipedia)

The primary components of discs are water, cells–mainly chondrocyte like cells and fibroblasts, proteoglycan, collagen and other matrix components (Singh *et al.*, 2009). Fibrillar collagens, aggrecan and water are the three main structural components of the intervertebral disc (IVD) which together contributes around 90-95% of volume of the healthy IVD (Urban

and Roberts, 2003), although the ratio varies across the disc. For example, collagen is found highest in outer AF and lowest in the NP, whereas reverse is true for water and aggrecan content. Specific matrix structure maintained by distinct cell population makes these tissues differ in function (Pattappa *et al.*, 2012). Although cell density in the human disc is low at around 6×10^6cells/cm^3, extracellular matrix (ECM) produced by them is essential to regulate mechanical response. Endplates are the outer region of IVD where AF and NP are embedded in. During development, blood vessels penetrate into the endplates and provide nutrition to the developing IVD and until skeletal maturity IVD becomes completely avascular. Nutrients and metabolites are therefore reaching to the IVD mainly by diffusion (Moore, 2000).

1.2.1 Nucleus pulposus

The emergence of the nucleus pulposus begins through mesodermal somites during the embryonic development and in later stages notochord goes through a transition to form nucleus pulposus progenitor cells ($Tie2^+$ and $GD2^+$ positive). NP is originated from the notochord and between the vertebrae this notochord enlarges to form NP (Hsieh and Twomey, 2010). During developing vertebrae notochord is replaced by bone whereas in NP, notochordal cells get replaced by chondrocytes like cells. Presently it is still unclear whether this replacement of cell population is because of apoptosis of resident cells causing consequential invasion by mesenchymal cells or dedifferentiation of notochordal cells (Hunter *et al.*, 2004). However at maturity, the NP cells are 10 µm small, round chondrocyte like cells, present in a density of about 4×10^6cells/cm^3(Roughley, 2004). Nucleus pulposus is mainly comprised 80% of water (wet weight) and 20% collagen (dry weight) where, collagen II and proteoglycans mainly predominates in NP with small amount of types VI, IX and XI collagen (**figure 2**). Hydrophilic nature NP is responsible for high water content, due to 70-90% of water content and high proportion of proteoglycans (ca. 50% of dry weight) (Kepler *et al.*, 2013). Presence of hydrophilic proteins called proteoglycans enriches nucleus pulposus with high water content, which is almost 90 % at birth and then decreases over the age up to 70% (Buckwalter, 1995).

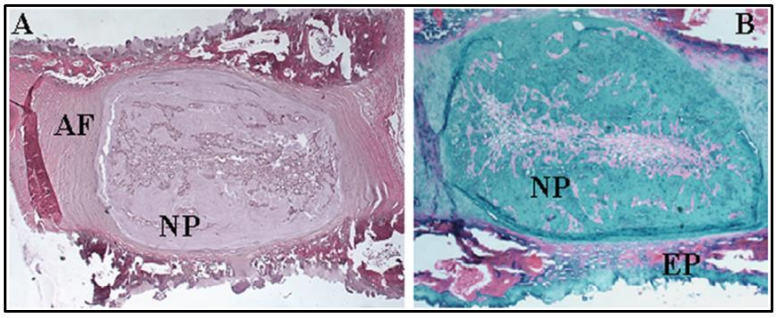

Figure 2: Rat intervertebral disc, sagittal section. (A) Hematoxylin and eosin stain, original magnification 4x: the nucleus pulposus (NP) contains chondrocyte-like cells immersed in an abundant matrix, surrounded by the anulus fibrosus (AF), (B) Alcian blue stain, original magnification 10x: the matrix in NP is mostly proteoglycans (blue stain) and type II collagen, and is directly in contact with the vertebral endplate (EP). (Courtesy of Makarand V. Risbud, PhD) (Di Martino *et al.*, 2005).

Out of 15% of proteoglycan (wet weight); aggrecan in major and decorin, biglycan and lumican in small amount, and glycoproteins like elastin, fibronectin, laminin, lubricin, link protein and chondromodulin-I organized to form matrix microenvironment. Aggrecan and biglycan are highly present proteoglycans within NP (Pattappa *et al.*, 2012) and together with cells are embedded in collagen fibers (especially collagen type II) mesh, which is randomly oriented and makes up to 20% of the dry weight (Buckwalter, 1995). Ratio of collagens:GAG differs NP from hyaline cartilage endplate which is 1:5 and 5:2 respectively (Mwale *et al.*, 2004). Proteoglycans are the most abundant macromolecules which are loosely bound together with type II collagen fibers; making NP a highly hydrated and forms gel like structure (Roberts *et al.*, 2006) and therefore allows NP to be elastic and deform under stress (Colombier *et al.*, 2014). Additionally, proteoglycans; a multiple chains of glycosaminoglycan together with hyaluronic acid forms non-covalently linked complexes that helps in water absorption and therefore enables NP to withstand compressive forces (Roughley, 2004). Hydrated healthy NP thus generates intradiscal pressure which separates two vertebral bodies, tensions the AF and distributes the pressure evenly over the two adjacent endplates. Generated hydrostatic pressure further enables NP to resist compression under load. During loading and different movement of spine, NP can later its shape and position and thus can act as nature of loading dependent (Iatridis *et al.*, 1996). NP primarily absorbs the loads and equalize the compressive stress on the vertebral cartilaginous endplates (Iatridis *et al.*, 1996; Colombier *et al.*, 2014).

1.2.2 Annulus fibrosus

AF derives from the mesenchymal tissue enclosed the notochord. It is a fibrocartilage whose ECM is comparable to knee meniscus (Nerurkar *et al.*, 2010). AF is primarily composed of fibroblasts which mainly synthesize collagen I and therefore, proportion of collagen I predominates in the AF. It is a tough fibrocartilaginous outer layer of the intervertebral disc which primarily consists of collagen type I interconnected via elastic fibers which are normally oriented in alternating direction forming successive layers, provides mainly tensile force resistance (Colombier *et al.*, 2014). Structural and cellular differences within AF mainly distinguish into inner and outer part of AF, where outer AF is highly organized with fibroblasts like cells with elongated nuclei which are aligned with collagen fibers and relatively low proteoglycan and water content (Colombier *et al.*, 2014). Moving towards the inner AF region, cell are more rounded and chondrocyte like with poorly organized ECM which mainly composed of collagen II, I, proteoglycan and high water content (Risbud and Shapiro, 2011). However, other types of collagen for example: type V, VI and IX are also present along with a minor amount of type III as it gradually differentiates from the periphery of the nucleus to form outer layer. Outer AF region is highly tension resistant than inner AF and overall AF serves as a boundary for the NP (Freemont, 2009a; Colombier *et al.*, 2014). Cell density in the AF is almost double than that of NP, which is roughly about 9×10^6cells/cm^3 (Roughley, 2004). Though AF entirely derived from mesenchyme, cells from different regions within AF, has a different morphology and so ECM component they produce as well varies. Bundle of collagen and GAG (ratio is 3:1) elements enables AF to tension and compression resistant and therefore, it is known to be viscoelastic (rate-dependent) and anisotropic (direction-dependent). Mechanical properties of AF are dependent on highly organized lamellar structure and therefore, based on the axial, circumferential and radial directions, order of magnitude of tensile, compressive, and shear stress may differ on AF (Nerurkar *et al.*, 2010). Collagen percentage in the outer and inner AF makes up to 40-60% and 25-40% of the dry weight respectively (Smith and Fazzalari, 2009). Although collagen I and II are the most prevalent, their relative proportion gradually changes as move towards the inner AF from outer. Therefore, type I collagen is most abundant in outermost region whereas collagen II close to NP. Depending on the circumferential location, spinal level and age, number of distinct lamellae (bundle of collagens) varies between 15-25 from one vertebral to other and as well amongst individual (Kepler *et al.*, 2013). Alternative orientation of lamellae with respect to spinal axis thus forms angle ply structure in which inter-lamellar septa mainly contains proteoglycans. Proteoglycan makes up 58% of the outer AF and 11-20% of the inner

AF (Smith and Fazzalari, 2009), which is primarily responsible for tissue hydration. Through their water binding capacity, it enables to distribute force around the circumference of AF (Pattappa *et al.*, 2012). Aggrecan and versican are major abundant proteoglycan present in AF, however small traces of biglycan, decorin, fibromodulin and lumican are well present (Singh *et al.*, 2009).

Cartilaginous endplate (CEP) is a thin hyaline and fibrocartilage layer. Hyaline cartilage is located opposite the vertebral body whereas fibrocartilage is fond adjacent to the IVD (Cramer Gregory *et al.*, 2014). It is mainly composed of chondrocytes and ECM rich in collagen II and proteoglycan (ratio is 1:2) (Colombier *et al.*, 2014). Healthy cartilaginous endplate is a 1 mm thick homogenous layer of hyaline cartilage which distributes pressure of the NP and tension of the AF to the subchondral bone uniformly (Rutges *et al.*, 2013). Moreover, it prevents the NP from bulging into the adjacent vertebral body during mechanical load of the spine. In addition, CEPs are very important for disc nutrition, since vascular buds present in the endplate and multiple perforations are very much essential source of nutrition and water exchange into the IVD during growth and development (Urban *et al.*, 2004).

1.3 Intervertebral disc degeneration

Substantial changes in composition and progressive loss of structural integrity is the hallmark of the intervertebral disc degeneration (Walter *et al.*, 2015), which occurs mostly in adults at the age over 30 in one or more discs or during trauma. With aging or in case of trauma, water retention capacity of proteoglycans starts diminishing with loss of proteoglycan content, which consequently leads to inability of nucleus pulposus to resist compression pressure. Subsequently, AF lamellae loses their physiological orientation / arrangement leading to further compromise in the structural integrity as well as mechanics of the discs (Walker and Anderson, 2004). As the degeneration process is age dependent, their pathologic changes characterized right from second decade in life (Walker and Anderson, 2004; Eskola *et al.*, 2012). Pathologic intervertebral disc degeneration (**figure 3**) is associated with pain due to AF fissure, AF collapsing, structural changes in vertebral bodies and nerve ingrowth (de Schepper *et al.*, 2010; Adams and Dolan, 2012). Although a biochemical change within intervertebral discs has no direct association with pain, it is difficult to distinguish the changes are either due to aging or due to pathology (Brinjikji *et al.*, 2015). Several etiological factors such as aging, smoking, infection, genetic predisposition, abnormal biomechanical loading, and nutrition insufficiency are thought to be involved in the pathogenesis (Urban and Roberts, 2003;

Roberts *et al.*, 2006). Moreover, genetic heritability estimates up to 74% (MacGregor *et al.*, 2004).

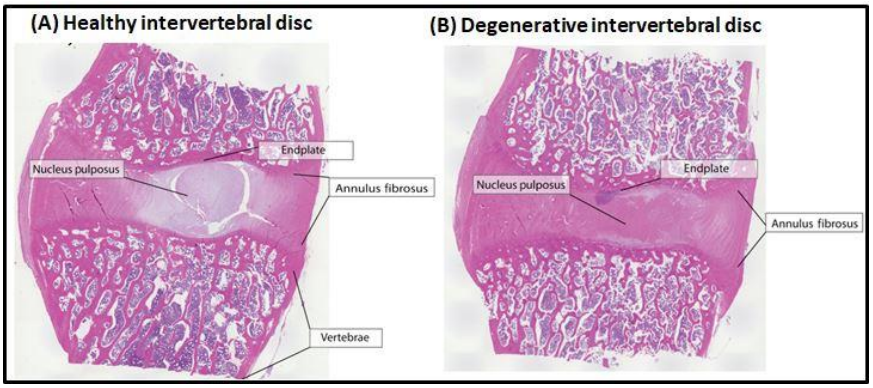

Figure 3. Histology of intervertebral disc. (A) Normal histological depiction of healthy intervertebral disc between the two vertebrae, where annulus fibrosis, nucleus pulposus and endplate is clearly distinguishable, (B) histology of degenerative intervertebral disc where annulus fibrosis has bulge beyond the endplate edge and nucleus pulposus is mildly replaced by fibrocartilaginous tissue (Sakai and Schol, 2017).

Downregulation of the endplates diffusion efficiency due to loss of blood vessels with aging mainly limits the nutrient supply (Buckwalter, 1995; Urban *et al.*, 2004; Walker and Anderson, 2004). It therefore produces low oxygen tension, procuring acidic environment and accumulating lactic acid, which all together affects ability of disc cells to synthesize and maintain their ECM (Kepler *et al.*, 2013). Disc cells on the other hand undergo phenotypic changes including morphology, metabolism (Ahsan *et al.*, 2001; Jiang *et al.*, 2014) and insufficient amount of active and viable cells therefore makes it unable to maintain ECM which in turn accelerates the loss of proteoglycan and collagen synthesis.

Progressive structural failure is a salient feature of the intervertebral disc degeneration, which is a consequence of mechanical trauma, injuries, smoking, obesity, and / or aging. It is a cell mediated response where extracellular matrices mainly gets deteriorates (Setton and Chen, 2006). Inadequate nutrient supply, reduced cell viability, cell senescence, and programmed cell death contributes to this deterioration (Urban *et al.*, 2004; Shiri *et al.*, 2010; Ding *et al.*, 2013), which is mainly characterized by elevated levels of inflammatory cytokines, increased proteoglycan (aggrecan) and collagen type II degradation in the NP, and alterations in IVD cell phenotypes. Loss of aggrecan in the NP mainly triggers a complex of growth factors, cytokines and catabolic enzymes which consequently penetrates into the disc, causing the vascular and neural ingrowth. Matrix degradation during intervertebral disc degeneration, alters their turnover through a multiple biochemical processes (Bachmeier *et al.*, 2009).

Previous studies have shown that degenerated disc contains high levels of matrix metalloproteinases (MMPs), which are catabolic enzymes that encourage matrix degradation. Healthy disc otherwise inhibit the activity of MMP by using tissue inhibitors of MMPs (TIMPs) where, TIMP-1 specifically increases the proteoglycans and matrix production. Activation of serine proteinases and MMPs, cytokines (specifically IL-1 & IL-6), nitric oxide (NO), and prostaglandin E2 (PGE2) specifically degrades proteoglycans and other ECM proteins (Kang *et al.*, 1995; Ishihara and Urban, 1999). Activation of MMP1, MMP-2, MMP-3, MMP-8, MMP-9, and aggrecanases (a disintegrin and a metalloprotease with thrombospondin motifs (ADAMTS)-1, ADAMTS-4, ADAMTS-5, ADAMTS-9, and ADAMTS-15) promotes the degradation of collagens and hyaluronic acid binding region which slower proteoglycans synthesis within the extracellular matrices of intervertebral disc (Bachmeier *et al.*, 2009; Freemont, 2009b; Shamji *et al.*, 2010). In addition, direct implication of MMP-1 (collagenase), MMP-2 (gelatinase), and MMP-3 (stromelysin) in aggrecan, collagen types I and II, and collagen types IV and V, respectively has also been identified (Cassinelli and Kang, 2000). IL-1 upregulates the MMPs release thereby decreasing the proteoglycan production (Kang *et al.*, 1997). Change in different collagen types and as well in their ratio ultimately alters the collagen crosslinking and therefore the ability of disc to support mechanical loads deteriorates (MacGregor *et al.*, 2004). Increase of disorganized collagen type I with corresponding loss of type II collagen and proteoglycan leads to fibrous structure of the disc and thus the disc becomes less elastic, preventing its ability to absorb and dissipate spinal forces (Roughley, 2004; Kepler *et al.*, 2013). There is as well a theory which suggests that cell death due to low pH primarily affects the proteoglycan content (Ohnishi *et al.*, 2018). With aging and / or during degeneration chemical composition of the nucleus pulposus changes, causing the change in the proteoglycan concentration while increase in keratin sulfate / chondroitin ratio. Loss of proteoglycans and decrease in the ratio of proteoglycan:collagen (Urban and Roberts, 2003) consequently loses hydrostatic properties inducing structural wear of the intervertebral disc (Noble, 2002) and thus progresses towards the fibrotic nature. Stress distribution over the nucleus pulposus therefore tends to reduce at the centre and the more pressure around the periphery, essentially unable the nucleus pulposus to perform its function of load transfer. As nucleus pulposus dehydrates, it shrinks its size causing the additional load on annulus fibrosis (McNally and Adams, 1992). Disintegration of collagen lamellae with increased inter-bundle spaces and increase in the thickness of remaining lamellae fails to maintain AF lamellar organization and therefore affects the stability of the disc (Nerurkar *et al.*, 2010). Subsequently, annulus fibrosis is subjected to

abnormal compressive stress and therefore is more prone to injuries and hence radial tears, cracks and fissure arise within the annulus fibrosis (Osti *et al.*, 1992). Due to lack of intra-discal pressure; the load absorption and transmission in such dehydrated discs is significantly altered (**figure 4**) and subsequently it results in disc height reduction, osteophyte formation, facet joint arthritis, and deformation of vertebral bodies (Freemont, 2009a). Dehydration of nucleus pulposus and gradual disappearance of nucleus pulposus and annulus fibrosis border defines the loss of normal architecture. With continued degeneration, the structural deficit is accompanied by leakage of central nucleus pulposus material which migrates through the crack developed in annulus fibrosis towards the periphery that results in immune cell activation thereby evoking pain (Bao *et al.*, 1996; Vaday and Lider, 2000).

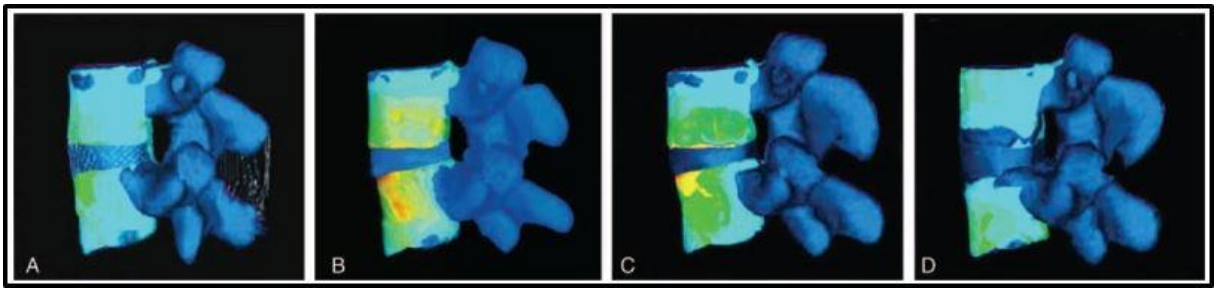

Figure 4: The stress distribution of the vertebral body under the axial load of 500 N in the 4 models. (A) Normal IVD; (B) degenerative IVD; (C) IVD with NP removal; (D) IVD with NP replacement; the colour form blue to red represented stress rise. IVD=intervertebral disc, NP=nucleus pulposus (Wang and Yi, 2017).

Intervertebral disc degeneration and its progression is dependent on the genetic and environmental factors such as nutrition, smoking (Nerurkar *et al.*, 2010). Moreover, the correlation between the state of degeneration and the age factor makes it difficult to distinguish the impact between the aging from that of degeneration on the biomechanical behavior of the intervertebral disc. IVD degeneration results in low back pain but is not always the case. Location of affected disc, nerve damage, pressure on the spinal column all together defines the degree of degeneration. For example, some patients may not feel pain while others, with exact equal amount of damage may come across chronic back pain. Degree of degeneration does not correlate with the degree of pain. Nonetheless, intervertebral disc degeneration is most common cause of the lower back pain (Lim *et al.*, 2017).

1.4 Conventional treatments

1.4.1 Conservative treatments

Current treatments are mostly symptomatic that have not shown repair strategy of IVD so far (Masuda and Lotz, 2010; Huang *et al.*, 2018). Bed rest is the most common conservative treatment that has been recommended as it helps in the reduction of the intra-discal pressure. Since the exact pathogenesis of intervertebral disc degeneration is poorly understood, many trials / therapies are nonspecific for low back pain and do not treat the root cause of the low back pain. Nevertheless, physiotherapy, muscle relaxant, spinal manipulation and anti-inflammatory drugs (*e.g.*: Cyclooxygenase-2 selective inhibitors) (van Tulder *et al.*, 2006), have been shown effective for short term pain relief, maintaining ordinary activity in patients with acute low back pain (Assendelft *et al.*, 2004; Arnau *et al.*, 2006; Koes *et al.*, 2010). In chronic low back pain, various interventions like physiotherapy, antidepressants, weak opioids, cognitive behavioral therapy sedatives, ultrasound, and electrotherapy have been shown to relief short term pain (Haldorsen *et al.*, 1998; Schnitzer, 2006). Some patients with suspected disc herniation and radicular pain or progressive neurologic deficits get benefit from epidural corticosteroid injections. However the effects of these treatments are temporary, and hence the patients are referred for surgery if these treatments fails.

1.4.2 Surgical treatments

Prior to surgery, intervertebral disc degeneration can be assessed with conventional radiography, computed tomography (MacGregor *et al.*, 2004), discography, and magnetic resonance imaging (MRI). Microdiscectomy is routinely used procedure to excised herniated disc fragment which otherwise impinging on the nerve roots, causing the pain. Moreover, this is recommended if the annulus fibrosis damage is not severe and results to eliminate the back pain in 90-95% of the cases (Le *et al.*, 2003).

1.4.2.1 Spinal fusion

Spinal fusion was the gold standard for many decades, which is normally recommended if the annulus fibrosis is severely damaged. It is a highly invasive treatment, foremost aiming for pain relief for the patient. It involves the fixation across the two adjacent vertebrae (**figure 5**) by inducing the bone growth. It thereby stabilizes the damaged intervertebral disc joint by eliminating the motion between the vertebral bodies. Several studies have shown wise range of success rate, ranging from 30-95% (Bao *et al.*, 1996). Fusion certainly alters the biomechanics of the entire spinal column thereby increasing the stress on the adjacent vertebrae (Javedan and Dickman, 1999). Lack of motion often leads to secondary complications like degeneration of adjacent discs and this in turn creates more instability and

pain (Adams and Dolan, 2012; Bridwell *et al.*, 2013). Elevated degree of degeneration in adjacent discs due to this internal rigid fixation consequently suspected of causing osteoporosis, stress shielding which results in decrease bone density, muscle atrophy, pseudoarthosis, and spinal stenosis (Lee *et al.*, 1991; Javedan and Dickman, 1999). Although the number of spinal fusions performed each year is continually increasing (de Kleuver *et al.*, 2003), the clinical success rate of lumbar fusion is variable ranging from 16-95%, as long-term results are poor due to increased risk of complications.

Figure 5: Post-operative radiograph (lateral view) with posterior spinal fusion performed (Wong *et al.*, 2010).

Ultimately patients require revision of surgery (van den Eerenbeemt *et al.*, 2010). Although procedure aimed to alleviate the back pain, it fails to repair the intervertebral disc or to restore the biomechanics and thus has become a controversial issue (Zhang *et al.*, 2016).

1.4.2.2 Arthroplasty

In an effort to overcome the demerits of spinal fusion and so to restore the physiological motion, arthroplasty have been developed where total disc replacement and nucleus pulposus replacements were studied extensively (Schizas *et al.*, 2010; Lewis, 2012b). The scaffold or biomaterial aiming for intervertebral disc arthroplasty should be biocompatible that should not cause local tissue reaction or toxicity (Lee *et al.*, 1991). In addition, wear resistance is a key consideration, because the foreign body response generated due to wear particles may result in secondary complications like hypersensitivity (Cunningham, 2004; Schizas *et al.*, 2010). Ideally, mechanical properties including stiffness, viscoelastic properties, fatigue properties of the material should withstand the cyclic compression to which intervertebral disc is otherwise subjected (Lee *et al.*, 1991).

1.4.2.2.1 Total disc replacement

Theoretically, total disc replacement aims removal of damaged or degenerating intervertebral disc thereby replacing it with the mobile and potentially shock absorbing artificial biomaterial. Principle advantage of this technique is that, success of the surgery is independent of the annulus fibrosis integrity or the state of degeneration. Ideally it should preserve not only the spinal motion but also disc height thereby alleviating pain. Additionally, it should also avoid morbidity, stiffening associated with spinal fusion. Moreover, implant should have adequate fixation to the vertebral end plate and vertebrae, in order to simulate the natural structure and function of the intervertebral disc. In order to provide the structural support, biomaterial would be attractive approach that would provide immediate closure for the defects and thus aiming to restore the biomechanical properties of the intervertebral disc, while the cellular components would repopulate the defect site and enable new extracellular matrix synthesis (Guterl *et al.*, 2013). Restoration of biomechanical cues of the native tissue and tissue integration, enabling ECM organization are the prerequisites of the biomaterial (Nerurkar *et al.*, 2010). It was also suggested that material should be wear and corrosion resistance and in addition, it should withstand the fatigue loading up to cyclic 100 million cycles that equivalents to 40 yr. life span (Bao *et al.*, 1996; Cunningham, 2004).

Large efforts have been made over the last couple of years to develop artificial intervertebral disc. Broadly, artificial disc consists of a body embedded within two endplates. Few designs were tested clinically out of which, Fernstrom made the first attempt (Fernstrom, 1966). **Fernstrom ball** is one of the earliest prosthetic discs made of stainless steel (McKenzie, 1995). The advantage of considering complete metal was the fatigue strength and compressive load. Prosthetic resulted excellent in 79% of the cases during clinical investigation. In spite of these results, resettling of balls in to the vertebral bodies plus migration of disc into spinal and moreover, stiffness mismatch was one of the reasons to abandon the scaffold design. **Spring System** is yet another type of metal based prosthetic where, disc either made of Ti-6Al-4V (Ti alloy with 6 wt % Al and 4 wt % V) springs placed between either hot isotactically pressed or CoCrMo endplates with CoCr beads sintered to the endplates (Kostuik, 1997). Design was aimed to withstand 100 million cycles, equivalent to 40 years of use. Later studies showed that Ti-6Al-4V wear particles between 1 μm to 30 μm and CoCrMo wear particles between 5 μm and 30 μm does generate from both the spring / endplate interface and hinge / pin interfaces (Schmiedberg *et al.*, 1994). Bone resorption and no tissue ingrowth were seen in to the springs, was one of the major drawbacks. The SB **Charité disc** is commercially available in Europe (Büttner-Janz *et al.*, 1989), mainly made of an ultra-high molecular weight

polyethylene (UHMWPE) positioned between two CoCrMo endplates. Since 1984, over 7000 prostheses have been implanted in patients worldwide. As reported by Cinotti, further modification to the original design achieved good results at a 2 yr. follow up in 69% of the patients (Cinotti *et al.*, 1996). Early clinical tests showed high occurrence of problems like plate dislodgement and fracture, improper fixation at implant and endplate interface. Similarly, clinical outcomes of **Prodisc** (Delamarter *et al.*, 2003) and other metallic implants made of Ti-6Al-4V (Ti alloy with 6 wt % Al and 4 wt % V), CoCrMo, CoCr were equivalent to those with spinal fusion (Zigler and Delamarter, 2012). Total disc replacement implants are therefore resulted in susceptible to wear interfacial bonding, causing aseptic loosening (Schmiedberg *et al.*, 1994; Kostuik, 1997; Cunningham, 2004). In addition, due to lack of wear resistance and unable to withstand fatigue, implants showed inadequate fixation to the vertebral endplate and vertebrae leading to the failure. The apophyseal joints of the vertebrae are often gets degenerated when intervertebral disc is replaced. In order to maintain motion segment and two adjacent vertebrae, function of the facet joints needs to be integrated in the intervertebral disc prosthetic. Since long term results with all these prosthetics don't seems optimal, there is a need to develop an alternative strategy for intervertebral disc (Cunningham, 2004; Huang *et al.*, 2018).

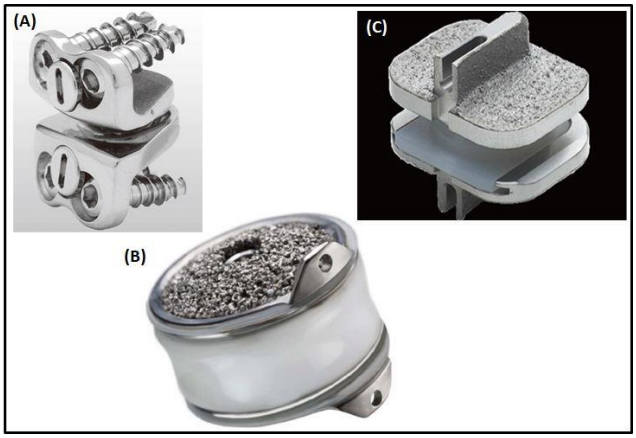

Figure 6: Total disc replacement scaffolds. (A) Prestige artificial cervical disc, (B) Bryan artificial cervical disc, (C) ProDisc-C artificial cervical disc (Park *et al.*, 2018).

1.4.2.2.2 Nucleus pulposus replacement

Nucleus pulposus replacement is only possible if the annulus fibrosis is intact and therefore this technique aims to facilitate the preservation of the natural disc structure along with their function. It is also known as a minimal invasive technique, in contrast with current surgical

procedures like the total disc replacement or spinal fusion (Di Martino *et al.*, 2005; Goins *et al.*, 2005). The potential benefit of only replacing the dehydrating nucleus while preserving annulus fibrosis and endplates could be a less invasive posterior surgery. While maintaining the natural tension of the healthy annulus fibrosis during this procedure, prosthetics are not intended to be fixed into the vertebral bodies and therefore endplate fixation problem is also avoided (Di Martino *et al.*, 2005; Goins *et al.*, 2005). Nucleus replacement might not be suitable for the later stages of disc degeneration. Nonetheless, Scaffold meant for nucleus pulposus replacement as well need to maintain certain requirements such as biocompatibility, fatigue strength, cyclic compression, wear and corrosion resistant (Bertagnoli *et al.*, 2005; Joshi *et al.*, 2005).

First human implanted nucleus scaffold was developed by **Fernstrom** in 1966, which was made of stainless steel ball; aimed to allow the movement between the two vertebrae (Fernstrom, 1966). However it did not maintain the biomechanics of the disc which led further to implant migration problem. It was then realized that the metal blocks as a scaffold are too stiff to replace the nucleus pulposus replacement. Later, evolution of using polymer either into injectable form or preformed state (Liu *et al.*, 2017) allowed curing the nuclear cavity with better stability.

1.4.2.2.2.1 Hydrogels

It is the most relatable class of material mainly made of polymer. Their swelling property and the ability to hold the water uptake, make them similar to those of natural soft tissues. **Newcleus** is one of the examples of nucleus replacement device (**figure 7**), composed of polycarbonate urethane (PCU) (Di Martino *et al.*, 2005). The material has a 35% water absorption property and this elastic spiral design allows for easy uncoiling and coiling facilitating a minimally invasive implantation. Fatigue test of 50 million cycles showed no change in terms of implant stability (Goins *et al.*, 2005). It is no longer under clinical evaluation due to adverse preclinical events such as incidents of migration or extrusion (Coric and Mummaneni, 2008).

1.4.2.2.2.2 Polyacrylonitrile based hydrogels

Ray and Corbin in 1980s, designed a cylindrical implants consisted of fiber-woven shells of biodegradable poly (glycolic acid) (PGA) that were filled with a thixotropic hydrogel such as hyaluronic acid once inserted after removal of the nucleus (Ray, 1988; Ray, 1990; Ray *et al.*, 1991). With the intention of tissue ingrowth, implants shell intends to degradation upon swelling. Therefore, implants were further investigated for the controlled release of

therapeutic anti-inflammatory drugs (Ray, 1990). Difficulties with fluid sealing within capsules led this design to sit back (Bao *et al.*, 1996). Later improvement to the early design, Ray *et al* proposed yet another design that involved side by side positioning in the medial-lateral position and implant made of polyacrylonitrile (PAN) copolymer hydrogel enclosed in polyethylene fiber (Ray *et al.*, 1997; Ray *et al.*, 1998; Ray, 2002). PAN was further renamed as the **PDN (ProstheticDisc Nucleus)**. Fatigue testing with 50 million cycles showed no change in hydrogel properties (Ray, 2002; Di Martino *et al.*, 2005; Goins *et al.*, 2005) and viscoelastic behavior as well tested using cadaver disc which revealed the progressive disc height reduction (Bain *et al.*, 2000). Moreover, its *in vivo* compatibility (using baboon lumbar spine model) showed endplate degeneration and dysfunctioning of adjacent vertebrae, scaffold migration as a potential problems (Di Martino *et al.*, 2005). Also, leaching of acrylonitrile and acrylamide monomers from the hydrogel was one of the major drawbacks of using this material.

Di Martino *et al.* reported that, 10% of PDNs implanted patient suffered with endplate failure or extrusion (Di Martino *et al.*, 2005). Similar results were seen in another clinical study demonstrated by Bao *et al.* (Bao *et al.*, 1996) and it was then assumed that improper positioning of the implant do not ensure compressive stresses on the disc would translate in to tensile stresses in the annulus, leading change in the biomechanical behavior, unlike healthy intervertebral disc. **PDN-SOLO** (Shim *et al.*, 2003), an upgraded version of the PDN implant (**figure 7**) later showed an improvement in clinical follow up study, showing no evidence of failure or dislocation in any of the patients (Jin *et al.*, 2003).

Replication Medical, Inc. developed another implant called **Neudisc**, composed of hydrolyzed polyacrylonitrile (Aquacryl) and polyester mesh (**figure 7**). Design is aimed to implant in dehydrating state and to be hydrated to 80% once in position. Biocompatibility tests in New Zealand rabbits (Di Martino *et al.*, 2005) and in addition, another study by Bertagnoli *et al.* demonstrating fatigue tests of 10 million cycles (Bertagnoli *et al.*, 2005), reported Neudisc as a promising strategy. Layers of polyester mesh designed to act as resistance against radial deformation or bulging (Bertagnoli *et al.*, 2005)

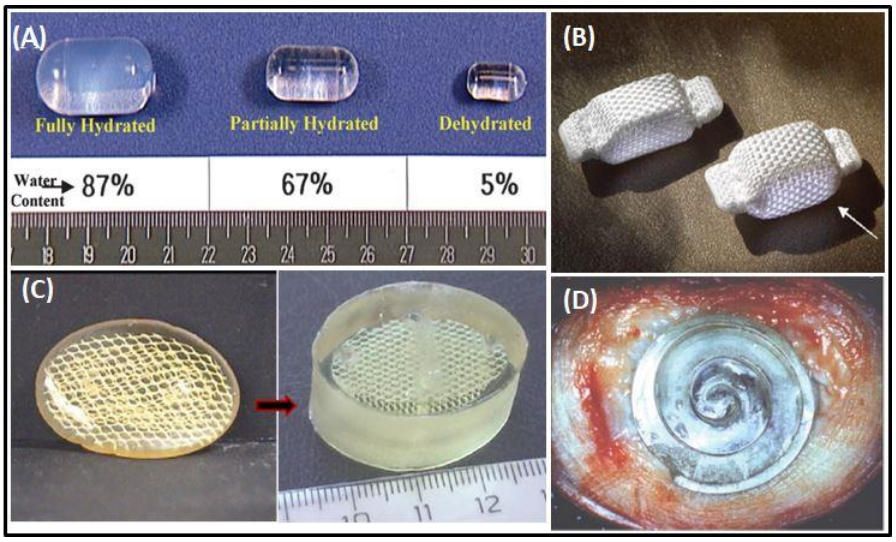

Figure 7: Nucleus replacement devices (A) The **Aquerelle** Poly (vinyl alcohol) hydrogel has a swelling pressure similar to the nucleus pulposus *in vivo*. Once implanted, its final volume depends on the water content at equilibrium. (Reprinted with permission from Stryker Spine, Allendale, NJ), (B) **PDN-SOLO** device in dehydrated and hydrated states. The PDN-SOLO device is designed to swell both in height and in width within the disc space. The porous polyethylene weave allows fluid to pass into the hydrophilic core, which causes the device to expand vertically and horizontally (Milner *et al.*). This process maximizes the device's footprint on the vertebral endplates. (Reprinted with permission from Raymedica Inc., Minneapolis, MN), (C) The **Neudisc** hydrogel, pre-hydration (left) and post hydration (right) Hydration occurs in an anisotropic fashion, mainly in the vertical plane. (Reprinted with permission from Replication Medical, Inc., New Brunswick, NJ), (D) The **Newcleus** Spiral Implant; once implanted, the device reconstitutes its original spiral shape. It localizes in place of the nucleus pulposus of which reconstitutes the volume, sparing the anular fibers. (Reprinted with permission from Zimmer Spine, Warsaw, IN) (Di Martino *et al.*, 2005).

1.4.2.2.2.3 PVA-based hydrogels

Poly (vinyl alcohol) (**PVA**) made nucleus pulposus replacement device developed by Bao and Higham aimed to mimic physiological properties of the disc (Bao and Higham, 1993; Bao and Higham, 1996; Bao *et al.*, 1996; Bao *et al.*, 1998; Bao and Yuan, 2000; Bao and Higham, 2001). Design is similar to Rays design with ease of insertion and reduced size of hole needed in the annulus (Bao and Higham, 1991). No adverse local or systemic tissue reaction was reported when PVA model tested in a baboon model (Bao and Yuan, 2000). Bao and Yuan further proposed a concept of aperture sealing, to correct the annulus fibrosis defects arose due to nucleus hydrogel implants (Bao and Yuan, 2001). Stammen *et al.* (Stammen *et al.*, 2001) introduced PVA hydrogel physically cross linked with freeze-thaw cycling and they found increase in tangent compressive modulus between 1-18 MPa from 10-60% strain. Partially hydrated PVA with 80% water (**Aquarelle**) is yet another nucleus implant (**figure 7**), which has been tested for fatigue up to 40 million cycles (Di Martino *et al.*, 2005). No systemic or local toxicity was observed up to 24 months post implantation in baboon model

(Allen *et al.*, 2004), although there was 20% extrusion rate. Nucleus replacement using Aquarelle into humans has been performed within Europe (Cunningham, 2004). Semi-crystaline, hydrophilic PVA polymer undergoes dissolution within the physiological condition, which mainly involves unfolding of PVA crystals chains that join the amorphous region of the polymer (Mallapragada and Peppas, 1996; Mallapragada *et al.*, 1997). It ultimately hampers the mechanical stiffness. Mar colongo and Lowman further introduced a combination of polyvinyl alcohol (PVA) and polyvinyl pyrrolidone (PVP) as a stable hydrogel over pure PVA (Thomas *et al.*, 2003). Also, their mechanical testing restored

1.4.2.2.3 Injectable nucleus replacements

Preformed nucleus implant compromises the annulus upon implantation. Moreover, the idea of using the dehydrating implants has a potential inability of a surgeon to accurately assess the nuclear cavity and appropriately implant dehydrated hydrogels. Therefore, the approach of replacing the damaged nucleus with the injection of liquid based compound (**figure 8**) became the wide interest. This technique could potentially fill the disc space; completely contact the surrounding annulus fibrosis (Joshi *et al.*, 2005). In 1955, David Cleveland made a first attempt at injectable nucleus replacement using methyl-acrylic into 14 patients undergoing discectomy (Cleveland, 1955; Goins *et al.*, 2005). Nachemson in late 1950s explored the use of liquid silicone rubber, which unfortunately turned out to be failure as degradation of the implant after 30,000 compression cycles was found out, which mimicked a walking road (Szpalski *et al.*, 2002). A fluid filled bladder was the next revolution since the designed was already explored for breast implants. Critical rupture was majorly seen in the implants and moreover, the biomechanics were also not comparable with that of disc, and therefore thought might not be suitable for the intervertebral nucleus pulposus replacement. Polyurethane elastomer (Langrana *et al.*, 1994), oligomers such as isocyanate or silane functionalized prepolymers (Milner *et al.*, 2001), polyurethane balloon (Di Martino *et al.*, 2005) etc. have also been evaluated in animal studies (Yue *et al.*, 2008) out of which, there is barely any suitable injectable hydrogel that have been utilized in clinical trial (Liu *et al.*, 2017). Injection of heated thermoplastic to the disc space is known as disc augmentation technology, where thermoplastic would harden after it cools within the disc space (Yue *et al.*, 2008). Exothermic process of polymer *in situ* is a major concern as it involves monomer, short chain oligomers, initiators and / or catalysts that in many cases are toxic and carcinogenic. Furthermore, herniation or fissure in the annulus fibrosis due to the injection pressure needs to be closely

monitored. BioDisc is yet another injectable hydrogel, mainly composed of protein hydrogel solution. Disc height restoration of de-nucleated disc is seen in fatigue study in the calf spine model; moreover disc remained intact, stable even after 10 million compression cycles (Yuksel *et al.*, 2002).

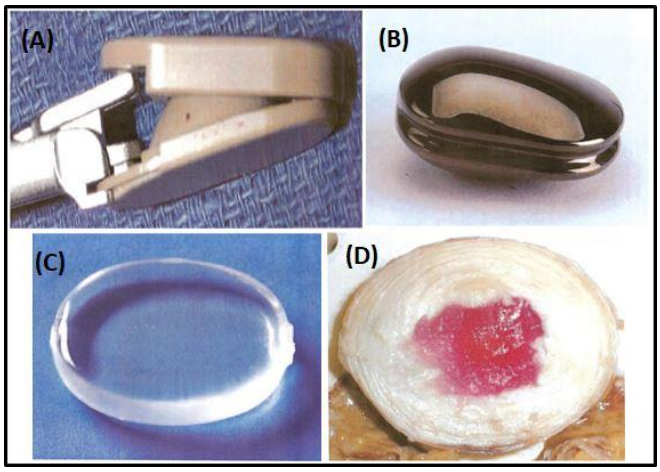

Figure 8: Rigid and injectable nucleus replacement devices. (A) **Nubac** 2-piece mechanical nucleus. Articulated PEEK-on-PEEK device ready for insertion. Picture used with permission from Pioneer Surgical, (B) **Regain** 1-piece mechanical/rigid nucleus replacement. Picture used with permission of Biomet, (C) **Dascor** injectable hydrogel elastomeric nucleus. Picture used with permission from Disc Dynamics, (D) **Nucore** Injectable Disc Nucleus (red), shown interdigitating with normal disc after injection into nucleotomy defect. Picture used with permission of Spine Wave (Coric and Mummaneni, 2008).

Nucleus pulposus replacement devices has been categorized into six types, such as *in situ* curable polymer, preformed polymer, composite polymer, one-piece mechanical, two-piece mechanical, and knitted mechanical.

Table 1: Commercial nucleus pulposus replacement materials (Lewis, 2012b)

Type	**Name**	**Material(s)/ Salient Features**	**Company**
In situ curable polymer	BioDisc	Albumin + glutaraldehyde hydrogel	CryoLife, Kennesaw, GA
	DASCOR	A polyurethane (PU) core and a PU balloon	Disc Dynamics, Eden Prairie, MN
	Hydrafil	Hydrophilic PVA and poly (vinyl pyrrolidone) (PVP) copolymer	Synthes USA, West Chester, PA
Preformed polymer	Aquarelle	A poly(vinyl alcohol) (PVA) hydrogel (80% water)	Stryker Howmedica Osteonics, Allendale, NJ

	NeuDisc	A modified hydrolyzed poly(acrylonitrile) reinforced with a Dacron mesh	Replication Medical, Cranbury, NJ
Composite polymer	HydraFlex	Flexible preformed hydrogel core encased in a jacket fabricated from tightly woven fibers of ultra-high-molecular-weight polyethylene	Raymedica, LLC, Minneapolis, MN
One-piece mechanical	IPD	An elastic component (elastic springs) attached to a fixation component	Dynamic Spine, Nahtomedi, MN
	Newcleus	A memory-coiling polycarbonate urethane	Centerpulse Orthopaedics, Winterthur, Switzerland
Two-piece mechanical	NuBacVR Disc Arthroplasty	Poly (etheretherketone) (PEEK)-on-PEEK	Pioneer Surgical Technology, Marquette, MI
Knitted mechanical	**Buck**	**Knitted Ti filaments**	**Buck GmbH & Co., Bondorf, Germany**

Theoretical advantages of arthroplasty especially the nucleus replacement (Schizas *et al.*, 2010) are to decrease the post-surgery risk factor like implant dislocation, lack of integration and thus to restore the biomechanical stability. Nonetheless, techniques are primarily focusing on restoration of mechanical integrity of the annulus fibrosis and do not offers a clear solution for delivery and fixation (Lewis, 2012b). In spite of so much of advancement, currently available nucleus implants are often associated with complications like changes in vertebral body, dislocation, vertical height loss of the disc and the lack of necessary associated mechanical rigidity (Cunningham, 2004). Therefore, it often limits in resulting load distribution, fatigue strength and *in vivo* compatibility concerning more about the post-surgery complications.

1.5 Titanium as a biomaterial

Titanium and their alloy are highly accepted material mainly because of its high resistance to corrosion. Especially pivot joint implants need mechanical strength and corrosion can erode the strength which ultimately leads to implant failure. Robust nature of titanium enables to withstand the loading during compression (Pohler, 2000). Moreover immunologically inert nature minimizes hypersensitivity reactions, which can be problematic with other metals like

nickel, cobalt (Geetha *et al.*, 2009). Therefore, it plays essential role from cyto-compatibility point of view. Further, scaffold surface modification by changing surface chemistry and/or topography uplifts its interaction with surrounding tissue, increasing the possibility of tissue integration (Puleo and Nanci, 1999; Mao and Li, 2014). Since tissue integration is critical for the long term success of the implant, it has been thought that scaffold surface modifications may optimize the conditions for rapid tissue integration. Physico-chemical properties of the scaffold are mainly thought to enhance the potential of tissue integration and at the same time minimize the chances of scaffold failure *in vivo*. Alteration to any of these characteristics influences the level of interaction with surrounding tissues.

1.5.1 Titanium and its alloys

Since 1964s, the use of titanium and its alloys have employed in the biomedical field after Branemark *et al.* (Brånemark *et al.*, 1964) proposed a phenomenon of osseointegration. Ti possess certain adequate properties such as excellent compressive strength, elastic moduli (110 GPa), corrosion resistant, low density and moreover the biocompatibility which ranks Ti high in the orthopedic field over other types of biomaterials such as stainless steel , CoCr (Niinomi, 2007). Layer of surface oxide (~5-29 nm) makes the material corrosion resistant. Pure titanium (cp-Ti), Ti-6Al-4V and NiTi are commonly used alloys (Pohler, 2000; Katti, 2004). Selection of appropriate alloy has an influence on the overall performance of the material and thus Ti alloy is of prime importance in clinical success (Geetha *et al.*, 2009). Compare to pure titanium, alloys are stronger and less prone to fatigue and therefore mainly explored for pivot joints replacements such as intervertebral disc (Hallab and Singh, 2014).

1.5.2 Surface modification

Apart from choice of material to be used in cartilage tissue engineering, it is equally important to have suitable scaffold properties and thus to function in accordance with host tissue upon implantation. Therefore it is foremost important that implant should be able to bond to the tissue in succession manner at the site of implantation (Geetha *et al.*, 2009), with the direct contact between the tissue and implant without a growth of fibrous tissue at the interface. Implant surface properties plays pivotal role in influencing the tissue integration as the interactions takes place at the interface (Geetha *et al.*, 2009). Hence, a striking balance between bulk and surface properties of the scaffold is necessary for effective performance (Geetha *et al.*, 2009). For instance, a thin layer of oxides on the surface of Ti and its alloy provides the resistance to corrosion however, despite, this bio-inert surface unable to develop

anchorage directly to the tissue upon implantation which ultimately corroborates longer tissue integration period (Burns *et al.*, 2009). Thus surface modification is an effective strategy which not only improves corrosion resistance of the implant but also renders the surface bioactive (Boyan *et al.*, 1996). It is a way to improve the implants biocompatibility and bioactivity while retaining the bulk properties of the material (Boyan *et al.*, 1996; Geetha *et al.*, 2009). Surface properties of titanium and its alloys can alter by means of various physical, chemical and biological methods. In mechanical way of surface modification, machining, grinding, blasting techniques are employed, whereas physical methods involves, thermal, kinetic / electrical energy is utilized to deposit a thin films on the surface. Chemical surface modification involves alteration of atoms, compounds or molecules on the surfaces modified (Kurella and Dahotre, 2005).

Table 2: Mechanical surface modification strategies (Tallawi *et al.*, 2015)

Mechanical methods	Modified layer	Objective
• Grinding • Polishing • Machining • Blasting	Rough or smooth surface formed by the subtraction process	– Produce specific surface topographies; – Clean and roughen surface; – Improve adhesion in bonding.

Table 3: Surface modification strategies to improve cell material interactions (Tallawi *et al.*, 2015)

Surface modification	Modified biomaterial properties
Physical	coatings containing pores to enhance tissue ingrowth
	topography induced (groves, morphology, roughness)
	fibrous materials
	porous materials
Chemical	glow discharge to increase surface energy and tissue adhesion
	cross-linked polymeric surfaces to decrease surface permeability and increase surface hardness
	plasma treatment with reactive gases to create new functional groups on polymer surface
	grafting macromolecules such as polyethylene glycol to reduce protein adsorption and cell adhesion
	functional groups used to produce positively or negatively charged surface

Biological	immobilization of biomolecules to promote cell adhesion and growth
	heparin, heparin sulfate binding peptides
	natural ECM proteins (fibronectin, laminin, collagen)
	peptide sequences (RGD)
	growth factors

Any targeted biomaterial primarily owes the requirement of achieving favorable surface properties that certainly influence the cell material interactions. Despite the fact that titanium and its alloy exhibit suitable biomechanical and biocompatible properties, negligence of specific requirements of site specific scaffold does limit their application. Therefore, scaffold bio-functionalization is being widely investigated using classical approaches such as mechanical, physical, chemical and biological.

1.6 Cell-material interactions

The main objective of implantology is that, scaffold material should induce controlled, guided and rapid healing. Although the interaction between the tissue and material is a dynamic complex process which is mainly dependent upon the scaffolds physico-chemical properties and respective host response (Alghazali *et al.*, 2015; Patel *et al.*, 2018). A scaffolds physico-chemical property includes surface roughness, topography, surface composition, wettability, pore size, porosity (El-Ayoubi *et al.*, 2011). Protein adsorption is the very first event that takes place at the interface during cells material interaction (Puleo and Nanci, 1999). Cell interaction is mediated by adsorbed protein from physiological fluids if it is *in vivo*, else in the cell culture medium *in vitro*, it is mainly fibronectin, vitronectin, fibrinogen, collagen as well as laminins (Wilson *et al.*, 2005). Protein adsorption on the scaffold surface is followed by cell attachment, spreading and then late events takes place such as cell proliferation, differentiation and matrix formation (Griffith and Naughton, 2002; De Bari *et al.*, 2006). Cellular response towards scaffold surface is mainly dependent scaffold surface properties (**figure 9**) such as composition, stiffness, roughness, chemistry, topography, surface energy, pore size, and porosity. Since the present study aims to characterize the novel knitted titanium scaffold scaffold for the replacement of intervertebral disc nucleus pulposus, it is extremely important to understand the response of the human primary intervertebral disc cells and mesenchymal stromal cells (MSCs). Besides in terms of their, cell adhesion, proliferation and so differentiation on the knitted titanium scaffold surface in order to achieve better tissue integration as well as for developing suitable design for rapid tissue healing (Raghunath *et al.*,

2007). Physico-chemical properties are generally interconnected and often it is difficult to distinguish the cellular response as a consequence of individual characteristics. Nonetheless, several studies have demonstrated the effect of individual parameter on cellular response by exploiting each surface characteristics as well as studying the synergy thereby eliminating the effect of other properties (Zhu *et al.*, 2004; Gittens *et al.*, 2014; Rupp *et al.*, 2014).

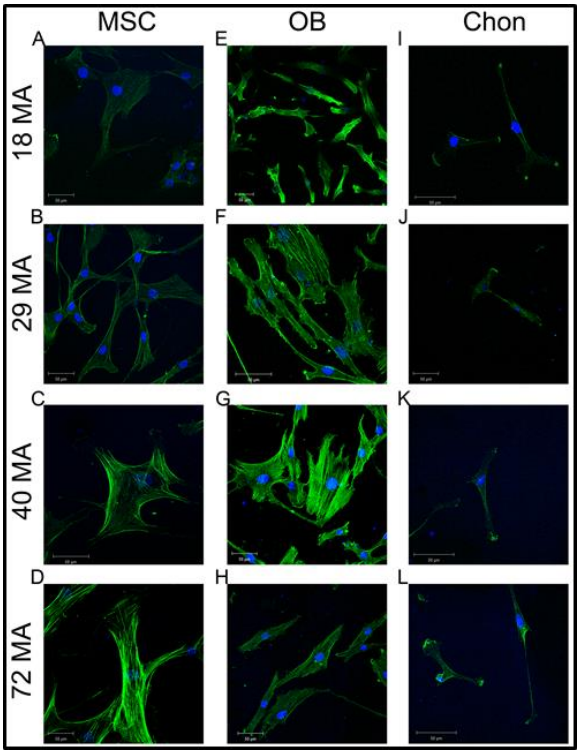

Figure 9: Cytoskeleton arrangement was altered by substrate stiffness. Representative staining of F-actin by phalloidin (green) and nuclei by DAPI (blue) in human MSCs (A-D), osteoblasts(E-H), and chondrocytes cultured on surfaces of varying stiffness. (Scale bars: 100 μm for A,B,D; 50 μm for all others) (Olivares-Navarrete *et al.*, 2017).

1.6.1 Surface roughness and topography

Surface topography is predicted as an important factor for better tissue integration which in turn regulates cellular behavior. Micro and / or nano structured scaffold surfaces are known to modulate the cellular behavior such as cell morphology, cell adhesion and RhoA activity (Nishimura *et al.*, 2018). Physical and chemical surface modification alters the topographical features (**figure 10**) thereby forming pits and grooves, moreover affecting pores at macro, micro and / or nano scale, which in turn affects surface roughness at microscale and / or nanoscale (Singh *et al.*, 2013). Degree of surface roughness is described by the height descriptive parameter of Sa or Ra i.e. arithmetic mean deviation of a profile (Ra) or a surface (Sa). Since the cell adhesion and spreading further guide and subsequently influence the

capacity of cells to proliferate and differentiate, it thus establish a mesh between the implant surface and tissue.

Cell adhesion is mediated by transmembrane protein receptors called integrins. Cell morphology on the other hand is mainly driven by surface topography (Lord *et al.*, 2010). It has been demonstrated that smooth surface roughness allows full cell spreading with filopodia, whereas rough surface allows elongated, spindle shaped cell spreading which normally oriented in the directions of grooves. Actin organization defines the quality of cell adhesion. This kind of behavior was reported by Jayaraman *et al.* (Jayaraman *et al.*, 2004) and many other, confirming that cell morphology is a complete topography driven phenomenon (Lord *et al.*, 2010; Ross *et al.*, 2012). It has been demonstrated that roughened surface have a greater tissue integrative potential than smooth and / or machined surfaces with an optimal roughness being in the range of 1-10 µm, although there are also contradictory findings (Alla *et al.*, 2011).

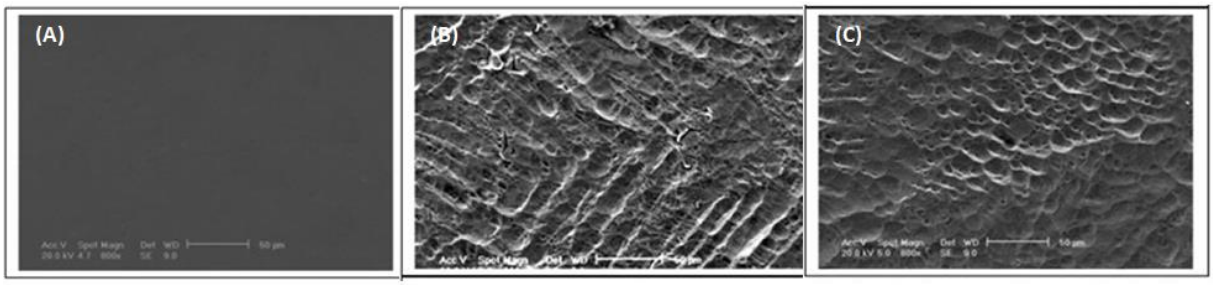

Figure 10: Scanning electron microscopy of titanium disk surfaces. Smooth surface (A), HF/HNO_3-etched surface – 15 min (B), HF/HNO_3-etched surface – 30 min (C). Scale= 50µm, magnification= 800x (Silva *et al.*, 2009).

Smooth surfaces are more prone to fibrous encapsulation which ultimately results in failure of tissue integration (Bobyn *et al.*, 1995; Gittens *et al.*, 2014). Fibrous encapsulation is the formation of a poorly vascularized collagenous capsule around the scaffold and number of factors such as sustained inflammatory response, lack of vascularization at the implant site and low levels of cell migration or attachment to the scaffold surface are involved in the formation of fibrous capsule coat (Bobyn *et al.*, 1995). As an outcome, tissue does not directly attach to the implant surface and thus fluid gets entrapped in a space between the fibrous capsule and implant. This fluid is an ideal environment for bacterial infiltration and subsequent infection which then cause bone resorption via sustained inflammatory reactions. On contrary, rough surface has thicker titanium oxide layer which thought to has superior influence on cell attachment and thus enhancing the implant stability. Also, increased

adherence of fibrin clot to the rough implant surface increase the possibility of cell progenitor migration and thus expected to increase the rate of the tissue integration. Increased adherence of the initial fibrin clot to the implant surface primly lowers the events of fibrous encapsulation around roughened implant surface (Bobyn *et al.*, 1995). The effect of various micro and nanoscale micro-topography on chondrocytes behavior were studied by Martínez *et al.* (Costa Martínez *et al.*, 2007) and others (Boyan *et al.*, 1996; Murakami *et al.*, 2000; Malda and Frondoza, 2006; Jäger *et al.*, 2007). With increase value of surface roughness, decrease in cell adhesion, proliferation while increase in cell differentiation phenomenon has been observed (Neves *et al.*, 2011; Ross *et al.*, 2012). However, an optimized method to create roughened surface thereby procuring tissue integration is yet to be investigated.

1.6.2 Wettability

Scaffold surface wettability is yet another physicochemical parameter that has been reported to play a critical role in establishing initial cell interactions (**figure 11**) at material interface such as cell adhesion and morphology (Gittens *et al.*, 2014; Rupp *et al.*, 2014). In particular, higher wettability / hydrophilic surface have been shown to have the specific capacities to enhance cellular behavior (Zhu *et al.*, 2004; Rupp *et al.*, 2014). On contrary, a number of studies also suggested that hydrophobic surface over hydrophilic is superior from clinical point of view (Wennerberg *et al.*, 2011). At molecular level, RhoA (small GTPase protein of the Rho family, involved in cytoskeleton regulation) activity and subsequent cell adhesion has been shown significantly higher in cells on hydrophobic surfaces compare to hydrophilic surfaces (Nishimura *et al.*, 2018). Moreover, time dependent wettability reduction and subsequent alteration in surface energy has also been reported (Att *et al.*, 2009). Contact angle is a measure of wettability of the solid surface by a liquid drop. Theoretically, contact angle should fall between 0-180^{o}. Surfaces are classes as hydrophilic if the contact angle is less than 90^{o}. If the wetting angle is more than 90^{o} then the surfaces are known as hydrophobic. When contact angle reach either 0 or 180^{o} then, surfaces are considered either super-hydrophilic or super-hydrophobic respectively. Dynamic contact angle mainly defines the hysteresis, meaning the difference between the advancing contact angle (the maximum value of the contact angle) and receding contact angle (the minimum value of the contact angle) (Gittens *et al.*, 2014; Rupp *et al.*, 2014).

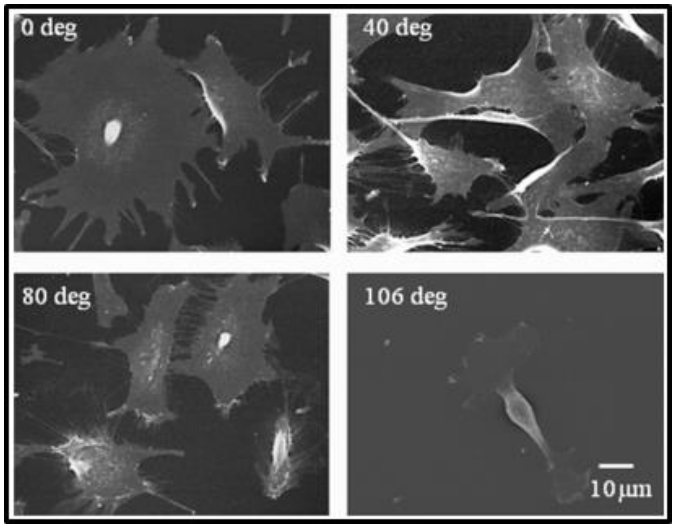

Figure 11: Typical SEM images of cell morphology with different contact angles at 180 min incubation. (Wei *et al.*, 2009b)

Titanium and its alloy although has a high surface free energy, are the example of poor wetting, weak hydrophilic surface with corresponding high contact angle about 80-90^{O}. Although titanium is well known suitable biomaterial, its surface modification may yield a hydrophilic surface with low contact angle which then enhance the cell material interactions. Plasma surface modification is one of the rapid processes to change the surface chemistry using either cold or atmospheric plasma system, thereby modify the surface hydrophilicity (Dowling *et al.*, 2011). Previously it has been reported that oxygen plasma treatment has a positive influence on the cellular behavior in terms of the initial cell adhesion, proliferation and also in the differentiation process (Yamamura *et al.*, 2015). In this study, we used the oxygen plasma in order to obtain low range of water contact angles. At laboratory level; plasma is generated through an electric gas discharge by creating a potential difference between the two electrodes into a fixed chamber, maintaining a pressure below 100 Pa. Balance between the hydrophilicity and hydrophobicity does influence the cell adhesion and growth (Gittens *et al.*, 2014; Rupp *et al.*, 2014). It has been previously shown that cells preferentially anchored to hydrophilic surface. Yamaguchi *et al.* on parallel showed that surfaces contact angle below 60^{o} are more suitable for better cell adhesion (Yamaguchi *et al.*, 2004). Although there have been several studies reported on the cellular behavior on the response of surface properties, no clear evidence yet exist with regards to human primary chondrocytes and mesenchymal stromal cells response on porous knitted titanium. As such, studies on the influence of surface chemistry and surface roughness on cell behavior has already been reported, their specific role in the cell response especially, cell adhesion,

proliferation and differentiation is still unclear. Moreover, it is extremely important to understand the specific role of surface properties on the human chondrocytes and mesenchymal stromal cells performance at material interface. This formed the basis of the one of the objective of this study.

1.7 IVD tissue engineering

Tissue engineering approaches over the past few years have been addressing the objective to recapitulate functional and structural features of the healthy intervertebral disc. Reparative treatment mainly targets intervention at early stages of intervertebral disc degeneration so to alleviate ECM homeostasis restoration, control of inflammation and prevention of angiogenesis. As current surgical procedures only focuses on alleviating symptoms associated with IVD degeneration, it does not promote tissue remodeling. On the other hand, tissue engineering offers an alternative to design a biomaterial by encompassing cells and growth factors that will aid in the IVD tissue regeneration. Thereby, it offers multiple strategies to prevent and possibly cure degenerated disc by encouraging disc repair. The exact mechanism of cartilage regeneration is still not known, however the several studies have been focused on the effect of segmental distraction in IVD disease (Buric and Pulidori, 2011; Guterl *et al.*, 2013; Fontana *et al.*, 2015). Recently, stimulatory factor together with cells either unaided or together with biomaterials has thought to provide suitable repair site to ensure maximum cell differentiation or deposition of appropriate ECM. Nonetheless selection of biomaterials, cells and appropriate stimulatory factor is very much important as the ideal combination is yet to be established. In this chapter we have explicitly discussed synthetically modified messenger RNA therapy.

1.7.1 *In vitro* transcribed mRNA therapy

The potential application of recombinant proteins and nucleic acid therapy has been widely explored in tissue engineering to produce specific growth factors, transcription factors, or molecules with therapeutic effects (Lieberman *et al.*, 2002; Henry *et al.*, 2018) to stimulate regenerative responses in the tissue. Ideally, gene therapy can overcome the recombinant growth factor delivery limitations, including supra-physiological dose, short half-life and poor distribution. The use of synthetic peptides as drugs is also associated with similar challenges and moreover, their pronounced conformational flexibility sometimes leads to a lack of selectivity and the activation of undesired cells, which can lead to adverse effects (Vlieghe *et al.*, 2010). Although viral and plasmid mediated gene delivery has demonstrated the ability to

effectively produce desired proteins, it also has several disadvantages, such as high risk of insertional mutagenesis leading to tumorigenicity due to genome integration, high immunogenicity, inefficient transduction in non-dividing cells , high levels of pre-existing immunity, and other potential serious complications (Katz *et al.*, 2013; Steinle *et al.*, 2017). Limitation of DNA based gene therapy has led to intense research on messenger RNA delivery as a promising alternative. Exogenous delivery of *in vitro* transcribed messenger RNA encoding protein of interest results in rapid but transient production of protein of interest (Mitchell and Nair, 2000; Bettinger *et al.*, 2001) and thus holds promising therapeutics in variety of medical indication (Tavernier *et al.*, 2011; Steinle *et al.*, 2017). Upon exogenous delivery of *in vitro* transcribed mRNA, cells intend to produce functional proteins which are not naturally synthesized or not needed. Besides, targeted cell after *in vitro* transcribed (IVT) mRNA delivery exhibit a new protein profile aiming to improve a cellular functions. The translational efficacy of synthetic mRNA has also improved compared to plasmids, since it bypasses the need for nuclear trafficking and it is immediately translated upon entering the cytoplasm. The risk of genomic integration and the nuclear entry doesn't remain major obstacles during the mRNA delivery. Moreover, their effectiveness as well in non-dividing cells holds a central advantage (Steinle *et al.*, 2017). IVT mRNA tends to trigger severe, undesirable immune response and besides, conventional form of mRNA is instable and labile, leading to early decay of the administered mRNA product in the target cell. Although, the use of mRNA as a therapeutic for protein replacing is not a new concept, it was also not widespread for many years due to mRNA's high instability and immunogenicity. Further Kariko *et al.* and others have demonstrated that modification of mRNA by incorporating modified nucleoside (replacing the uridines and cytidines with thio-uridine and 5-methyl-cytidine respectively) into mRNA elevates the stability mRNA and also lowers down the immunogenicity (Karikó *et al.*, 2005; Karikó *et al.*, 2008; Nallagatla and Bevilacqua, 2008; Kormann *et al.*, 2011).

mRNA can be synthetically synthesized using DNA templates targeting protein of interest by *in vitro* transcription (**figure 12**). In order to increase the mRNA stability and as well to reduce the immunogenicity, generated mRNA can be modified. Delivery of mRNA by transfection into the cells, allows direct translation into protein in the cytosol. Delivery of modified mRNA, which is non-integrating into the host genome, provides a transient pulse of protein expression. Therefore, it also avoids the possibility of oncogenic mutation and allows efficient delivery in dividing, non-dividing cells (Steinle *et al.*, 2017). It thus suggests an alternative to traditional DNA based gene therapy which allowed delivering therapeutic proteins either unaided or together with a scaffold.

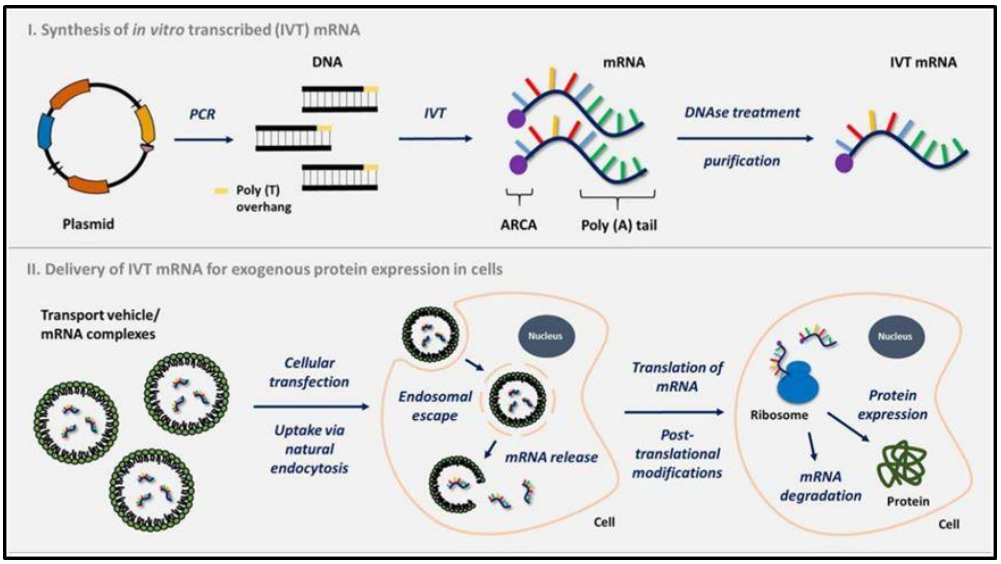

Figure 12: Schematic overview of (I) synthesis of IVT mRNA and (II) delivery of IVT mRNA into cells. In the PCR, the DNA template containing the coding DNA sequence of the desired protein is generated with a 50-T100-250 overhang from the corresponding DNA plasmid. To produce the mRNA, an *in vitro* transcription reaction is performed. During *in vitro* transcription, a 30-poly (A) tail is generated to prevent the mRNA from nuclease degradation. Additionally, mRNA can be generated using modified nucleosides (*e.g.*, 5-methylcytidine and pseudouridine) and a 50-cap structure (e.g. ARCA) to improve translation and mRNA stability. The presence of RNAse inhibitor during the *in vitro* transcription protects the mRNA from nuclease attack. To transfect cells, mRNA molecules are complexed with a cationic lipid-based transport vehicle. The complexes are taken up via endocytosis. After endosomal escape of the IVT mRNA into the cytoplasm, the mRNAs are translated by ribosomes into the desired protein(s). Abbreviations: ARCA, anti-reverse cap analog; IVT, *in vitro* transcribed; mRNA, messenger RNA; PCR, polymerase chain reaction (Steinle *et al.*, 2017)

Although there have been studies reported on nucleic acid therapy, delivery of Link N mRNA were not explored for intervertebral disc regeneration. Furthermore, although there are reports on the improved intervertebral disc height restoration using peptide form of Link N, the exact mechanism of cell behavior upon delivery of messenger RNA encoding Link N remains uninvestigated. We have evaluated the possibility of Link N mRNA delivery either unaided or

together with knitted titanium and explored their chondrocytes specific anabolic ability with emphasis on the effect of messenger RNA delivery on the functionality of human primary chondrocytes as well as mesenchymal stromal cells. The details form the basis for chapter 4.

1.7.2 Link N peptide

Link protein is a membrane bound glycoprotein that stabilizes the interaction between aggrecan and hyaluronan (Bach *et al.*, 2014) in extracellular matrices including in intervertebral disc matrix. The N terminal proteolytic cleavage of Link protein leads to the generation of Link N peptide, which is a 16 amino acid long peptide (Bach *et al.*, 2017). Positive relevance of Link N peptide has shown in the matrix of degenerating intervertebral discs; in addition, it appears to have additive effect on intervertebral disc metabolism, which stimulates the proteoglycan synthesis (Wang *et al.*, 2013). Recently, the Link N peptide has been identified as promising growth factor that stimulates the ECM synthesis in IVD tissue (Wang *et al.*, 2013; Gawri *et al.*, 2013a; Gawri *et al.*, 2013b; Gawri *et al.*, 2014; Bach *et al.*, 2017) and therefore, acts in IVD repair. Furthermore Antoniou *et al.* and Mwale *et al.* demonstrated that, Link N has suitable properties to drive chondrogenesis and therefore it serves as a potential growth factor during the phases of IVD healing (Mwale *et al.*, 2011a; Antoniou *et al.*, 2012a; Gawri *et al.*, 2014; Mwale *et al.*, 2014).

Although these studies reported on the possible role of Link N peptide as a novel growth factor in IVD response in terms of their anabolic effect, Link N application using nucleic acid therapy for intervertebral disc regeneration is yet to be investigated. We have explored the influence of Link N messenger RNA delivery in human primary chondrocytes and mesenchymal stromal cells *in vitro*. This formed the basis of one of the objective of the study.

2 Aim of the study

In order to overcome the drawbacks of currently available nucleus implants, Kettler *et al.* reported the development of a nucleus prosthesis made of knitted titanium wires (Buck GmbH & Co.) which proved to have low migration tendency and thus aimed to restore the physiological axial deformability (Kettler *et al.*, 2007; Buck and Kaps, 2014). Introducing knitted titanium implant in the clinical setting requires further characterization; therefore the current study was aimed to characterize and investigate the cytocompatibility aspect of knitted titanium scaffold for the replacement of intervertebral disc nucleus pulposus.

2.1 Knitted titanium scaffold

The very first design of the scaffold had a shape as that of the bovine NP with a rough surface roughness (Kettler *et al.*, 2007). Biomechanical test (**figure 13**) concerning axial deformity (AD) and disc height reduction was carried out on bovine lumbar spine (L2-L3 and L4-L5 segments). Quasi-static loading (increased from 100 to 1000 N) revealed that the median value of AD was same as that obtained immediately upon implantation. However, cyclic complex loading (axial force of 100–600 N, at 5 Hz) changed the median of AD by 33% and also disc height reduction was seen by small amount compare to intact case (Kettler *et al.*, 2007). Further, migration / expulsion assessment of the scaffold showed no extrusion but there was an evidence of migration within the implant cavity and also towards anterior border of the disc (Kettler *et al.*, 2007). Double the range of motion (ROM) as high in extension as it was in flexion, showed lordotic tilt caused upon implantation. However ROM effect on lateral bending and in axial rotation was marginal (Kettler *et al.*, 2007).

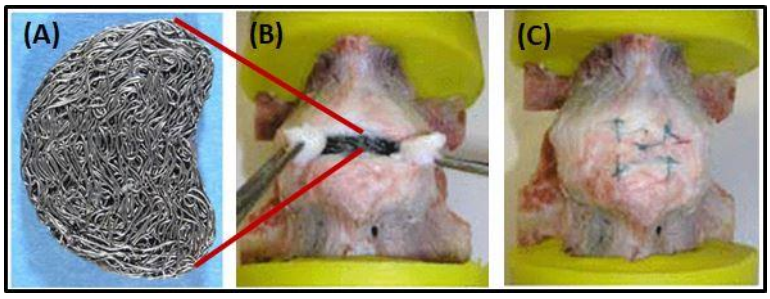

Figure 13: Biomechanics Experimental setup: knitted titanium nucleus scaffold (A) was implanted after anterior fenestration of the annulus fibrosus (B). Two lateral annulus flaps were created and sutured after implantation (C) (Kettler *et al.*, 2007)

Thesis objective

The objective of this thesis was to evaluate the cytocompatibility of the knitted titanium nucleus implant. This was achieved by investigating the following aspects-

To perform comparative analysis of unpolished and electro-polished scaffold with respect to their physicochemical properties, wear particle characterization, hemocompatibility and cellular response cell- material interface.

To further execute the surface hydrophilisation of the electro-polished scaffold and investigate the cell adhesion, spreading and proliferation behavior of the mesenchymal stromal cells and human primary chondrocytes.

To generate synthetically modified Link N mRNA and to evaluate its effect on mesenchymal stromal cells and human primary chondrocytes in terms increase anabolic response *in vitro* in 2D and together with knitted titanium scaffold.

CHAPTER 2

3 Results

Publication 1-

Tendulkar G, Grau P, Ziegler P, Buck A Sr, Buck A jr, Badke A,Kaps H-P, Ehnert S, Nussler AK: **Imaging cell viability on non-transparent scaffolds—using the example of a novel knitted titanium implant**, *Journal of Visualized Experiments*, 2016 Sept 7, 115:e54537

3.1 Synopsis:

Ideal biomaterial for an intervertebral disc nucleus pulposus replacement is on rise. Chronic back pain associated with intervertebral disc degeneration is of major socioeconomic concern (Melrose, 2016; van Uden *et al.*, 2017). The major significant discussion in the field of arthroplasty related to intervertebral disc is the need for nucleus replacement. Various biomaterials including hydrogels, polymers, metal and composites have been investigated to treat these conditions with wide range of success (Thomas *et al.*, 2003; Allen *et al.*, 2004; Goins *et al.*, 2005; Lewis, 2012a). A number of these materials have been used for total disc replacement depending on the site and degree of injury.

However, the major concern is the suitability of materials for soft tissue repair together with load bearing application. Thus, pivot joint replacement scaffold must possess certain properties to meet the requirement of lead bearing application. Adequate biomechanical properties including elasticity, fatigue properties so as to able to withstand compression pressure and suitable biological properties for effective *in vivo* functioning are the two main requirements (Goins *et al.*, 2005; Coric and Mummaneni, 2008). Until now, the choice of the material was limited to the hydrogel, as far as nucleus replacement is concerned (Di Martino *et al.*, 2005; Goins *et al.*, 2005). On contrary, metals with their good compressive and tensile strength mainly limit other materials such as ceramics, polymers and composites for load bearing applications for bone tissue engineering and hard tissue repair (Patel *et al.*, 2018).

Although metals such as titanium and its alloy, cobalt-chromium alloys, stainless steel are the man classes of metal that has been intensely investigated for total disc replacement, their mismatched elasticity lost its prominence in the long term success and so for the nucleus

pulposus replacement. Nonetheless, functionality with such low elastic modulus is required for load bearing application and therefore might be suitable for nucleus pulposus replacement if material is modified. Titanium and its alloy has gained much importance over stainless steel and cobalt chromium alloy for biomedical applications due to their excellent corrosion and wear resistance, strength (Geetha *et al.*, 2009).

Buck GmbH & Co. has developed a knitted mechanical based nucleus implant made of titanium filaments. Further Kettler *et al.* investigated their biomechanical properties, demonstrating suitable alternative of currently available nucleus scaffolds (Kettler *et al.*, 2007). In this study, we have further evaluated the biocompatibility including the wear particle characterization and tested their *in vitro* cytotoxicity and cellular behavior of human mesenchymal stromal cells and human primary chondrocytes when seeded on the knitted titanium scaffold by investigating the adhesion and proliferation behavior.

Video Article

Imaging Cell Viability on Non-transparent Scaffolds — Using the Example of a Novel Knitted Titanium Implant

Gauri Tendulkar[1], Phillip Grau[1], Patrick Ziegler[1,2], Alfred Buck, Sr.[3], Alfred Buck, Jr.[3], Andreas Badke[1,2], Hans-Peter Kaps[1,2], Sabrina Ehnert[1], Andreas K. Nussler[1]

[1]Siegfried Weller Institute for Trauma Research at the BG Trauma Center, Eberhard Karls Universität Tübingen

[2]Department of Orthopaedics, BG Trauma-Center

[3]Buck GmbH and Co.KG

Correspondence to: Andreas K. Nussler at andreas.nuessler@gmail.com

URL: https://www.jove.com/video/54537
DOI: doi:10.3791/54537

Keywords: Bioengineering, Issue 115, Nucleus implant, knitted titanium wires, biocompatibility, osteochondro-integration

Date Published: 9/7/2016

Citation: Tendulkar, G., Grau, P., Ziegler, P., Buck, Sr., A., Buck, Jr., A., Badke, A., Kaps, H.P., Ehnert, S., Nussler, A.K. Imaging Cell Viability on Non-transparent Scaffolds — Using the Example of a Novel Knitted Titanium Implant. *J. Vis. Exp.* (115), e54537, doi:10.3791/54537 (2016).

Abstract

Intervertebral disc degeneration and disc herniation is one of the major causes of lower back pain. Depletion of extracellular matrix, culminating in nucleus pulposus (NP) extrusion leads to intervertebral disc destruction. Currently available surgical treatments reduce the pain but do not restore the mechanical functionality of the spine. In order to preserve mechanical features of the spine, total disc or nucleus replacement thus became a wide interest. However, this arthroplasty era is still in an immature state, since none of the existing products have been clinically evaluated.

This study intends to test the biocompatibility of a novel nucleus implant made of knitted titanium wires. Despite all mechanical advantages, the material has its limits for conventional optical analysis as the resulting implant is non-transparent. Here we present a strategy that describes *in vitro* visualization, tracking and viability testing of osteochondro-progenitor cells on the scaffold. This protocol can be used to visualize the efficiency of the cleaning protocol as well as to investigate the biocompatibility of these and other non-transparent scaffolds. Furthermore, this protocol can be used to show adherence pattern of cells as well as cell viability and proliferation rates on/in the scaffold. This *in vitro* biocompatibility testing assay provides a propitious tool to analyze cell-material interaction in non-transparent and opaque scaffolds.

Video Link

The video component of this article can be found at https://www.jove.com/video/54537/

Introduction

Chronic back pain is a multifactorial disease. The interest in a minimally invasive treatment option for the degenerative disc disease has grown since the 1950s. Until today, multi-segmental fusion of the spinal column is the most widely used treatment. Since, this method often leads to limitations in the mobility of the affected segment[1,2], exploration of the arthroplasty era became a wide interest. Significant advancements in total disc replacement and nucleus replacement has become a good alternative to treat chronic back pain[1]. Despite the huge progress, none of the methods has been clinically evaluated. The less rigid nucleus implants represent a promising alternative to total disc replacement, provided that the annulus fibrosus is intact[3,4]. However, the currently present nucleus implants on the market are often associated with complications like changes in vertebral body, dislocation, vertical height loss of the disc and the lack of necessary associated mechanical rigidity[5]. In order to overcome the current drawbacks, a novel nucleus implant made of knitted titanium wires has been successfully developed[6]. Due to the unique knitted structure, this newly developed scaffold has shown distinguished biomechanical characteristics, *e.g.*, damping feature, pore size, loading capacity and reliability[7]. Aiming to test the biocompatibility of this novel nucleus implant, depicted severe limitations in the (optical) analysis techniques attributed to the non-transparent nature of the implant.

In order to test the biocompatibility, cell-metal interaction plays a prominent role[8-10]. An interaction between the cells and the scaffold is necessary for the stabilization and hence for the better implant integration within the host system. However, an increasing ingrowth depth might alter the mechanical properties of the scaffold. Aiming to investigate whether the scaffold surface provides a base for cell attachment, proliferation and differentiation or whether the metal affects cell viability, it is important to troubleshoot the common well-known problem of imaging cells on/in non-transparent and opaque scaffolds. In order to overcome this limitation several fluorescent based techniques were explored. Companies provide a large range of fluorophores to visualize living cells, cellular compartments, or even specific cellular states[11]. Fluorophores for this experiment were chosen with the help of the online tool spectral viewer in order to best fit our fluorescent microscope.

The developed strategy for the analysis of the adherent cells behavior on/in the non-transparent knitted titanium scaffold involves the following: 1) fluorescent (green fluorescent protein/GFP) labeling of the osteochondro-progenitor cells to allow tracking of the cells on the scaffold, 2) measuring the viability (mitochondrial activity) of the cells, and 3) visualizing cell-cell and cell-material interactions within the scaffold. The

procedure has the advantage that it can be easily transferred to other adherent cells and other non-transparent or opaque scaffold. Furthermore, viability and ingrowth pattern can be monitored over several days, thus it can be used with limited amounts of scaffold material or cells.

The present study demonstrates the successful use of our current protocol to measure the cell viability and visualize in-growth pattern of osteochondro-progenitor cells on/in the non-transparent knitted titanium scaffold. Furthermore, the developed protocols might be used in order to determine the scaffold impurities and to check cleaning protocols.

Protocol

NOTE: Immortalized human mesenchymal stromal precursor cells (SCP-1 cells) were used for the experiments. SCP-1 cells were provided by Prof. Matthias Schieker[12].

1. Expansion of SCP-1 Cells

1. Prior to working with the SCP-1 cells, properly clean the working area (designated biosafety cabinet I) with 70% ethanol (v/v) wearing gloves.
2. In the cleaned biosafety cabinet prepare an appropriate volume of cell culture medium by mixing the required components as indicated in **Table 1**. In order to maintain sterility of the basal medium, add supplements by passing through sterile filters with a pore size of 0.22 µm.
    1. To prevent contamination, prepare medium at least 24 hr before use. In order to test its sterility, incubate 1 ml medium in a cell culture plate without cells in the standard cell culture incubator: 37 °C, 5% CO_2, 20% O_2 and 90% humidity. After 24 hr, check medium microscopically using a magnification of at least 200X.
3. Maintain SCP-1 cells in a standard cell culture incubator with supportive condition: 37 °C, 5% CO_2, 20% O_2 and 90% humidity.
4. For maintenance and expansion, grow the SCP-1 cells until they reach 80-90% confluency. During this time period culture, change medium every 2-3 days. Upon reaching 80-90% confluency, split SCP-1 cells (in general a 1:2 ratio) to the next passage for expansion or plate for the experiments (as indicated).
5. For splitting the SCP-1 cells, warm the culture medium at 37 °C and thaw trypsin/EDTA using a water bath at 37 °C.
6. Completely aspirate the culture medium from the 80-90% confluent cells and discard it into a waste container.
7. Wash the cells at least twice with DPBS (Dulbecco's Phosphate buffered saline without magnesium and calcium, pH 7.2).
    1. Pipette an appropriate volume of DPBS onto the cells (5 ml DPBS for a T75 culture flask and 12 ml for a T175 culture flask).
    2. Aspirate DPBS carefully and discard it into a waste container.
8. Pipette an appropriate volume of 0.25% trypsin/EDTA onto the cells (1 ml DPBS for a T75 culture flask and 2 ml for a T175 culture flask) and incubate for 5-10 min at 37 °C in the standard cell culture incubator with 5% CO_2, 20% O_2 and 90% humidity.
9. Dislodge the cells by tapping the vessel and ensure all cells are detached from the culture plastic (trypsinization) by observing the floating cells under the microscope.
10. Inactivate the trypsin reaction by adding 10 ml of culture medium. Mix the trypsin and cells with the medium carefully by repeated pipetting.
11. Transfer the cell suspension into a reaction tube and centrifuge at 600 x g for 10 min at room temperature.
12. Aspirate the supernatant and resuspend the cell pellet in 10 ml culture medium.
13. Count the cells by Trypan Blue exclusion method as described in protocol 2.
14. Seed the cells depending on the experimental design.

2. Counting of SCP-1 Cells

1. Perform a viable cell count (Trypan Blue exclusion method) of the resuspended cells using a hemocytometer.
2. Prior to the cell count, clean the hemocytometer using tap water. Dry the hemocytometer components using a lint free tissue. Assemble it by moistening the cover glass and pressing it inversely onto the two glass runners on each side of the counting area. Ensure that Newtonian rings are seen on the glass runners (**Figure 1**).
3. Take 10 µl of the resuspended cells and mix with 10 µl of 0.1% Trypan Blue solution to obtain a dilution factor of 2.
4. Load 10 µl of the total sample on the pre-cleaned and assembled hemocytometer chamber.
5. Count the number of live (white/transparent cells) and dead (blue nuclei) cells on the 4x4 squares (see **Figure 1B**).
6. Calculate the total number of cells following the given formula:

$$\frac{\text{Total number of cells counted} * \text{dilution factor} * 10\text{^}4}{\text{number of squares}} = \frac{\text{number of cells}}{\text{mL}}$$

3. GFP Transfection of SCP-1 Cells

NOTE: In order to observe SCP-1 cell growth on and into the knitted titanium scaffold over a certain culture period we marked the cells with green fluorescent protein (GFP). Overexpression of GFP is achieved by infection with adenovirus particles coding for GFP. Replication incompetent (-E1/-E3) adenovirus particles coding for green fluorescent protein (GFP) were used to infect SCP-1 cells. The virus particles were obtained from Prof. Steven Dooley[13] by collecting culture supernatant of recombinant adenovirus (Ad5-GFP) transfected HEK293T cells (Biosafety lab II). Three repeated freeze (-80 °C) and thaw (37 °C in the water bath) cycles ensured that no HEK293T cells remain viable to produce new virus particles. Using this adenovirus seed stock can efficiently infect the SCP-1 cells without producing new virus particles. Thus, the infected cells can be handled in a Biosafety Lab I.

1. Resuspend the target cells (SCP-1 cells) with a seeding density of 50,000 cells/ml in culture medium. Pipette 2 ml per well into a 6-well tissue culture plate.
2. Incubate at 37 °C in the standard cell culture incubator; 5% CO_2, 20% O_2 and 90% humidity, till SCP-1 cells reach a confluency of 70-80%.

NOTE: Confluency depends on the seeding density of the cells. For above stated conditions, SCP-1 cells reach a confluency of 70-80% in 1.5-2 days.

3. At a confluency of 70-80%, without aspirating the culture medium add 100 µl of the adenovirus seed stock per 1 ml of culture medium.
    1. Determine the concentration range individually depending on the amount of virus particles in each virus seed stock preparation. In case the infection efficiency is too low, purify and concentrate virus particles using various commercially available kits.
4. Incubate for an hour in the standard cell culture incubator at 37 °C (5% CO_2, 20% O_2 and 90% humidity).
5. Remove the culture medium containing the virus seed stock and collect it for disposal. Add fresh culture medium 2 ml per well of a 6-well-culture-plate to replenish.
    1. Make sure that prior to disposal, virus particle containing medium is autoclaved.
6. Evaluate the intracellular GFP expression (infection efficiency) 24 hr after the infection using a fluorescence microscope with a GFP LED cube/filter set.
    1. Observe the cell morphology (**Figure 2**). Cells detaching from the culture plastic can give false positive results.

4. Cleaning of Knitted Titanium Scaffolds

1. Place up to 5 scaffolds into a 50 ml reaction tube.
2. Wash the scaffold (6-7 mm thickness) three times with 30 ml distilled-deionized water for 20 min at room temperature, using rotor conditions (8 x g).
3. Replace the distilled-deionized water with 30 ml 1% (w/v) Triton-X-100 solution (dissolved in distilled-deionized water) and then wash the scaffolds once for 20 min at room temperature, using rotor conditions (8 x g).
4. Discard the Triton-X-100 solution followed by washing with 30 ml distilled-deionized water twice (5 min each at room temperature) maintaining rotor conditions (8 x g).
5. Replace the distilled-deionized water. Rinse the scaffolds sequentially with reagent grade 99% acetone, 99% isopropanol and 99% ethanol (30 ml each) for 2 x 5 min each in an ultrasonic bath (~ 50 Hz, 50 W, 220-240 V).
6. Wash again three times with 30 ml distilled-deionized water for 5 min, keeping the ultrasonic bath treatment constant.
7. Place the scaffolds on a lint-free tissue in order to air dry overnight at room temperature.
8. Autoclave the scaffold for 15 min at 121 °C with 15 psi.
9. Confirm the cleaning protocol by indirect fluorescence as described in protocol 5.

5. Imaging Scaffold Structures by Indirect Fluorescence

NOTE: The present protocol describes the imaging of scaffold structures by indirect fluorescence using the fluorophore sulforhodamine B which gives a bright red fluorescence at an ex/em wavelength of 565/586 nm. However, the fluorophore can be changed to better fit for given microscope settings or possible auto-fluorescence of the scaffold.

1. Prepare the sulforhodamine B staining solution (0.04%) in 1% acetic acid and store at room temperature with protection from light.
2. Take a 24-well tissue culture plate and immerse the cleaned scaffold in 500 µl of the sulforhodamine B staining solution by placing it inside the well using forceps.
3. Capture the negative images of the scaffold using fluorescence microscope.
    1. Take pictures with a RFP LED cube/filter set with an excitation wavelength of 531/40 nm and an emission wavelength of 593/40 nm. Alternatively choose the adequate excitation and emission wavelength with the help of the fluorescence spectral viewer[20]. Sulforhodamine B has its peak excitation at 578 nm and its peak emission at 593 nm.
    2. In order to visualize the scaffold structure, take pictures at lower magnifications, *e.g.,* 4X or 10X (**Figure 3**). Using these pictures, determine characteristics, *e.g.,* the pore size and shape with the help of the ImageJ.
    3. In order to detect scaffold impurities, take pictures at higher magnifications, *e.g.,* 20X or 40X, considering that this will limit the analysis depth. Ensure that dirt particles/substances are not seen (see representative results; **Figure 3**).

6. *In Vitro* Biocompatibility Assay

1. Pre-warm the culture medium at 37 °C in a water bath.
2. Take a 24-well tissue culture plate and using forceps, place the cleaned and sterilized scaffolds in each test well aseptically. Work under the pre-cleaned biosafety cabinet I!
3. Soak/incubate the scaffolds with a culture medium for about 15 min (500 µl per well of a 24-well tissue culture plate), in order to remove air from inside of the scaffold.
4. Meanwhile, resuspend 500,000 Ad-GFP-infected SCP1 cells in 1 ml of culture medium.
5. After 15 min of scaffold soaking, aspirate the medium completely off the scaffold.
6. For seeding the cells on the scaffold, dispense 100 µl of cell suspension carefully on the scaffold (which is placed in 24-well plate) surface. Maintain a minimum volume of cell suspension while seeding the cells, so to ensure no medium flows out of the scaffold.
7. Incubate the cells for 30 min at 37 °C in the standard cell culture incubator (5% CO_2, 20% O_2 and 90% humidity).
8. Add 500 µl more culture medium and incubate for 24 hr in the standard cell culture incubator (37 °C, 5% CO_2, 20% O_2 and 90% humidity).
9. Evaluate the cell adherence pattern and cell spreading on the scaffold surface using a fluorescence microscope.
    1. Take pictures with a GFP LED cube/filter set with an excitation wavelength of 470/22 nm and an emission wavelength of 510/42 nm. Alternatively choose the adequate excitation and emission wavelength with the help of the fluorescence spectral viewer. GFP has its peak excitation at 488 nm and its peak emission at 507 nm.

2. In order to visualize cell adherence pattern capture pictures at lower magnifications, *e.g.,* 4X or 10X (**Figure 4**). In order to observe cell spreading a higher magnification (at least 100X) is needed — limiting the focus depth.

10. For further evaluating cell spreading on the scaffold surface, fix the cells with 4% formalin and proceed with conventional fluorescence staining of cellular structures, *e.g.,* actin filaments (Phalloidin). However, adapt incubation times and fluorescent labelling of the antibodies in order to fit the individual scaffold characteristics, *e.g.,* diffusion times or auto-fluorescence[14].
11. The next day, change the culture medium to remove non-adherent cells.
12. Calculate the percentage of adherent cells on the scaffold by resazurin conversion measurement as described in protocol 7.

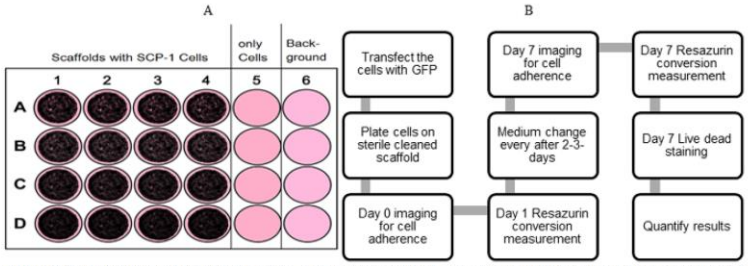

Figure 5: Timeline of *in vitro* assay. (**A**) Experimental setup for plating cells. (**B**) Illustration of procedure, emphasizing importance of beginning protocol and cell functionality validation till day 7. Please click here to view a larger version of this figure.

7. Resazurin Conversion measurement

NOTE: Resazurin conversion assay is used for measuring the mitochondrial activity and thus indirectly cell proliferation. Resazurin reduction to resorufin generates a fluorescent signal, which is based on the mitochondrial activity associated with viable cell numbers (**Figure 7A**).

1. Completely aspirate the culture medium from the SCP-1 cells and discard it into a waste container.
2. Wash the SCP-1 cells once with DPBS to remove detached cells. Add 500 µl DPBS per well of the 24-well tissue culture plate containing SCP-1 cells on the scaffold.
3. Cover the cells with a required amount of sterile resazurin working solution (0.25% resazurin in culture medium) and incubate at 37 °C in the standard cell culture incubator (5% CO_2, 20% O_2 and 90% humidity) for 30 min.
    1. Make a note that; incubation time depends on the cell type and cell density. It can vary between 10 min and 6 hr. Optimized incubation time for SCP-1 cells is 30 min.

4. As a background control, include at least one well with the resazurin working solution but without cells, that is incubated at 37 °C in the standard cell culture incubator (5% CO_2, 20% O_2 and 90% humidity) for the same amount of time.
5. Transfer 100 µl conditioned supernatant from each well of the 24-well tissue culture plate into a 96-microwell plate.
6. Wash the remaining cells three times with 1 ml DPBS for 5 min at room temperature in order to remove residual resazurin working solution. After the third wash add culture medium to the implants with SCP-1 cells (500 µl per well of the 24-well tissue culture plate) and continue incubation at 37 °C in the standard cell culture incubator (5% CO_2, 20% O_2 and 90% humidity) for further time course measurements.
    1. Make sure to set up replicates at this step (2-4) in order to minimize pipetting errors.

7. In the meantime, place the 96-microwell plate into the microplate reader and measure the fluorescence of the formed resorufin.
    1. In order to reduce background signal, measure fluorescence at an excitation wavelength of 545 nm and an emission wavelength of 585 nm.
    2. Alternatively choose the adequate excitation and emission wavelength with the help of the fluorescence spectral viewer. Resorufin has its peak excitation at 572 nm and its peak emission at 585 nm. The given signal intensity is an average of 25 individual readings (25 flashes per well).

8. Measure the fluorescence of formed resorufin in conditioned medium, using a bottom optic.
    1. Make a note that, the gain depends on the average amount of resazurin converted and can vary between 10 and 4,000. Adjust the gain to the individual microplate reader used by pipetting a resorufin standard curve, such that the fluorescent signal is below 80% of the maximum signal intensity detectable (in this case 20,000). The optimized gain for SCP-1 cells is 800.

9. Subtract the background signal (resazurin working solution without cells) from signal of the test samples.
10. Depending on the experimental setup/purpose, proceed with further steps:
11. Calculate the percentage of viability of the cells on the scaffold using a standard curve. Make an individual standard curve separately for each cell line used.
12. Analyze cell growth/proliferation by estimating the relative increase in resazurin conversion throughout the cultivation time. For this calculation, set the resazurin conversion on day 1 as reference. Freshly prepare the resazurin working solution for this kind of analysis. Furthermore, incubation times have to be equal between the different measurements.
13. Repeat the entire protocol of resazurin conversion measurement at least three times to get consistent results.

8. Live-dead Staining

1. Plate the SCP1 cells on the scaffold with a seeding density of 50,000 cells/scaffold and allow it to grow on the scaffold keeping the standard cell culture conditions (refer to protocol 1 and 2).
2. After 24-48 hr completely aspirate the culture medium from the SCP-1 cells and discard it into a waste container.
3. Wash the SCP-1 cells once with DPBS to remove detached cells. Add 500 µl DPBS per well of the 24-well tissue culture plate and incubate for 5 min at room temperature.
4. Stain SCP-1 using fluorophores (all three stains at the same time):
    1. From now on keep the scaffolds in the dark in order to protect the fluorophores bleaching from daylight!
    2. Set an incubation time to 30 min in order to allow equal distribution throughout the scaffold. If transferring to other scaffolds, make sure to optimize the incubation times to fit the individual scaffold characteristics (pore size, scaffold depth, *etc.*).
    3. In order to detect viable cells on the scaffold, stain the cells with calcein AM at a final concentration of 2 µM (in culture medium).
    4. In order to detect all cells on the scaffold, stain the cells with Hoechst 33342 at a final concentration of 0.002 µg/µl (in culture medium).
    5. In order to detect dead cells, incubate the scaffold with ethidium homodimer at a final concentration of 4 µM (in culture medium).
5. After the incubation time, wash the cells 3 times with DPBS (1 ml per well) for each 5 min at room temperature.
6. Immediately take pictures by using a fluorescence microscope.
    1. Take pictures of the calcein (living cells) with a GFP LED cube/filter set (excitation and emission wavelength of 470/22 nm and 510/42 nm, respectively). Alternatively choose an adequate excitation and emission wavelength with the help of the fluorescence spectral viewer. Calcein has its peak excitation at 488 nm and its peak emission at 507 nm. Note: Ensure not to use GFP transfected cells for fluorescence staining with Calcein or other green fluorescent stains.
    2. Take pictures of the Hoechst 33342 with a DAPI LED cube/filter set with an excitation wavelength of 357/44 nm and an emission wavelength of 447/60 nm. Alternatively choose the adequate excitation and emission wavelength with the help of the fluorescence spectral viewer. Hoechst 33342 has its peak excitation at 347 nm and its peak emission at 483 nm.
    3. Take pictures of the ethidium homodimer with a RFP LED cube/filter set (excitation and emission wavelength of 531/40 nm and 593/40 nm, respectively). Alternatively choose the adequate excitation and emission wavelength with the help of the fluorescence spectral viewer. Ethidium homodimer has its peak excitation at 530 nm and its peak emission at 618 nm.

Representative Results

Preliminary results showed that the described novel nucleus implant not only has good damping features but also is biocompatible with SCP-1 cells. During the production process of the implant, it comes in contact with strong corrosive and toxic substances (lubricant, mordant, electro-polishing solution). With the help of indirect fluorescent staining techniques we were able to visualize remaining impurities and consequently optimize a cleaning protocol showing significant reduction in substance load on the scaffold. **Figure 3** shows the efficiency of established cleaning protocol.

The success of implants used for arthroplasty treatment is determined by events that takes place at the cell-material interface. **Figure 4** shows the cells attached on the scaffold after 24 hr of plating, as described in the protocol section 6. A significant transfection efficiency of SCP-1 cells was observed as we could image the growth pattern of mesenchymal stromal precursor cells on the scaffold (refer **Figure 2**). Direct visualization confirms the biocompatibility of the scaffold and also depicts the adherence pattern on the scaffold surface (**Figure 4**). Fluorescence staining can be done further to examine cell interaction with and spreading on the scaffold surface.

Fluorophores were successfully applied in order to examine cell death and proliferation over a period of time on the scaffold. Live-dead-staining images exemplify how staining can successfully be done on the scaffold to confirm the percent viability of cells over a period of time. **Figure 6** shows blue nuclear staining (Hoechst 3342) in all cells, red fluorescently labelled (ethidium homodimer) dead cells, and green labelling for incorporation of calcein-AM as viability marker. Calcein AM is converted to calcein which exhibits a bright green fluorescence in the presence of calcium ions in the cytoplasm of the cells. Hoechst 33342 is cell wall permeable and intercalates into the cellular DNA. This way all cells will show blue nuclei (refer **Figure 6**). Ethidium homodimer is not cell wall permeable, thus it will only intercalate into the DNA of dead cells. This way, dead cells will show red nuclei. Furthermore, cell viability and fold increase in cell number on scaffold over a week was quantified by resazurin conversion assay and represented graphically (**Figure 7**).

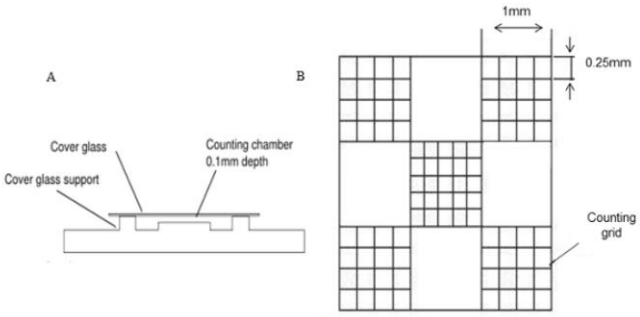

Figure 1: Cell counting with a Hemocytometer. (**A**) Setup of a chamber assembly. (**B**) Illustration of counting chambers; 4 x 4 counting chamber is used for a cell count. Please click here to view a larger version of this figure.

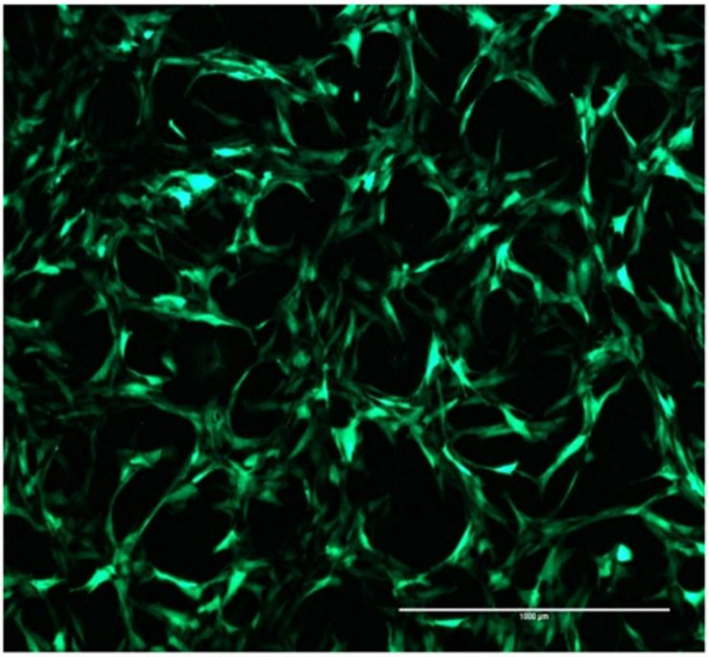

Figure 2: GFP transfection efficiency. SCP1 cells exhibit a strong green fluorescence indicating positive ad-GFP- transfection efficiency. Scale bar = 1,000 µm, 4X magnification. Please click here to view a larger version of this figure.

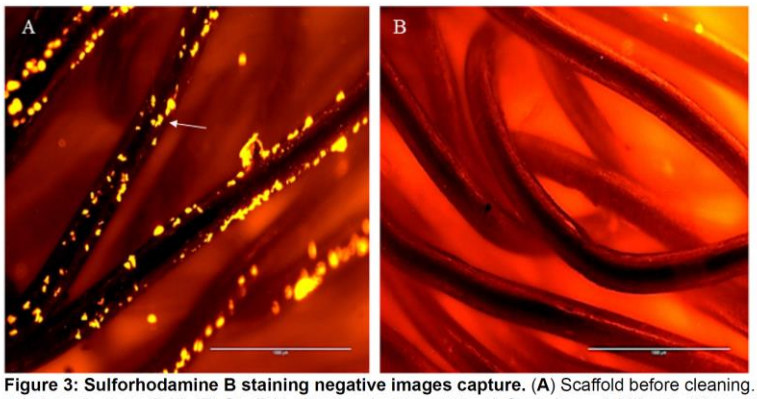

Figure 3: Sulforhodamine B staining negative images capture. (**A**) Scaffold before cleaning. Arrow indicates the presence of toxic/corrosive substances on scaffold. (**B**) Scaffold after the cleaning protocol. Scale bar = 1,000 µm, 4X magnification. Please click here to view a larger version of this figure.

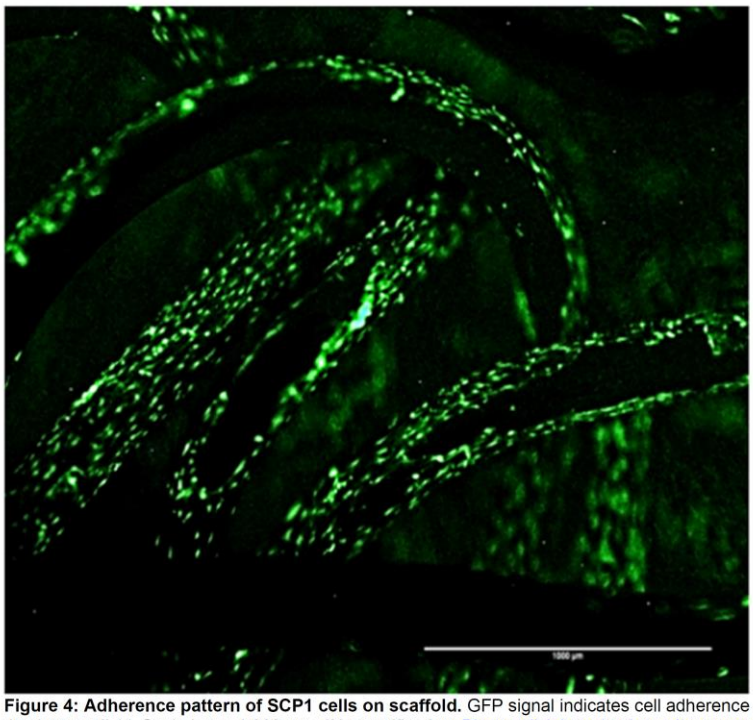

Figure 4: Adherence pattern of SCP1 cells on scaffold. GFP signal indicates cell adherence and growth pattern on the surface of the knitted titanium scaffold. Scale bar = 1,000 µm, 4X magnification. Please click here to view a larger version of this figure.

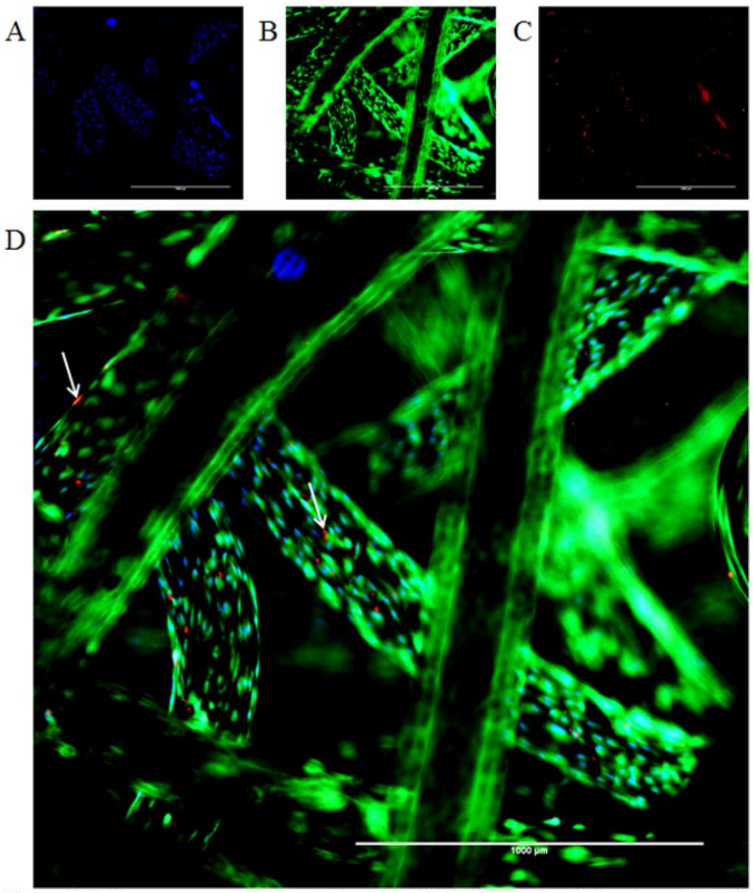

Figure 6: Co-fluorescence staining of cells on scaffold. (**A**) The Hoechst nuclear staining (blue) and (**B**) the Calcein-AM cytoplasmic staining (green). (**C**) Arrow indicates the presence of dead cell due to uptake of ethidium homodimer-1 stain (red). (**D**) shows the merged image. Scale bar = 1,000 µm, 4X magnification. Please click here to view a larger version of this figure.

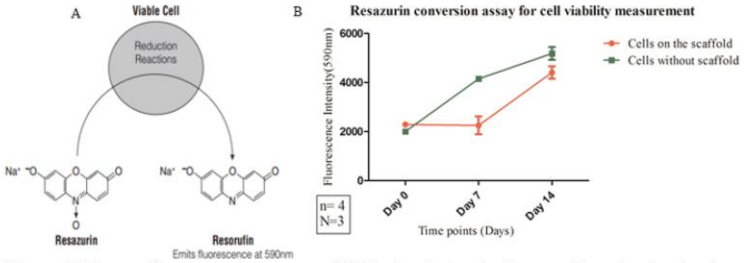

Figure 7: Resazurin conversion assay. (**A**) Biochemical reduction reaction of redox dye (resazurin) into an end product (resorufin) which emits fluorescence and undergoes colorimetric changes. (**B**) Mitochondrial activity was measured when cells were plated on 0.75 mg/cm³ density scaffold. Data was collected using fluorescence based measuring instrument. Fluorescence intensity at 590 nm (y-axis) at defined time points (x-axis) is depicted as a result of quantitative cell viability measurement (Ex = 540 nm, Em = 590 nm). The statistical significance was determined using Two way ANOVA and standard error of the mean (SEM) is shown as an error bars. Considering the scaffold physical properties, *e.g.,* pore size and mechanical properties (*e.g.,* damping feature) together, 0.75 mg/cm³ density scaffold was used for biocompatibility characterization. Please click here to view a larger version of this figure.

Media components	Concentration
Basal αMEM media (%)	90
Serum (%)	10
Pen/Strep (%)	1

Table 1: Cell culture (αMEM) Media composition.

Problem	Cause	Solution
Cell viability imaging on Non-transparent scaffold	Scaffold prevents light from penetrating without distortion	Use fluorophore based imaging technique for cell assessment.
Interference of fluorescence intensity	Auto fluorescence, background signal	Pay attention to the fluorophores and use appropriate based on particular scaffold properties.
Cell viability assessment on scaffold over a culture period	Repeated measurements over a long time	Transfect the cells with ad-GFP-virus particles.
Cell functionality assessment on non-transparent scaffold	Fluorescence imaging technique allows only cell spreading pattern analysis.	Perform resazurin conversion assay (quantitative cell viability measurement) in a combination with imaging technique.

Table 2: Summary table: troubleshooting the cell viability imaging on non-transparent scaffold.

Discussion

The scaffold surface plays an important role in its interaction with surrounding tissue *in vivo* thereby determining implants functional durability. Thus, the bio-compatibility of the scaffold is studied by *in vitro* assays using cells (SCP1 cell line), when plated on the scaffolds.

Microscopy techniques that function well with thin and optically transparent scaffolds are poorly suited for non-transparent scaffolds to study the biocompatibility. This is mainly because the non-transparent scaffolds prevent light from penetrating without significant distortion[15]. To partly overcome these problems we herewith establish a method for cell assessment on/in knitted titanium made scaffolds using various fluorophores.

In order to enable knitting followed by folding of the titanium wires, the material comes into contact with strong corrosive and toxic substances (lubricant, mordant, electro-polishing solution), which might alter the biocompatibility of the scaffold if traces remain in/on the scaffold. With the help of a developed indirect-fluorescence protocol (Protocol 5) we could visualize the scaffold structure. Furthermore, scaffold characteristics, *e.g.*, the material thickness, the individual pore size and shape, or the connective density, were analyzed using ImageJ. A higher magnified epifluorescence microscopic image allowed visualizing impurities in the scaffold as well as on the scaffold surface. **Figure 3b** thus represents the confirmatory result of the successfully developed cleaning protocol. The principle of this indirect staining protocol can be easily reproduced to other non-transparent scaffolds, taking into consideration the individual scaffold properties, *e.g.*, pore size and corresponding diffusion which affects the incubation time. Also, auto-fluorescence of the scaffold and microscopic settings affects the choice of fluorophores used. The online tool fluorescence spectral viewer can help to choose the adequate fluorophores.

Cell-metal interaction has been examined indirectly by analyzing the adherence pattern of cells on the scaffold. Protocol 6 describes the methodology of how cells can be monitored *in vitro* if plated on non-transparent scaffolds in culture systems by using a GFP transfection strategy. Based upon preliminary results of *in vitro* assays, it has been predicted that the surface properties such as composition, micro-topography and roughness[16] might play an important role in establishing adherence and spreading of target cells. Titanium being a biomaterial thus might be acting as a substrate template to provide base for cell attachment (refer **Figure 4**).

Implant surface topography has been reported to influence cell behavior[16]. In the present study, we analyzed the cell growth/spreading and viability using fluorescence staining techniques in combination with quantitative viability measurements. Analysis revealed subtle variation in cell percent viability and spreading depending on the scaffold material. However, cell functionality assessed quantitatively by resazurin conversion assay (mitochondrial activity), was not significantly affected by the scaffold material. The measurement of the mitochondrial activity by resazurin conversion has the advantage that it is not cell toxic and thus can be performed repeatedly over a long culture period. Special care has to be taken when washing off residual resazurin working solution, so to not accumulate background signal (false positive results). Despite these advantages, the resazurin conversion assay will not give any information on the cell spreading on the scaffold. The GFP infected cells hence can be tracked over a long culture period (GFP signal remained constant for over 14 days), thereby enabling to visualize specific growth pattern on the scaffold surface. Visualization of cells deeper in the scaffold is still limited by the scaffold material and thus will require dissection of the implant. The combination of these two techniques has the major advantage that it can be easily transferred to other cell types, considering that incubation time might have to be adapted to the cell type of interest. However, care has to be taken when transferring this method to other non-transparent scaffolds, *e.g.,* collagen based scaffolds which generally exhibit a strong green auto-fluorescence[17]. In this case other fluorescent tags might be used. The combination of above stated two methods therefore has several advantages (see **Table 2**).

Scaffold characteristics, *e.g.*, pore size might trap cells inside the scaffold. If not enough nutrients are supplied, these cells might die and secrete proteases that affect cell viability of the surrounding cells/tissue. We were able to adapt a fluorescent based staining protocol that is able to visualize live and dead cells in and on the knitted titanium scaffold. Similar to the indirect fluorescence staining protocol, the principle of this staining protocol can be easily transferred to other non-transparent scaffolds. While doing so, the individual scaffold properties, *e.g.*, pore size and corresponding diffusion as well as possible auto-fluorescence, microscopic setting have to be taken into consideration as they might

affect the incubation time and the choice of fluorophores used. Here, again the online tool fluorescence spectral viewer can help to choose the adequate fluorophores.

In summary, *in vitro* results indicate that the proposed knitted titanium nucleus implant model has a biological profile. Initial attachment of mesenchymal stromal precursor cells (SCP-1 cells) on this material suggests that this titanium alloy implant material is biocompatible. Although we have not analyzed association of different topographical parameters, scaffold surface modification might enhance cell adherence proliferation as well as differentiation[18]. Optimum compatibility between scaffold and cells raise the probability of better implant integration into the surrounding tissue and so improving *in vivo* longevity after the treatment[19]. Using the above stated test setup opens up the possibility to measure and visualize improvements in the biological performance of the scaffold induced by surface modifications. The preference of scaffolds with bioactive surface over unmodified implant designs suggests the better performance[20] in terms of osteo-chondrogenic integration. This study is further enhanced by other reports on the knitted titanium implant where its mechanical property and bioactivity have been reported [6,7].

Disclosures

The authors declare that they have no competing interests. No portion of the work has been or is currently under consideration for publication or has been published elsewhere.

Acknowledgements

Project is partially funded by Zentrales Innovationsprogramm Mittelstand (ZIM) des Bundesministeriums für Wirtschaft und Energie - KF3010902AJ4. The publication fee has been covered by the BG trauma hospital Tübingen, Germany.

References

1. Bridwell, K. H., Anderson, P. A., Boden, S. D., Vaccaro, A. R., & Wang, J. C. What's new in spine surgery. *J Bone Joint Surg Am.* **95**, 1144-1150 (2013).
2. Adams, M. A., & Dolan, P. Intervertebral disc degeneration: evidence for two distinct phenotypes. *J Anat.* **221**, 497-506 (2012).
3. Schizas, C., Kulik, G., & Kosmopoulos, V. Disc degeneration: current surgical options. *Eur Cell Mater.* **20**, 306-315 (2010).
4. Lewis, G. Nucleus pulposus replacement and regeneration/repair technologies: present status and future prospects. *J Biomed Mater Res B Appl Biomater.* **100**, 1702-1720 (2012).
5. Cunningham, B. W. Basic scientific considerations in total disc arthroplasty. *Spine J.* **4**, 219S-230S (2004).
6. Buck, A. E., & Kaps, H.-P. *Implant for surgical use in humans or vertebrates.* US8728164 B2. Google Patents, (2014).
7. Kettler, A., Kaps, H. P., Haegele, B., & Wilke, H. J. Biomechanical behavior of a new nucleus prosthesis made of knitted titanium filaments. *SAS J.* **1**, 125-130 (2007).
8. Nerurkar, N. L., Elliott, D. M., & Mauck, R. L. Mechanical design criteria for intervertebral disc tissue engineering. *J Biomech.* **43**, 1017-1030 (2010).
9. Elias, C. N., Lima, J. H. C., Valiev, R., & Meyers, M. A. Biomedical applications of titanium and its alloys. *JOM.* **60**, 46-49 (2008).
10. Hallab, N., Link, H. D., & McAfee, P. C. Biomaterial optimization in total disc arthroplasty. Spine *(Phila Pa 1976).* **28**, S139-152 (2003).
11. Gustafsdottir, S. M. et al. Multiplex cytological profiling assay to measure diverse cellular states. *PLoS One.* **8**, e80999 (2013).
12. Bocker, W. et al. Introducing a single-cell-derived human mesenchymal stem cell line expressing hTERT after lentiviral gene transfer. *J Cell Mol Med.* **12**, 1347-1359 (2008).
13. Ehnert, S. et al. Transforming growth factor beta1 inhibits bone morphogenic protein (BMP)-2 and BMP-7 signaling via upregulation of Ski-related novel protein N (SnoN): possible mechanism for the failure of BMP therapy? *BMC Med.* **10**, 101 (2012).
14. Morgan, S. P., Rose, F. R., & Matcher, S. J. *Optical Techniques in Regenerative Medicine.* CRC Press, (2013).
15. Vielreicher, M. et al. Taking a deep look: modern microscopy technologies to optimize the design and functionality of biocompatible scaffolds for tissue engineering in regenerative medicine. *J R Soc Interface.* **10**, 20130263 (2013).
16. Curtis, A., & Wilkinson, C. Topographical control of cells. *Biomaterials.* **18**, 1573-1583 (1997).
17. Niu, G. et al. Fluorescent imaging of endothelial cells in bioengineered blood vessels: the impact of crosslinking of the scaffold. *J Tissue Eng Regen Med.* (2014).
18. Chan, B. P., & Leong, K. W. Scaffolding in tissue engineering: general approaches and tissue-specific considerations. *Eur Spine J.* **17 Suppl 4**, 467-479 (2008).
19. Navarro, M., Michiardi, A., Castano, O., & Planell, J. A. Biomaterials in orthopaedics. *J R Soc Interface.* **5**, 1137-1158 (2008).
20. Priyadarshani, P., Li, Y., & Yao, L. Advances in biological therapy for nucleus pulposus regeneration. *Osteoarthritis Cartilage.* (2015).
21. *Thermofisher Fluorescence Spectraviewer.* Source: https://www.thermofisher.com/de/de/home/life-science/cell-analysis/labeling-chemistry/fluorescence-spectraviewer.html (2016).

CHAPTER 3

Publication 2-

Tendulkar G, Sreekumar V, Rupp F, Teotia AK, Athanasopulu K, Kemkemer R, Buck A Jr, Buck A Sr, Kaps H-P, Geis-Gerstorfer J, Kumar A, Nussler AK: **Characterisation of porous knitted titanium for replacement of intervertebral disc nucleus replacement**, *Scientific Reports*, 2017 Nov 30; 7(1):16611.

3.2 Synopsis:

For successful *in vivo* functioning, suitable implants should possess certain biological properties as the biocompatibility is the prime requirement for any type of scaffold (Griffith and Naughton, 2002; De Bari *et al.*, 2006; Chang and Wang, 2011; El-Ayoubi *et al.*, 2011). Biomaterial should be able to function in the physiological environment without causing any inflammatory and adverse response upon implantation into the host system. Therefore, tissue integration is the foremost requisite for long term success of the material. Scaffold surface plays pivotal role in directing cell response, and moreover physicochemical properties of the scaffold surface such as surface energy, surface roughness, topography, surface composition, porosity and pore size have been demonstrated to modulate the cellular response either directly or in an interdependent manner. For example, Ross *et al.*demonstrated that, cell adhesion and proliferation behavior is inversely correlated on rough surface (Ross *et al.*, 2012). However, it should be noted that there is no conclusive evidence with regard to effect of surface roughness on the cell behavior pattern.

We have focused on the aspect of cell material interaction by investigating the behavior of mesenchymal stromal cells and human primary chondrocytes on unpolished and electro-polished surface of the scaffold in terms of the surface properties. Surface roughness profiles of these two surfaces were in the sub-micron range although the chemical composition remained the same. Electro-polishing treatment improved the surface roughness without affecting the wettability. Furthermore, we have observed a significant difference in the surface energy upon the electro-polishing treatment, although the difference was not enough in modulating the cellular responses thereby resulting the similar cell adhesion and proliferation behavior on electro-polished surface. We can interpret the possible role of

surface wettability in influencing the cell behavior, with the initial cell spreading highly accelerated by the high surface energy.

Initial protein adsorption on the scaffold surface modulates the signal transduction and thereby determines the fate of the cells with respect to cell morphology, adhesion, spreading and proliferation. Surface modification is the effective strategy to improve the biocompatibility of the scaffold surface without hampering the materials bulk properties (Puleo and Nanci, 1999). Various mechanical, physical, chemical and biological surface modification strategies have been investigated for improving the bioactivity of the scaffold at cell material interface (Morra, 2006; Mao and Li, 2014). Studies in the past have shown that hydrophilic surface is favorable to cellular behavior. Therefore, it becomes important to understand the contribution of surface hydrophilicity of knitted titanium on the cellular response of SCP1 cells and human primary chondrocytes. Thus, we modified the scaffold surface using oxygen plasma treatment to create hydrophilisation at the scaffold surface. The cellular responses were tested towards the modified surfaces and the observed differences in the differential expression of cell proliferation and cell spreading gave further insights into the behavior of chondrocytes and mesenchymal stromal cells on the material. The selective choice of cells, in this *in vitro* cytocompatibility testing provides further opportunities for studies, thereby looking at the possible outcome in the *in vivo* environment.

SCIENTIFIC REPORTS

OPEN

Characterisation of porous knitted titanium for replacement of intervertebral disc nucleus pulposus

Received: 22 May 2017
Accepted: 16 November 2017
Published online: 30 November 2017

Gauri Tendulkar[1], Vrinda Sreekumar[1], Frank Rupp[2], Arun K. Teotia[3], Kiriaki Athanasopulu[4], Ralf Kemkemer[4], Alfred Buck Jr.[5], Alfred Buck Sr.[5], Hans-Peter Kaps[1], Jürgen Geis-Gerstorfer[2], Ashok Kumar[3] & Andreas K. Nussler[1]

Effective restoration of human intervertebral disc degeneration is challenged by numerous limitations of the currently available spinal fusion and arthroplasty treatment strategies. Consequently, use of artificial biomaterial implant is gaining attention as a potential therapeutic strategy. Our study is aimed at investigating and characterizing a novel knitted titanium (Ti6Al4V) implant for the replacement of nucleus pulposus to treat early stages of chronic intervertebral disc degeneration. Specific knitted geometry of the scaffold with a porosity of 67.67 ± 0.824% was used to overcome tissue integration failures. Furthermore, to improve the wear resistance without impairing original mechanical strength, electro-polishing step was employed. Electro-polishing treatment changed a surface roughness from 15.22 ± 3.28 to 4.35 ± 0.87 µm without affecting its wettability which remained at 81.03 ± 8.5°. Subsequently, cellular responses of human mesenchymal stem cells (SCP1 cell line) and human primary chondrocytes were investigated which showed positive responses in terms of adherence and viability. Surface wettability was further enhanced to super hydrophilic nature by oxygen plasma treatment, which eventually caused substantial increase in the proliferation of SCP1 cells and primary chondrocytes. Our study implies that owing to scaffolds physicochemical and biocompatible properties, it could improve the clinical performance of nucleus pulposus replacement.

Chronic low back pain is the most common ailment among people aged 40–80 years, affecting men and women alike globally. It is a common cause of disability and one of the top ten disorders causing high socio-economic burden with a global prevalence of 22–65%[1].

Intervertebral disc degeneration has been implicated as a causative factor in chronic lower back pain, since an inability in the disc function is closely linked with degeneration of its components[1]. Till date, numerous therapeutic strategies like spinal fusion, drug treatments, physiotherapy, cell therapy, arthroplasty etc. have been developed aimed at maintaining disc function by preventing further downstream collapse and reduction of inflammatory pain[2,3]. Nevertheless the potential of these interventions in treating the chronic back pain is debated and continues to progress[4,5]. In addition, a considerable motivation of using biomaterial has been advanced, aimed at restoring the function of intervertebral disc. A number of studies have been reported on scaffolds primarily made of stainless steel, cobalt-chromium alloys, titanium based alloys, hydrogels as potential therapeutic alternatives[6,7] for such injuries. A more substantial approach through nucleus pulposus replacement[5] will necessitate as a minimal invasive technique, aiming to decrease the post-surgical risk factors. However, currently available nucleus implants have failed due to associated complications such as corrosion, inflammation, hypersensitivity, fibrous encapsulation, low fracture toughness, mismatched bone and implant modulus of elasticity, leading to revision surgery[7,8]. These factors along with patient response (poor compliance with rehabilitation), surgical techniques and implant surface characteristics results in inadequate benefit of this treatment strategy.

[1]Siegfried Weller Institute for Trauma Research at the BG Trauma Center, Eberhard Karls Universität Tübingen, Schnarrenbergstr.95, Tübingen, Germany. [2]Section Medical Material Science & Technology, University Hospital Tübingen, Ossianderstr. 2-8, Tübingen, Germany. [3]Department of Biological Sciences and Bioengineering, Indian Institute of Technology Kanpur, Kanpur, 208016, UP, India. [4]Hochschule Reutlingen, Reutlingen University, Alteburgstraße 150, Reutlingen, Germany. [5]Buck GmbH and Co.KG, Bondorf, Germany. Ashok Kumar and Andreas K. Nussler contributed equally to this work. Correspondence and requests for materials should be addressed to A.K.N. (email: andreas.nuessler@gmail.com)

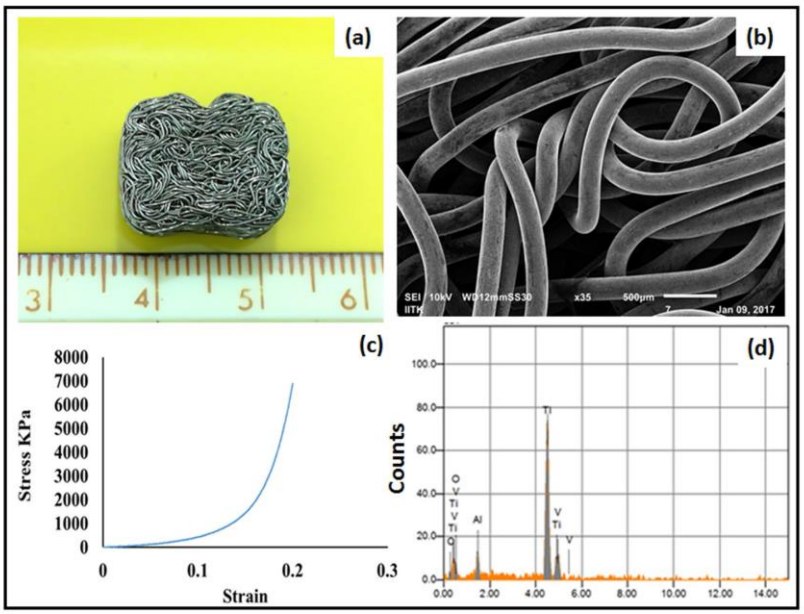

Figure 1. Physical characterization of the titanium scaffold. (**a**) 2D digital image of scaffold structure; (**b**) SEM micrograph depicting knitted scaffold microstructure; (**c**) EDX spectra of the mesh surface; (**d**) Compressive elastic modulus of the scaffold.

Thus, several modifications of these artificial implants are in progress to overcome the diminutive emergences and limitations[9]. However for a scaffold to be used in tissue engineering applications, it is essential to be biocompatible, have sufficient mechanical strength, integrate with biological tissue and should support cell proliferation[10]. Interaction between the implant and the surrounding tissue *in vivo* mainly depends, not only on the bulk properties of the implant material but also on the surface properties such as surface roughness, composition, surface energy, microstructure, porosity and the pore size[11]. Modifications in material surface physical properties persuade various cellular responses, resulting in changes of cell adhesion and proliferation. Various scaffold surface modifications are promising in terms of modulating and improving wear resistance, inducing long term stability in the host system and osseo integration[12]. Previously, Kettler *et al.*[13] in their study reported that this unique knitted titanium scaffold possessed adequate biomechanical properties and showed low migration tendency, thereby restoring the physiological axial deformability. Further, we have demonstrated that the knitted scaffold enable the cell attachment and promote cell proliferation[14]. Subsequently, in this current study we have shown for the first time the influence of oxygen plasma surface treatment towards cellular response. Earlier studies have proven that, hydrophilic implant surfaces favor the cellular response like cell adhesion and proliferation of various cell types. Further it has also been reported that the surface wettability plays a role in determining events that takes place at cell material interface and modification of surface wettability effectively enhances the biological response[15,16]. Nevertheless, the contact angles usually observed for titanium and its alloy varies between 70–90°, indicating weak hydrophilicity[15,16]. The main interest of the current study was therefore to hydrophilize the surface of knitted titanium implant for which, this plasma treatment was applied as a favorable approach to increase the wettability, thus augmenting the mesenchymal as well as primary chondrocyte cell growth. Since, introduction of this knitted titanium implant in the clinical setting necessitates further characterisation with respect to host bio-compatibility and bio-functionality, our present study consequently investigated the physio-chemical properties of the scaffold and cellular responses of human bone marrow derived mesenchymal stem cell as well as the primary chondrocytes upon surface modification by oxygen plasma treatment.

Results

Physio-chemical characterization of the scaffold. Microscopic image of the knitted scaffold revealed the mesh construct and the cross sectional view depicting the non-woven structure. Microstructure analysis using SEM, Fig. 1b illustrates the knitted wire porous architecture of the scaffold having a heterogeneous pore distribution with pore size of 150–400 μm. Surface topography determined at micro scale using SEM and optical profilometry, confirmed that electro-polished scaffold surface is comparatively smooth as that of unpolished scaffold (Fig. 2a,b) and additional, surface finish has been improved without affecting microstructures. The optical

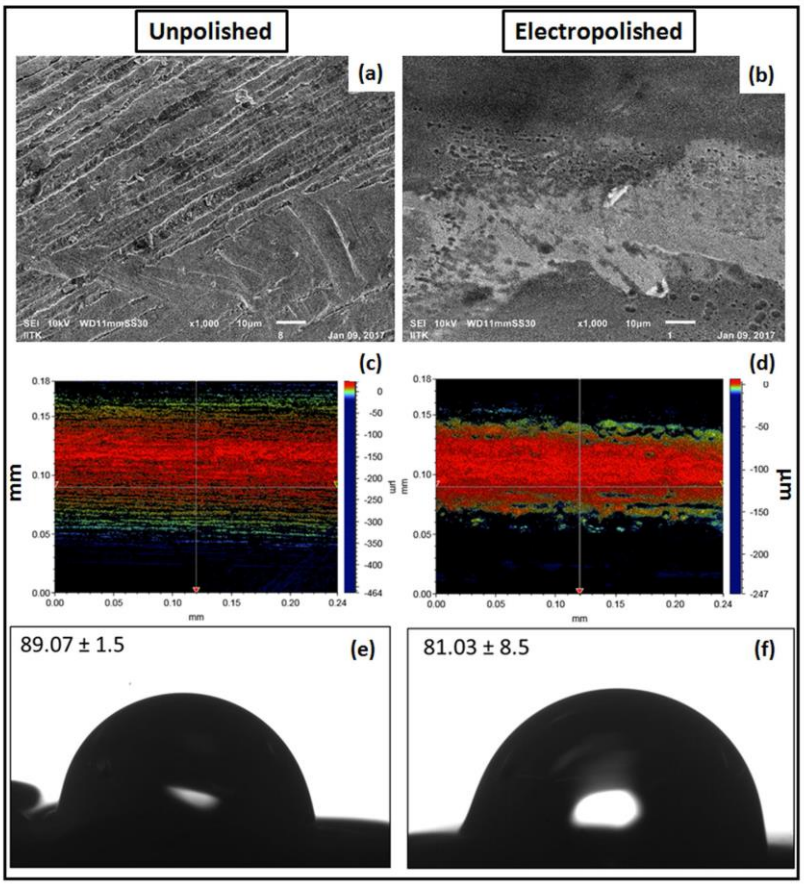

Figure 2. Surface characterization of electro-polished scaffold. (**a**,**b**) SEM image illustrating surface topography; (**c**,**d**) optical profilometry; (**e**,**f**) wettability measurements by sessile drop method; of unpolished and electro-polished scaffold respectively. For optical profilometry, surface area of 240 μm × 180 μm was scanned and the average surface roughness (Ra) was calculated. Ra value of unpolished and electro-polished scaffold was calculated to be 15.22 ± 3.28 μm and 4.35 ± 0.87 μm respectively. Subsequently, wettability measurements showed the weak hydrophilic scaffold surface property which has not affected upon electro-polishing treatment.

profilometry analysis revealed the unpolished surface has average surface roughness (Ra) of 15.22 ± 3.28 μm and the electro-polished surface has average surface roughness of 4.35 ± 0.87 μm (Fig. 2c,d). Energy dispersive X-spectroscopy (EDX) analyses of the unpolished scaffold denoted the elemental constitution mainly consisting of Ti, Al, V (Fig. 1d), which remained unchanged upon electro-polishing treatment. In addition, small traces of oxygen and nitrogen were found as a minor contamination on the scaffold surfaces, which could have originated either during manufacturing process, handling/storage or electro-polishing treatment. Surface energy and wettability are considered as the key factors playing role in cell behavior, cell material interaction and the scaffold integrity. Titanium alloy based scaffold represented weak hydrophilic surfaces; exhibiting contact angles of 83.3 ± 12.19° (Fig. 2e,f). The statistical analysis revealed that there was no considerable difference between the unpolished and electro-polished scaffold wettability (Fig. 2e,f). The observed low wettability of knitted titanium scaffold is a result of a low surface energy. Moreover, the change in surface roughness due to electro-polishing treatment didn't induce any change in wettability.

Mechanical properties of the scaffold play a crucial role in load bearing application. Compression strength of a biomaterial is therefore considered as one of the main factors. The knitted scaffold illustrated an elastic modulus of approximately 0.02 GPa (Fig. 1c), which is comparable to cancellous bone (0.01–3.0 GPa), but is too low in comparison with cortical bone (4.4–28.8 GPa) as revealed by mechanical analysis[17].

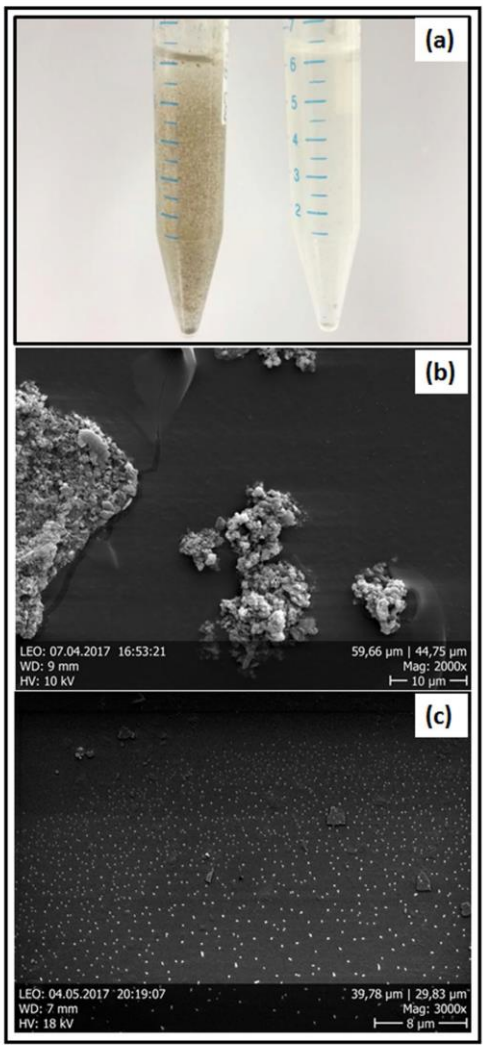

Figure 3. Wear debris particle analysis. (**a**) Digital image of unpolished (left) and electro-polished (right) wear debris particles; (**b**,**c**) SEM images representing morphology and size based distribution of wear debris particles of unpolished and electro-polished scaffold.

Wear debris particle characterization. The morphologies of the titanium debris showed considerable differences, both in size and shape of the particles. There are two precise differently sized particle groups in the unpolished scaffold based probe (Fig. 3b) ranging from 10–25 µm and sub-micrometer, contrarily there are impartial sub-micron ranged particles in electro-polished scaffold based probe (Fig. 3c). This was already noticeable with the high turbidity of the abrasion solution (Fig. 3a). The particles from unpolished scaffold based probe are very robust and not just clusters of small particles as we initially thought. Since, ultra-sonication as well did not affect these particles thus; we believe that these are solid particles (Fig. 3b). In addition, the particles are far from being spherically shaped. Subsequently, we measured all sort of shape descriptors since the titanium wear particle shape is rather anisotropic.

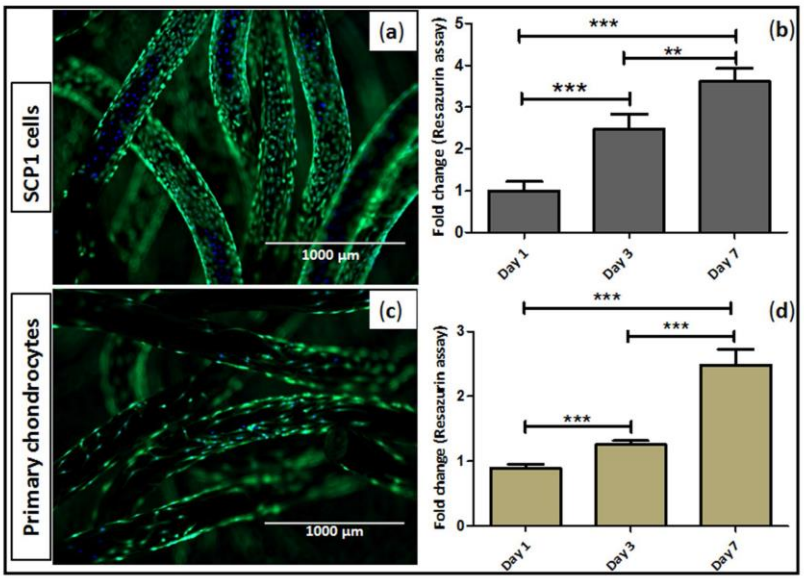

Figure 4. Cell viability and proliferation on the knitted titanium scaffold. (**a**,**c**) Live dead staining - viable cells; calcein-AM (green) and nucleus; Hoechst 33342 (blue) staining of SCP1 cell and human primary chondrocytes upon seeded on the scaffold respectively; (**b**,**d**) Resazurin conversion – indirect assay for cell proliferation of SCP1 cells and human primary chondrocytes respectively. Data represented as mean ± SEM; analyzed by Mann Whitney test. $P \leq 0.05$ was considered to be minimum level of significance. *$p \leq 0.05$, **$p \leq 0.01$, ***$p \leq 0.001$. Scale bar = 1000 µm.

Assessment of cell-material interaction. The physical characterization of the scaffold was followed by cytocompatibility assessment *in vitro*, where cells were cultured on scaffolds and the cell material interactions like cell adhesion, cell spreading and cell proliferation were observed. The cell culture studies indicated that the cells were able to adhere and survive on the scaffold in spite of low initial cell attachment at day 1. Furthermore, day 3 following cell seeding, we observed a noteworthy increase in the cell growth on the scaffolds. Since electro-polished scaffold exhibited considerably increased wear resistance, we decided to use this scaffold for further cell interaction studies. Cell viability was qualitatively visualized using live-dead assay, where the nucleus was stained blue with Hoechst and cytoplasm stained green with calcein-AM (Fig. 4a,c). Additionally, cell proliferation of human bone marrow derived mesenchymal stem cells as well as of human primary chondrocytes was determined by resazurin assay for cell mitochondrial activity. When the fluorescence was normalized with those on day 1, significant fold change increase in the fluorescence intensity and subsequent cell number was observed, demonstrating the bio-functional potential of the scaffold (Fig. 4b,d).

Cell adhesion and spreading on the scaffolds was determined by staining cells with phalloidin actin fibers (red fluorescence) and nucleus (blue fluorescence) at day-3 and day-7 post seeding. It was evident that, cells were effusively spread with extended fliopodia and cytoplasmic protrusions at day 7. In majority cells, orientation was found to be longitudinal along the direction of the knitted wires (Fig. 5). These results further confirm the cytocompatibility of the scaffolds.

Effect of scaffold surface modification by plasma treatment on the wettability. In order to enhance the cell material interactions, we further modified the electro polished scaffold surface by oxygen plasma treatment. Tensiometric measurements showed shifts to increased wetting tension values (force/length) likewise during immersion (wetting) as well as to a minor degree during emersion (de-wetting) after the plasma treatment (Fig. 6e). As a result of these shifts, hysteresis of the force loops was diminished. Advancing as well as receding contact angles were lowered in consequence to plasma treatments, indicating an overall change towards hydrophilicity. Mean (±standard deviation) advancing contact angles decreased from 72 ± 14° to 52 ± 14°, receding angles from 34 ± 4° to 25 ± 8°.

Whereas the Wilhelmy experiments yielded contact angle data of the pure material surfaces, the sessile drop experiments characterized the wetting behavior of a heterogenic system, *i.e.*; the material/air composite surfaces. Static drops set stable on untreated scaffold surfaces showing contact angles of 83.3 ± 12.19° (Fig. 6, see also Fig. 2). In contrast, the experiments clearly indicated water drops being spontaneously infiltrated into the plasma treated scaffold (Fig. 6d).

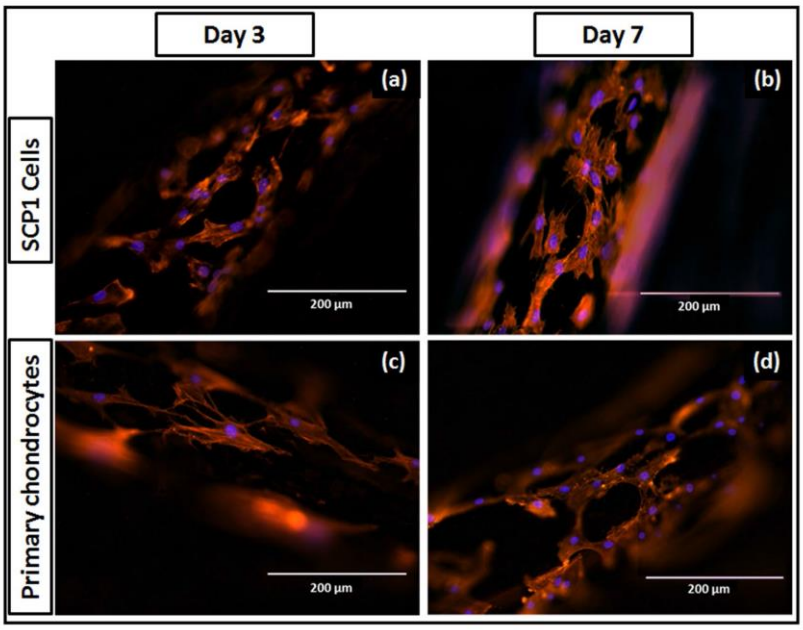

Figure 5. Cell spreading pattern on the knitted titanium scaffold. Image represents actin-phalloidin; alexa 555 (red) and nucleus; Hoechst 33342 (blue) fluorescent staining of (**a**,**b**) SCP1 cells on the scaffold at day 3 and 7 respectively; (**c**,**d**) human primary chondrocytes on the scaffold at day 3 and 7 respectively. Scale bar = 200 µm.

Effect of plasma treatment on the cellular response. To elucidate the effect of scaffold pretreatment with oxygen plasma on the cellular response, cell viability and proliferation were assessed post treatment. Figure 7 represents viable cells at day 3; calcein-AM (green fluorescence) and nucleus (blue fluorescence) staining as indicated in plasma treatment and control group, where more cells were evident on plasma treated scaffolds compare to non-treated scaffolds. There was no substantial change in terms of cell adhesion, however cell growth was found to be enhanced upon plasma treatment (Fig. 7c,f). Significant fold increase was observed in the fluorescence intensity and subsequent cell number at day 3 and 7 when it normalized with those on day 1. Additionally, significant difference between the two groups was observed (Fig. 7c,f). SCP1 cell proliferation at day 7 was almost similar in both controls and plasma treated scaffolds, whereas primary chondrocyte cell growth was higher upon plasma treatment; showing a positive effect of oxygen based plasma treatment. Furthermore, we confirmed that the plasma treatment had an influence on the cell morphology as the cells appeared more spread out with longer extensions following actin (red fluorescence) and nuclear staining (blue fluorescence) as observed on plasma treated scaffolds (Fig. 8).

Discussion

Titanium and its alloys are well established in the biomedical field due to their worthy mechanical properties, biocompatibility and low immunogenicity[6]. To further pursue this goal, we used titanium scaffold with a unique knitted geometry simulating the porous structure, precisely to create suitable conditions for cell attachment and tissue ingrowth. Ideally the scaffold should retain their dimensions, integrity and strength along with the biological integrity during the process of wound healing/tissue regeneration after the implantation[10]. One of the critical reasons for implant failure is the mobility of the implant leading to local abrasion and immune reaction[18–20]. Therefore the manufacturing procedure and surface modifications have a definite impact on the quality, performance and integrity of the implant *in vivo*[12,21]. In a previous study, Kettler *et al.* showed that cyclic loading of this knitted titanium scaffold did not cause implant expulsion. A potential advantage of using porous titanium knitted scaffold was its elasticity that in the range of that of cancellous bone. This upon mismatch possibly leads to stress shielding around the scaffold causing bone atrophy and induction of local inflammation which ultimately results in implant failure. Nevertheless, with respect to biomechanics, one of the most vital factors to be considered is wear and corrosion resistance. Wear debris particles have been reported to have role to induce toxicity, especially particle mediated inflammation triggers the granuloma cascade, necrosis and/or fibrosis all together causing the aseptic loosening[18,22] and therefore the excessive amount of the wear debris particles within the host system can cause adverse cellular host reactions. The intensity of local inflammation mainly depends on debris characteristics

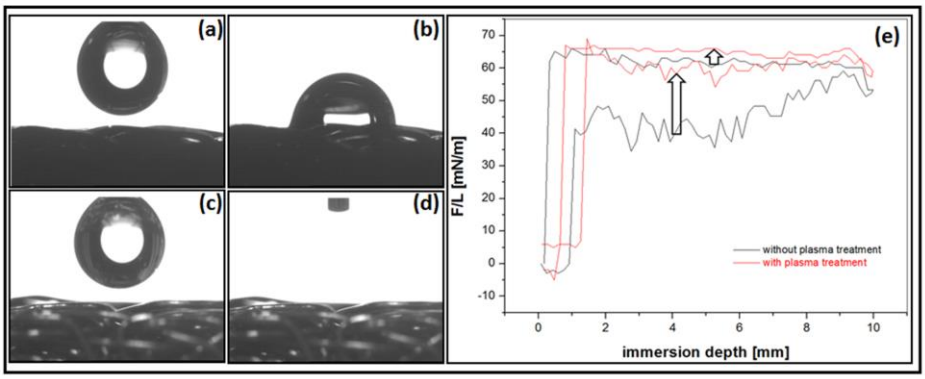

Figure 6. Effect of plasma treatment on the wettability. (**a**) Drop before application on the untreated scaffold by drop shape analysis system; (**b**) the drop after set from the needle onto the untreated scaffold surface; (**c**) drop before application on plasma treated scaffold by drop shape analysis system; (**d**) drop after set onto a plasma treated scaffold was immediately infiltrated into the scaffold; (**e**) tensiometric hysteresis loops of plasma treated and untreated electro-polished wires. The left arrow indicates shifts towards increased wetting tension values F/L of the advancing (adv) and the right arrow of the receding (rec) curves due to plasma treatment.

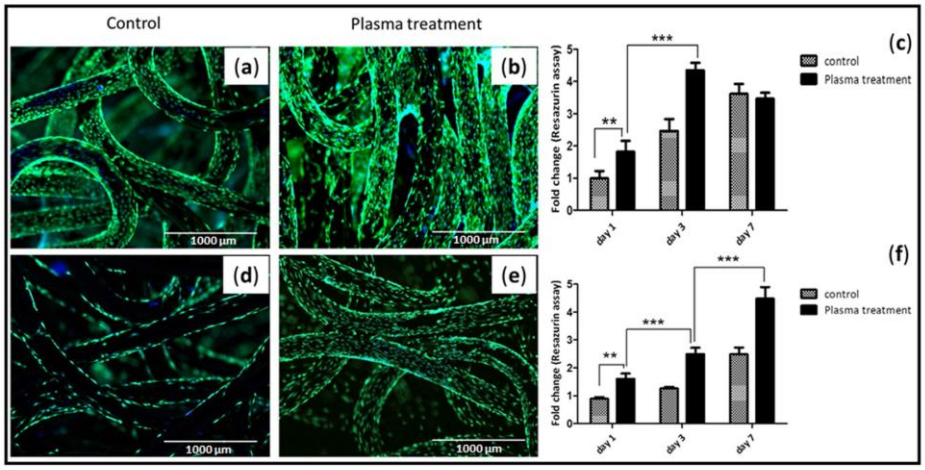

Figure 7. Effect of plasma treatment on cell viability and proliferation. Live dead staining - viable cells; calcein-AM (green) and nucleus; Hoechst 33342 (blue) staining of SCP1 cell and human primary chondrocytes upon seeded on the (**a**,**d**) non-plasma treated scaffold; (**b**,**e**) oxygen plasma treated scaffold respectively. Scale bar = 1000 µm. More cells are evident on the oxygen plasma treated scaffolds compare to the non-treated scaffolds; (**c**,**f**) Resazurin conversion – indirect assay for cell proliferation of SCP1 cells and human primary chondrocytes respectively. Fold increase was significant upon oxygen plasma treatment. Data represented as mean ± SEM; analyzed by Mann Whitney test. $P \leq 0.05$ was considered to be minimum level of significance. $^{*}P \leq 0.05$, $^{**}p \leq 0.01$, $^{***}P \leq 0.001$.

such as: particle load (size and volume) and chemical reactivity. Wear debris prone implant failure is prime suspect in the field of arthroplasty as attrition evoking immune reaction cannot be omitted[19]. In our study, the purpose of explicitly considering the electro-polished knitted scaffold was to emphasize the fact of wear resistant material goods. Moreover, the purpose of the wear debris analysis was not the elucidation of such body reactions, but rather to obtain a better understanding of the morphology of titanium wear particles. This information may have future implications for the design and adapting of the scaffold employed in musculoskeletal implants.

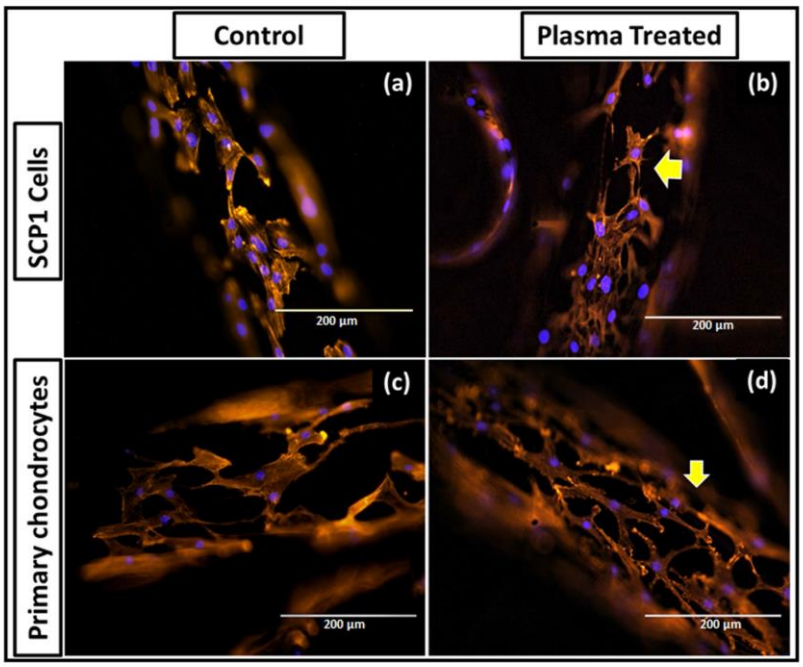

Figure 8. Effect of plasma treatment on cell spreading. Actin-Phalloidin; alexa 555 (red) and nucleus; Hoechst 33342 (blue) fluorescent stained SCP1 cells day 3 post seeded on the non-plasma treated (**a**), oxygen plasma treated scaffold (**b**); human primary chondrocytes seeded on the non-plasma treated (**c**), oxygen plasma treated scaffold (**d**). Scale bar = 200 µm.

Consequently, electro-polishing resulted in a substantial reduction of overall abrasion production which can ensure prolonged functional longevity of the scaffold *in vivo*.

Additionally, the success of an implant also depends on its biocompatibility which maintains its integration with the surrounding tissue and therefore will define its functionality *in vivo*[21]. In order to mimic the appropriate conditions, the human bone marrow derived mesenchymal stem cells and human primary chondrocytes were used for all experiments. As an early cell response towards the implant site, cell adhesion and cell proliferation were studied considering the scaffold surface characteristics *i.e.* surface roughness and wettability, as the desired physical properties of the scaffold are vital for its effective incorporation on the system. Owen *et al.* has described in earlier report that it is possible to modulate specific cell behavior by changing the surface topography[23]. Previously it has been reported that the optimum pore size range of 200–500 µm is suitable for tissue ingrowth[24]. However, there is no precise specification for optimal pore size that has been proved. He *et al.* earlier reported that the wire diameter influences the pore size[25]. Based on these reports, the scaffold used in our study presumed to have a favorable pore size distribution which can promote tissue in growth. Since it is possible that cell behavior could vary with pore size variation, in our study, we maintained uniform defined geometry of the porous knitted scaffold with a pore size of 150–400 µm and porosity roughly about 67.67 ± 0.824%, aiming to evaluate the scaffold cytocompatibility.

In order to obtain a realistic biomechanics prediction of *in vivo* situation, stress distribution within tissue–implant interface and its physio-chemical characteristics needs to be further analyzed. Scaffold surface properties such as surface roughness, composition, topography are known to influence the nature of cell adhesion which thereby directs the process of cell proliferation and differentiation. The role of surface roughness in deciding cell behavior is still debatable. A study by Hallab *et al.* shows that the surface roughness and the surface energy play crucial roles during initial cell response at the cell-material interface. Also, changes in the surface topography and increase in the roughness decreases the cell proliferation[26]. Surface energy of the material on contrary is proved to be a prime factor than the surface roughness in regulating the cell adhesion on the material surface[27]. Moreover in our study, the decrease in surface roughness upon electro-polishing treatment did not play any major role in initial cell attachment and neither affected the cell growth rate. Based on the obtained results, change in the scaffold surface roughness as observed in the study seems to have negligible effect on the cell proliferation which supports the possibility that the surface energy is a dominating factor in promoting cell growth[27]. Nonetheless,

surface roughness is highly required from a biomechanics prospective for a long term function of load bearing implant as it limits the micro crack formation and leads to better load distribution[28]. The host reaction towards the scaffold is mainly dictated by the adsorbed proteins during initial contact with body fluids. Since this reaction is preferential, it is influenced by the wide range of scaffold physical properties like surface roughness, topography, creating a porous material with high interconnectivity, wettability etc. For example, smooth and double acid-etched micro rough TiAl6V4 surfaces showed contact angles of 62° and 57°, respectively[16]. Moreover, surface modifications aimed at improving its bioactivity can be achieved by modification of these physical parameters. Therefore, desire scaffold structure and surface modifications are advantageous with respect to the site of scaffold in order to contribute the clinical success rate.

From clinical aspect, this study was aimed at investigating the biocompatibility of the proposed knitted titanium scaffold. Concerning the load bearing applications, targeted implant prerequisites to get stabilized first for which cell reaction towards the material surface is an important factor of selection. From the economic trait, the sooner tissue integration the better is the healing process. However, it is yet to be clear from clinical aspect that what all parameters are prime objects for faster healing. Therefore, it is important to develop scaffolds with appropriate surface properties. Here it could be proposed that, surface modifications should be mainly based on the site of implant within the body *in vivo*. In musculoskeletal prosthetics, a hydrophilic surface favors the tissue integration[29].

Surface wettability is another important factor that affects the extent of cellular responses on the implant surface. Hydrophilization and sterilization of biomaterial surfaces due to radio-frequency glow discharge (RFGD) plasma treatment is well known phenomena and occur due to cleaning of contaminants and by achieving of a high energy state[30]. The foremost intention of the surface modification by plasma treatment in our study was to improve the scaffold wettability and ultimately modulate cell attachment and proliferation of SCP1 cells and primary chondrocytes. Importantly, plasma treatment showed a positive influence on cell behavior in terms of cell viability, proliferation and the morphology; thus indicating a crucial role in mediating the cell response towards the scaffold surface. Further, studies on cell differentiation could be supportive for further understanding of the observed cell behavior with respect to SCP1 cells.

In summary, we have explored the potential of knitted titanium to allow viability and proliferation of adherent-cells. It has further shown that cells response with respect to viability and proliferation indeed remain unaffected upon electro-polishing treatment. This suggests that it is the wettability and not the surface roughness which could be the main cause for modulating the response at cell material interaction. Using oxygen plasma treatment, we have further demonstrated that the proliferation of the adherent-cells on the scaffold has been elevated as compared to non-treated conditions. Though our results shows *in vitro* cytocompatibility potential of knitted titanium scaffold, it needs to be verified further through *in vivo* studies to project it as a potential treatment option in the clinical settings.

Conclusion

This *in vitro* study demonstrated the potential of the knitted titanium scaffold as a possible replacement of intervertebral nucleus pulposus, while revealing some of the weaknesses especially because of the lack *in vivo* outcomes. Nonetheless, these results pave the way for establishing knitted titanium scaffold as an alternative solution for musculoskeletal tissue engineering, involving cell-material interaction. Combination of oxygen plasma treatment considerably affects cell proliferation compared to non-hydrophilized electro-polished scaffolds alone and thus seems to be a suitable additional surface modification for better tissue integration. It can be concluded that knitted titanium wire scaffold has shown a promising potential intervertebral nucleus substitute and can be used efficiently with oxygen plasma treatment to improve the tissue integration process.

Materials/Methods

Knitted titanium scaffold and surface modification. Knitted titanium scaffold was prepared as previously reported[31]. Briefly, medical grade titanium alloy (Ti6Al4V) wires with diameter of 0.25 mm were knitted to produce a mesh like cuboidal disk structure with 5 mm height and 14 × 11 mm dimension (Buck Co & GmbH, Bondorf, Germany), volumetric porosity of 67.67 ± 0.824%, and density of 0.75 mg/cm^3 and used in this study. Electro-polishing of the scaffolds was used to generate smooth wear resistant surface with defined finish. Scaffolds were cleaned with 1% Triton-X followed by ultrasonication in reagent grade acetone, iso-propanol, ethanol and distilled water[32] respectively for 15 min to remove impurities generated either during manufacture or due to electro-polishing. The scaffolds were then dried at room temperature, followed by sterilization at 121 °C and 15 PSI for 20 min before use.

Electro-polished scaffolds were further processed by oxygen plasma treatment, to yield hydrophillized surfaces. Single wires as well as scaffolds were treated in a low pressure Dentaplas PC plasma system (Diener electronic, Ebhausen, Germany). After generation of 0.3 mbar vacuum within 2 min, 160 W plasma was ignited at an oxygen flow of 3 sccm and applied for 15 min at 40 °C.

Scanning Electron Microscopy (SEM). Surface morphology of the knitted scaffold was determined using SEM (JEOL, JSM-7100F, Japan) after gold sputter coating. Images were recorded at an accelerating voltage of 15 kV. The surface roughness of unpolished and electro-polished scaffold was evaluated at 15,000× magnification. Chemical analysis of the material was studied by energy dispersive X-ray spectroscopy (EDX). Survey spectra were collected at pass energy of 80 eV.

All the SEM pictures were then used further to determine the pore size. The Image J software was used (https://imagej.nih.gov/ij/). The software was calibrated using the micron scale bar of each picture. An average pore size was determined by measuring the diameter of 50 different pores. Pores were identified as areas of void space bounded by fibers on all sides at or near the same depth of field, while their long and short diagonal axes were measured together to serve as their pore size range.

Optical profilometry. The effect of electro-polishing treatment on the scaffold surface roughness was analyzed using non-contact profilometry (Contour GT-K, Bruker, USA). Breifly, electro-polished and unpolished scaffold surfaces were scanned using 20× objective, area of 240 µm × 180 µm, and calculating the average roughness (Ra) of the surface using Vision-64 (Bruker) surface analysis software.

Sessile Drop Contact Angle Measurement. The contact angle measurements of unpolished and electro-polished scaffold were performed using surface goniometer (OCA 15 plus, Data-Physics Instrument GmbH, Germany) equipped with automatic drop application and contact angle evaluation.

Wettability of non-treated and plasma-treated electro-polished scaffolds was analyzed by automatic drop application and contact angle evaluation by a drop shape analysis system (DSA 10-Mk2, Kruess, Germany). Water droplets (2 µl) were deposited on the surfaces and the drop shape and infiltration behavior was recorded by a video camera (1 frame/s). If not infiltrated, contact angles of the sessile drops were measured 20 seconds after the initial surface contact analyzed from drop shapes by applying the circular segment method (circle fitting) implemented in the Kruess software (Kruess, Germany).

Dynamic Contact Angle Measurement. Dynamic wetting of the plasma-treated and untreated electro-polished single wires was investigated tensiometrically (KSV Instruments Ltd., Finland) using Wilhelmy balance method[15]. Prior to measurement in water, its surface tension was determined with a standardized, fully wettable platinum plate (39.4 mm wetted length; 19.6 mm width; 0.1 mm thickness). The samples were immersed and emersed with speed of 10 mm/min for one complete cycle with an immersion depth of 10 mm. From the recorded force loops, dynamic advancing (θadv) and receding (θrec) contact angles were calculated by extrapolating the corresponding immersion and emersion force/length-branches of the hysteresis loops to the zero immersion depth according to the following equation:

$$F = \gamma L \cos\theta \tag{1}$$

where γ: surface tension of the liquid, L: perimeter (wetted length) of the wires, and F: force at zero immersion depth where buoyancy is not apparent.

Compression analysis. The compression of scaffolds with 5 mm height and 14 × 11 mm dimension were analyzed[33] using uniaxial compression test by a mechanical tester (BiSS Ltd, India). The scaffold was placed between the two arms of load frame and compressed until mechanical failure with a speed of 0.5 mm/min. The applied force and displacement were continuously recorded during testing. The Young's modulus was calculated using the formula:

$$E = (F/A)/(\Delta l/l)\ \text{kPa} \tag{2}$$

where E: Young's modulus, F: applied force, A: cross-sectional area of the scaffold, l: initial length of the test sample, and Δl: change in length under the compressive force.

Porosity. The porosity of the knitted titanium scaffold was directly obtained by mass–volume calculation method[34] using following equation:

$$P = 1 - M/(V \times \rho s) \times 100 \tag{3}$$

where P: porosity; M: weight of the scaffold; V: volume of the scaffold; ρs: density of the scaffold.

Wear debris particle analysis. The wear test of the scaffold was done by Buck co & GmbH. During the test particles were collected in suitable lubricant, which then analysed further. Wear debris particle morphology and size was studied using SEM (Zeiss DSM962, Germany). Briefly, samples were prepared by precipitating the particles upon centrifugation at 10,000 rpm for 40 min (to remove the traces of lubricant) following resuspension in 70% ethanol. Spin coating was performed to deposit a uniform thin particle layer on a piece of a Si wafer (70 rps; t = 20 s; V = 100 µl, K.L.M. Spin Coater, Germany). To avoid agglomeration, the suspensions were sonicated for 10 min prior to spin coating process. Upon solvent evaporation following coating, the samples were sputter coated with gold.

Cell culture. Human immortalized bone marrow derived mesenchymal stem cell line (SCP1 cells)[35] was cultured in α-MEM (minimal essential medium; GIBCO, Germany) containing 1 g/L glucose supplemented with 10% FBS (fetal bovine serum; GIBCO, Germany) and 1% penicillin/streptomycin (Sigma, Germany) 10,000 units/ml 10 mg/ml respectively (P/S) in a humidified incubator (37 °C and 5% CO_2).

Human primary chondrocytes were isolated[36] from the donor samples (BG Klinik, Tübingen) after complete ethical clearance (338/2015BO2). Briefly, cartilage tissue was removed from the femoral condyles and transferred to Dulbecco's modified essential medium (DMEM)/F12 (1:1) medium containing 25 µg/ml Fungizone® Antimycotic and 1% P/S, Phosphitan: analogue of ascorbic acid (25 mg/mL; Sigma, Germany). The tissue was cut into small pieces, washed with phosphate-buffered saline (DPBS) and digested with collagenase II (GIBCO, Darmstadt, Germany) 1500 U/ml in chondrocyte medium for 16–24 hr at 37 °C with agitation (100–120 rpm). The suspension was passed through 70 µm cell strainer, centrifuged, resuspended in chondrocyte medium and incubated at 37 °C with 5% CO_2. At the time of seeding, sterile scaffolds were placed into each well of 24-well plates, pre-conditioned with media for 30 min; after which medium was aspirated. Cells were trypsinized (Trypsin-EDTA; 0.05%/0.02%, Sigma, Germany), centrifuged and resuspended to achieve a seeding density of 2×10^5 cells per scaffold. Cells seeded scaffold kept in incubator initially for 3 hr to allow cell attachment and thereafter, 700 µl of additional medium was added to each well and incubated further.

Resazurin assay. Cell proliferation was calculated using resazurin conversion assay[37]. Briefly, cells seeded scaffolds were incubated with a 1:10 volume of sterile resazurin (Sigma, Germany) working solution (0.025% in DPBS) at 37 °C for 30 min. Resulting fluorescence (ex/em = 540/590 nm) was then measured spectroscopically (BMG, Offenburg, Germany) and corrected to background control. Fluorescence value directly correlates with a cell number. Standard curve was generated which was then used to calculate the cell proliferation.

Live-dead staining. Cell viability was determined at day 3 post seeded by intracellular esterase activity using calcein-AM and ethidium homodimer to determine dead cells[14]. Briefly, cells were stained with 2 µM calcein-AM (Sigma, Germany), 4 µM ethidium homodimer (Sigma, Germany) and Hoechst 33342 (1:1000 in DPBS, Sigma, Germany) at room temperature (RT) for 30 min following DPBS wash. Images were taken using epifluorescence microscopy (Life technologies, Darmstadt, Germany).

Cell Morphology. Cells seeded scaffolds were washed with DPBS and then cells were fixed using 4% paraformaldehyde for 10 min at RT after which cell permeabilisation with 0.25% Triton-X 100 solution (Sigma, Germany) for 20 min at RT. 1% BSA (Bovine Serum Albumin, Sigma, Germany) blocking solution was added and incubated at RT for 1 hr. Further, it stained with Alexa Fluor® 555 Phalloidin (1:500, Santa Cruz, Germany) and Hoechst 33342 (1:1000) for actin fibers and cell nuclei respectively and incubated in dark for 45 min. Images were captured using epifluorescence microscopy.

Statistical analysis. Analysis was done using GraphPad Prism 5.0 software (El Camino Real, CA, USA) and PAST.exe (http://folk.uio.no/ohammer/past/index). Statistical significance of all experiments that were done in triplicates was analyzed using the Kruskal-Wallis H-test followed by a Dunn's test and Mann Whitney test. Minimum level of significance: $P \leq 0.05$. *$p \leq 0.05$, **$p \leq 0.01$, ***$p \leq 0.001$.

References

1. Hoy, D. *et al.* A systematic review of the global prevalence of low back pain. *Arthritis and rheumatism* **64**, 2028–2037, https://doi.org/10.1002/art.34347 (2012).
2. Urban, J. P. & Roberts, S. Degeneration of the intervertebral disc. *Arthritis Res Ther* **5**, 120–130 (2003).
3. Adams, M. A. & Roughley, P. J. What is intervertebral disc degeneration, and what causes it? *Spine* **31**, 2151–2161, https://doi.org/10.1097/01.brs.0000231761.73859.2c (2006).
4. Huang, R. C., Girardi, F. P., Lim, M. R. & Cammisa, F. P. Jr. Advantages and disadvantages of nonfusion technology in spine surgery. *The Orthopedic clinics of North America* **36**, 263–269, https://doi.org/10.1016/j.ocl.2005.02.006 (2005).
5. Schizas, C., Kulik, G. & Kosmopoulos, V. Disc degeneration: current surgical options. *Eur Cell Mater* **20**, 306–315 (2010).
6. Li, Y. H. *et al.* New Developments of Ti-Based Alloys for Biomedical Applications. *Materials* **7**, 1709–1800, https://doi.org/10.3390/ma7031709 (2014).
7. Reeks, J. & Liang, H. Materials and Their Failure Mechanisms in Total Disc Replacement. *Lubricants* **3**, 346–364 (2015).
8. Lewis, G. Nucleus pulposus replacement and regeneration/repair technologies: present status and future prospects. *Journal of biomedical materials research. Part B, Applied biomaterials* **100**, 1702–1720, https://doi.org/10.1002/jbm.b.32712 (2012).
9. Bagno, A. & Di Bello, C. Surface treatments and roughness properties of Ti-based biomaterials. *J Mater Sci-Mater M* **15**, 935–949, https://doi.org/10.1023/B:Jmsm.0000042679.28493.7f (2004).
10. Zohora, F. T. & Azim, A. Y. M. A. Biomaterials as porous scaffolds for tissue engineering applications: A review. *European Scientific Journal* **10** (2014).
11. Chang, H. I. & Wang, Y. Cell Responses to Surface and Architecture of Tissue Engineering Scaffolds. *Regenerative Medicine and Tissue Engineering - Cells and Biomaterials*, 569–588, https://doi.org/10.5772/837 (2011).
12. Wysocki, B. *et al.* Post Processing and Biological Evaluation of the Titanium Scaffolds for Bone Tissue Engineering. *Materials* **9**, https://doi.org/10.3390/Ma9030197 (2016).
13. Kettler, A., Kaps, H. P., Haegele, B. & Wilke, H. J. Biomechanical behavior of a new nucleus prosthesis made of knitted titanium filaments. *SAS journal* **1**, 125–130, https://doi.org/10.1016/SASJ-2007-0106-RR (2007).
14. Tendulkar, G. *et al.* Imaging Cell Viability on Non-transparent Scaffolds—Using the Example of a Novel Knitted Titanium Implant. *JoVE (Journal of Visualized Experiments)*, e54537–e54537 (2016).
15. Rupp, F. *et al.* A review on the wettability of dental implant surfaces I: theoretical and experimental aspects. *Acta biomaterialia* **10**, 2894–2906, https://doi.org/10.1016/j.actbio.2014.02.040 (2014).
16. Gittens, R. A. *et al.* A review on the wettability of dental implant surfaces II: Biological and clinical aspects. *Acta biomaterialia* **10**, 2907–2918, https://doi.org/10.1016/j.actbio.2014.03.032 (2014).
17. Geetha, M., Singh, A., Asokamani, R. & Gogia, A. Ti based biomaterials, the ultimate choice for orthopaedic implants–a review. *Progress in materials science* **54**, 397–425 (2009).
18. Hallab, N. J., Cunningham, B. W. & Jacobs, J. J. Spinal implant debris-induced osteolysis. *Spine* **28**, S125–138 (2003).
19. Bitar, D. & Parvizi, J. Biological response to prosthetic debris. *World journal of orthopedics* **6**, 172–189, https://doi.org/10.5312/wjo.v6.i2.172 (2015).
20. Hussein, M. A., Mohammed, A. S. & Al-Aqeeli, N. Wear Characteristics of Metallic Biomaterials: A Review. *Materials* **8**, 2749–2768, https://doi.org/10.3390/ma8052749 (2015).
21. Wieding, J., Jonitz, A. & Bader, R. The Effect of Structural Design on Mechanical Properties and Cellular Response of Additive Manufactured Titanium Scaffolds. *Materials* **5**, 1336–1347, https://doi.org/10.3390/ma5081336 (2012).
22. Pham, M. H., Mehta, V. A., Tuchman, A. & Hsieh, P. C. Material Science in Cervical Total Disc Replacement. *Biomed Res Int*, https://doi.org/10.1155/2015/719123 (2015).
23. Owen, G. R., Jackson, J., Chehroudi, B., Burt, H. & Brunette, D. M. A PLGA membrane controlling cell behaviour for promoting tissue regeneration. *Biomaterials* **26**, 7447–7456, https://doi.org/10.1016/j.biomaterials.2005.05.055 (2005).
24. Loh, Q. L. & Choong, C. Three-dimensional scaffolds for tissue engineering applications: role of porosity and pore size. *Tissue engineering. Part B, Reviews* **19**, 485–502, https://doi.org/10.1089/ten.TEB.2012.0437 (2013).
25. Cheng, M. Q. *et al.* A novel open-porous magnesium scaffold with controllable microstructures and properties for bone regeneration. *Sci Rep* **6**, 24134, https://doi.org/10.1038/srep24134 (2016).
26. Alves, N. M., Pashkuleva, I., Reis, R. L. & Mano, J. F. Controlling cell behavior through the design of polymer surfaces. *Small* **6**, 2208–2220 (2010).
27. Feller, L. *et al.* Cellular Responses Evoked by Different Surface Characteristics of Intraosseous Titanium Implants. *Biomed Res Int*, https://doi.org/10.1155/2015/171945 (2015).
28. Wiskott, H. & Belser, U. C. Lack of integration of smooth titanium surfaces: a working hypothesis based on strains generated in the surrounding bone. *Clin Oral Implan Res* **10**, 429–444 (1999).

29. Chan, B. P. & Leong, K. W. Scaffolding in tissue engineering: general approaches and tissue-specific considerations. *Eur Spine J* **17**(Suppl 4), 467–479, https://doi.org/10.1007/s00586-008-0745-3 (2008).
30. Baier, R. E. *et al.* Degradative Effects of Conventional Steam Sterilization on Biomaterial Surfaces. *Biomaterials* **3**, 241–245, https://doi.org/10.1016/0142-9612(82)90027-8 (1982).
31. Buck, A. E. & Kaps, H. P. Inventors; Buck GmbH & Co. KG, assignee. Implant for surgical use in humans or vertebrates. United States patent US 8,728,164. May 20 (2014).
32. Park, J. H. *et al.* Effect of cleaning and sterilization on titanium implant surface properties and cellular response. *Acta biomaterialia* **8**, 1966–1975 (2012).
33. Kumari, J., Karande, A. A. & Kumar, A. Combined Effect of Cryogel Matrix and Temperature-Reversible Soluble–Insoluble Polymer for the Development of *in Vitro* Human Liver Tissue. *ACS applied materials & interfaces* **8**, 264–277 (2015).
34. He, G., Liu, P. & Tan, Q. Porous titanium materials with entangled wire structure for load-bearing biomedical applications. *Journal of the mechanical behavior of biomedical materials* **5**, 16–31, https://doi.org/10.1016/j.jmbbm.2011.09.016 (2012).
35. Ehnert, S. *et al.* TGF-beta(1) As Possible Link between Loss of Bone Mineral Density and Chronic Inflammation. *Plos One* **5**, https://doi.org/10.1371/journal.pone.0014073 (2010).
36. Aurich, M. *et al.* Histological and cell biological characterization of dissected cartilage fragments in human osteochondritis dissecans of the femoral condyle. *Archives of Orthopaedic and Trauma Surgery* **126**, 606–614, https://doi.org/10.1007/s00402-006-0125-6 (2006).
37. Sreekumar, V. *et al.* BMP9 a possible alternative drug for the recently withdrawn BMP7? New perspectives for (re-)implementation by personalized medicine. *Archives of Toxicology* **91**, 1353–1366, https://doi.org/10.1007/s00204-016-1796-6 (2017).

Acknowledgements

Project is partially funded by Zentrales Innovationsprogramm Mittelstand (ZIM) des Bundesministeriums für Wirtschaft und Energie –KF3010902AJ4. The authors thankfully acknowledge Ingrid Stephan for her technical assistance with wettability measurements, and Diener electronics for providing the plasma equipment. We acknowledge support by Deutsche Forschungsgemeinschaft and Open Access Publishing Fund of University of Tübingen.

Author Contributions

We would like to thank all the authors who contributed to the study. Conceived and designed the experiments: G.T., A.B. sen., A.B. jun., H.P.K., A.K.N. Performed the experiments: G.T., A.K.T., K.A. Supervised the study: V.S., R.K., J.G., A.K., A.K.N. Analysed the data: G.T., A.K.T., F.R., R.K. Wrote the manuscript: G.T., V.S., F.R. Critically revised the manuscript and gave important intellectual input: A.K.N., A.K., J.G., R.K., K.A., A.K.T., F.R., V.S., G.T. All authors have given final approval of the version to be published.

Additional Information

Competing Interests: The authors declare that they have no competing interests.

Publisher's note: Springer Nature remains neutral with regard to jurisdictional claims in published maps and institutional affiliations.

CHAPTER 4

Publication 3-

Tendulkar G, Ehnert S, Sreekumar V, Chen T, Kaps H-P, Golombek S, Wendel H-P, Nussler AK, Avci-Adali M: **Exogenous delivery of Link N mRNA into chondrocytes and MSCs – the potential role in increasing anabolic response**, *International Journal of Molecular Sciences*, 2018 (submitted).

3.3 Synopsis:

Biomaterials have been routinely used into the IVD via minimal invasive procedures. In order to improve the effectiveness, they are commonly used as cell carriers and / or together with bioactive agents such as; growth factors (Fosgerau and Hoffmann, 2015; Melrose, 2016). Encapsulation of bioactive agent in a biomaterial also increases their systemic and local delivery with increased bioavailability and stability thereby alleviating side effects over a longer period of time (Chan and Leong, 2008; Stratton *et al.*, 2016). Instructive biological cue for tissue regeneration is an upcoming facet of tissue engineering where biomaterials, cell and biomolecules plays a pivotal role. Extracellular matrices and small signaling molecules are known to positively influence the chondrogenesis and thus recent strategy are being developed to encapsulate or direct embedding these biomolecules into synthetic and / or metal based biomaterials (Chan and Leong, 2008; Vadalà *et al.*, 2012; Monteiro *et al.*, 2015). Substances can also be trapped non-covalently. Controlled local release of these bioactive molecules to achieve desired tissue is what needs to be further optimized. Growth factors does play role in cell migration proliferation, differentiation thereby modulating the extracellular matrices. In previous studies, Link N peptide has been identified as a promising growth factor that stimulates the ECM synthesis in IVDs (Gawri *et al.*, 2013a; Gawri *et al.*, 2013b; Wang *et al.*, 2013; Gawri *et al.*, 2014). Link N peptide appears to have an effect on IVD metabolism, which stimulates the proteoglycan synthesis (Wang *et al.*, 2013). Furthermore, Antoniou *et al.* and Mwale *et al.* demonstrated that, Link N has suitable properties to drive chondrogenesis and therefore it serves as a potential growth factor during the IVD healing (Mwale *et al.*, 2011b; Antoniou *et al.*, 2012b; Gawri *et al.*, 2014; Mwale *et al.*, 2014). Number of factors such as; avascular nature of cartilage and IVD, short half-life of the bioactive molecules, systemic side effects, mainly limits or restrict the successful systemic local delivery of growth factors or other bioactive molecules like steroids.

In recent years, nucleic acid therapy using synthetically modified messenger RNAs is emerging as a promising substitute for gene and recombinant protein therapies (Steinle *et al.*, 2017). mRNA delivery primly escapes the insertional mutagenesis risk which otherwise is associated with gene delivery (Kormann *et al.*, 2011). In the field of musculoskeletal therapeutics, Aini *et al.* previously demonstrated the delivery of mRNA encoding the cartilage anabolic transcription factor runt-related transcription factor 1 (RUNX1) as a promising osteoarthritis (OA) treatment option (Aini *et al.*, 2016). The injection of RUNX1 mRNA into mouse OA knee joints significantly suppressed the progression of OA compared to the non-treated control. The use of synthetic mRNA abrogates the risk of integration to the host genome (Steinle *et al.*, 2017). The translational efficacy of synthetic mRNA has also improved compared to plasmids, since it bypasses the need for nuclear trafficking and it is immediately translated upon entering the cytoplasm. Additionally, chemical modification of desired mRNAs has elevated stability and significantly reduced immunogenicity (Steinle *et al.*, 2017).

In this part of the thesis, for the first time, we analyzed the potential of the exogenous delivery of synthetic mRNA encoding Link N peptide in human primary chondrocytes and bone marrow derived mesenchymal stromal cells (SCP1 cells). Therefore, synthetic mRNA encoding Link N was generated and moderate cell transfection efficiency (close to 75%) and low cell toxicity was resulted upon Link N mRNA delivery into both cell types. Moreover, Link N mRNA delivery augmented anabolic response in human primary chondrocytes as well as in SCP1 cells thereby promoting matrix synthesis related gene expression in 2D cell culture and in 3D culture after seeding of cells on knitted titanium scaffolds (Tendulkar *et al.*, 2016). Thus, the delivery of synthetic Link N mRNA into chondrocytes and MSCs presents a new therapeutic strategy to augment anabolic response of cells for improving the cartilage and/or IVDs.

While considering scaffold free approach in musculoskeletal therapy, it may be necessary to use scaffold since it can serve as a load bearing structure to support biomechanical forces and thus provide stable microenvironment for tissue regeneration (Richardson *et al.*, 2007; Lewis, 2012b). Thus, we suppose that, the delivery of synthetic Link N mRNA presents a new therapeutic strategy to ameliorate musculoskeletal disorders.

International Journal of Molecular Sciences

MDPI

Article

Exogenous delivery of Link N mRNA into chondrocytes and MSCs – the potential role in increasing anabolic response.

Gauri Tendulkar[1*], Sabrina Ehnert[1], Vrinda Sreekumar[1], Tao Chen[1], Hans-Peter Kaps[1], Sonia Golombek[2], Hans-Peter Wendel[2], Andreas K Nüssler[1], Meltem Avci-Adali[2]

[1]Siegfried Weller Institute for Trauma Research at the BG Trauma Center, Eberhard Karls Universität Tübingen, Schnarrenbergstraße 95, Tübingen, Germany; sabrina.ehnert@gmail.com (S.E.), vrindaskumar@gmail.com (V.S.), zzuchentao@yahoo.com (T.C.), hpkaps@gmx.de(H.P.K.), andreas.nuessler@gmail.com(A.K.N.)

[2]Department of Thoracic and Cardiovascular Surgery, University Hospital Tübingen, Calwerstraße 7/1, Tübingen, Germany; sonia.golombek@klinikum.uni-tuebingen.de (S.G.), hans-peter.wendel@med.uni-tuebingen.de (H.P.W.), meltem.avci-adali@klinikum.uni-tuebingen.de (M.A.A.).

*Correspondence: gauritendulkar01@gmail.com (G.T.); Tel.: +49-(0)7071-606-1065

Received: date; Accepted: date; Published: date

Abstract: Musculoskeletal disorders, such as osteoarthritis and intervertebral disc degeneration are one of the causes of morbidity, which concomitantly burdens the health and social care systems worldwide with massive costs. Link N peptide has recently been described as a novel anabolic stimulator for intervertebral disc repair. Thus, in this study we analyzed by delivery of synthetic Link N encoding mRNA into primary human chondrocytes and mesenchymal stromal cells (SCP1 cells), the influence on anabolic response. Furthermore, both cell types were seeded on the knitted titanium scaffolds and the influence of Link N peptide mRNA for possible tissue engineering applications was investigated. Synthetic modified Link N mRNA was efficiently delivered into both cell types and, the transfection of cells resulted in an enhanced expression of aggrecan, *Sox 9* and type II collagen with a decreased expression of type X collagen. Thus, the exogenous delivery of Link N peptide mRNA into the cells augmented an anabolic response thereby increase in extracellular matrix synthesis. Considering these findings, we suppose that, the cultivation of cells on knitted titanium scaffold and the exogenous delivery of Link N peptide mRNA into the cells could mechanically support the stability of tissue engineered constructs and improve the synthesis of extracellular matrix by seeded cells. This method can provide a potent strategy for articular cartilage and intervertebral disc regeneration.

Keywords: Synthetic mRNA, Link N peptide, mRNA delivery, musculoskeletal disorders

1. Introduction

Osteoarthritis (OA) and Intervertebral disc (IVD) degeneration are primarily caused by an imbalance between the synthesis and degradation of extracellular matrix (ECM) [1]. They belong to musculoskeletal disorders with world's largest socioeconomic impact, which are certainly accompanied by join pain and low-back pain (LBP) [2], and consequently affect the quality of life [3]. Musculoskeletal debility, especially LBP is the most common health problem seen in elderly population worldwide with a global prevalence of 65 % [4], contributing highest to the physical

disability [5]. Therefore, non-pharmacological or pharmacological and non-invasive or invasive therapies [6] have been widely used to reduce the degree of pain. Despite progress, the treatment of OA and IVD degeneration remains a challenge [6], due to lack of structural and biomechanical restoration [7-9]. Thus, alternative treatments are required to restore the functionality of the damaged tissue. Although, there are substantial differences regarding the anatomy and embryonic origin between the human IVDs and articular joints, there are great similarities in terms of matrix-degrading factors and the response to mechanical loading in both types of joints [10].

In recent years, gene therapy has been widely explored in tissue engineering to produce specific growth factors, transcription factors, or molecules with therapeutic effects [9,11] to stimulate or induce regenerative responses in the tissue. Although viral and plasmid mediated gene delivery has demonstrated the ability to effectively produce desired proteins, it also has several disadvantages, such as high risk of insertional mutagenesis leading to tumerogenicity due to genome integration, high immunogenicity, inefficient transduction in non-dividing cells, high levels of pre-existing immunity, and other potential serious complications [12,13]. Therefore, in recent years, the synthetic messenger RNA (mRNA)-based protein expression in cells is gaining much attention. The use of synthetic mRNA abrogates the risk of integration to the host genome [13]. The translational efficacy of synthetic mRNA has also improved compared to plasmids, since it bypasses the need for nuclear trafficking and it is immediately translated upon entering the cytoplasm. Additionally, chemical modification of desired mRNAs has elevated stability and significantly reduced immunogenicity [13]. In a previous study, Aini *et al.* demonstrated the delivery of mRNA encoding the cartilage anabolic transcription factor runt-related transcription factor 1 (RUNX1) as a promising osteoarthritis treatment option [14]. The injection of RUNX1 mRNA into mouse OA knee joints significantly suppressed the progression of OA compared to the non-treated control. Moreover, it showed augmented expression of cartilage-anabolic markers and proliferation in articular chondrocytes, initiating a transcriptional cascade for therapeutic effects within chondrocytes.

Link protein is a membrane bound and constitutively expressed glycoprotein that stabilizes the interaction between aggrecan and hyaluronan [15] in extracellular matrices including in IVD matrix. The N terminal proteolytic cleavage of Link protein leads to the generation of Link N peptide, which is a 16 amino acid long peptide [15]. In previous studies, Link N peptide has been identified as a promising growth factor that stimulates the ECM synthesis in IVDs [16-19]. Link N peptide appears to have an effect on IVD metabolism, which stimulates the proteoglycan synthesis [18]. Furthermore, Antoniou *et al.* and Mwale *et al.* demonstrated that, Link N has suitable properties to drive chondrogenesis and therefore it serves as a potential growth factor during the IVD healing [17,20-22].

Thus, in this study, we examined the influence of exogenous delivery of synthetic mRNA encoding Link N peptide on anabolic response in human primary chondrocytes and bone marrow derived mesenchymal stromal cells (SCP1 cells). Therefore, synthetic mRNA encoding Link N was generated and the transfection efficiency was analyzed in both cell types. Functional Link N mRNA delivery augmented anabolic response in primary human chondrocytes and SCP1 cells thereby promoting extracellular matrix related gene expression in 2D cell culture as well as in 3D culture after seeding of cells on knitted titanium scaffolds [23]. Thus, the delivery of synthetic Link N mRNA into chondrocytes and MSCs presents a new therapeutic strategy to augment anabolic response of cells for improving the regeneration of cartilage and/or IVDs.

2. Results

Generation of synthetic modified Link N mRNA

To generate the Link N mRNA, PCR was performed with the template pEX-A128 vector containing Link N encoding sequence to amplify and add a poly T-tail to the Link N encoding sequence. Thereafter, DNA was *in vitro* transcribed into mRNA and the purity of the obtained mRNA was

demonstrated using 1 % agarose gel electrophoresis. The purified Link N mRNA showed the expected length of 351 nucleotides (Figure 1).

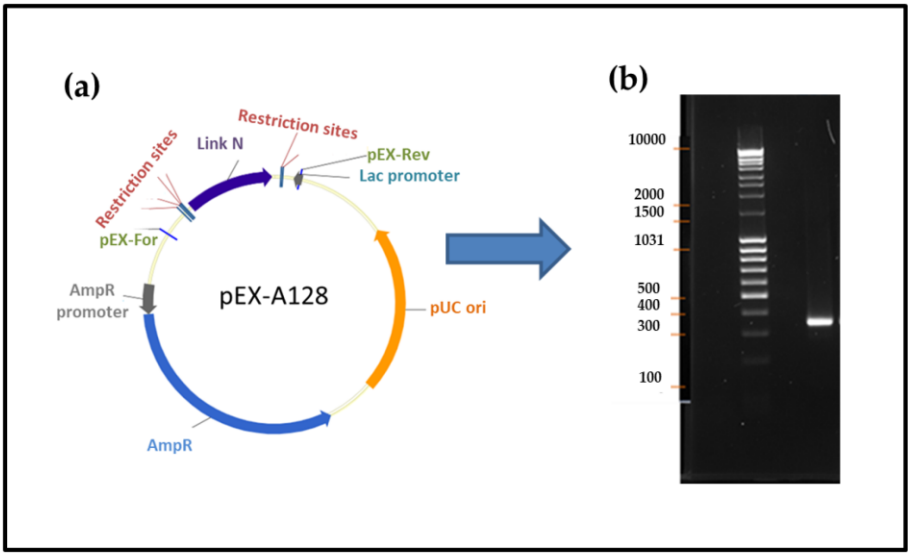

Figure 1: Synthesis of modified Link N mRNA. (a) Plasmid insert encoding Link N peptide was amplified using PCR and a poly T_{120} tail was added. DNA product was then in vitro transcribed into mRNA. (b) The generated mRNA product was purified and the specific length and purity were confirmed by 1 % agarose gel electrophoresis. Right Lane: Link N mRNA (351 nucleotides) after the purification, Left Lane: 0.5-10 kB RNA ladder.

Analysis of transfectability of human primary chondrocytes and SCP1 cells with synthetic mRNA

To confirm the transfectability of human primary chondrocytes as well as SCP1 cells with synthetic mRNA, first, in vitro transcribed (IVT) mRNA encoding eGFP was used. Transfection efficiency was analyzed using flow cytometry (Figure 2a, b) and the production of eGFP was confirmed using epifluorescence microscope (Figure 2c, d). Flow cytometry revealed that 24 h after the eGFP mRNA transfection, 59.65 ± 2.07 % of SCP1 cells and 67.72 ± 4.33 % of primary chondrocytes expressed eGFP. The successful mRNA transfection was easily investigated in human primary chondrocytes as well as in SCP1 cells using eGFP mRNA. Compared to the control (untransfected cells and cells treated with Lipofectamine 2000), the transfection of 100,000 cells with 1 µg mRNA complexed with Lipofectamine 2000 was sufficient to induce a significant increase in the protein expression.

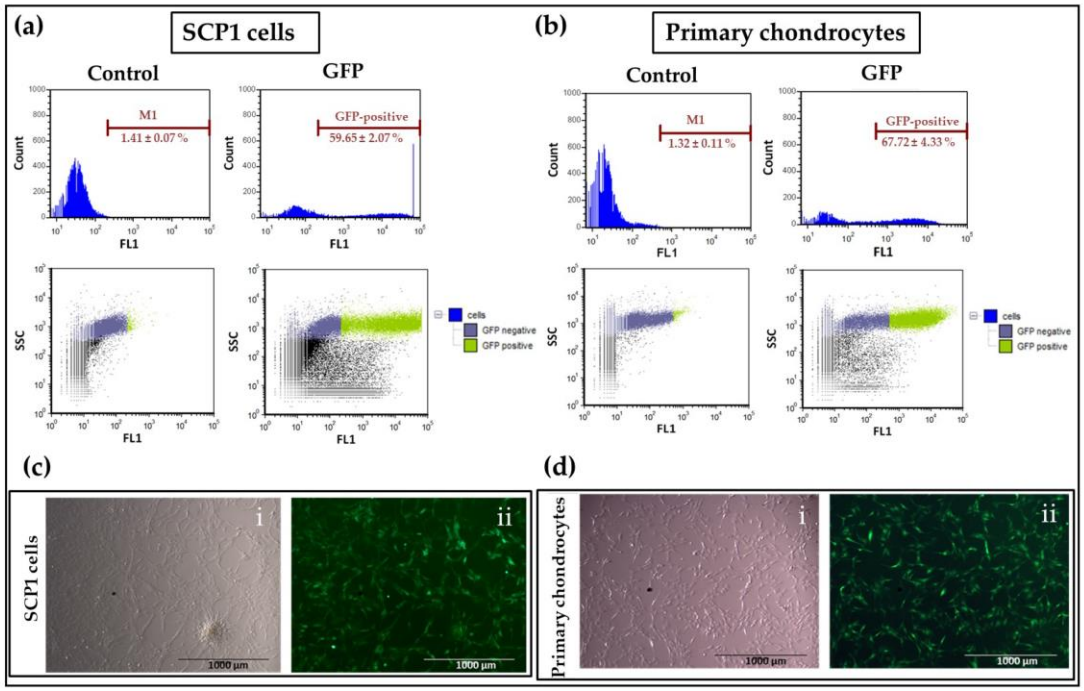

Figure 2: Analysis of transfection efficiency using eGFP mRNA in SCP1 cells and human primary chondrocytes. Flow cytometry analyses of (a) SCP1 cells and (b) human primary chondrocytes, 24 h post transfection with 1 µg eGFP mRNA using Lipofectamine 2000. Untransfected cells and cells treated with Lipofectamine 2000 were used as controls. Representative fluorescence microscopic images of eGFP mRNA transfected (c) SCP1 cells (i- Untransfected control cells, ii- eGFP mRNA transfected cells) and (d) human primary chondrocytes (i- Untransfected control cells, ii- eGFP mRNA transfected cells). Scale bar = 100 µm.

Similarly, the Link N mRNA transfection efficiency was analyzed in SCP1 cells and human primary chondrocytes using flow cytometry (Figure 3a, b) and fluorescence microscopy (Figure 3c, d). Therefore, 1 µg Cy3-labelled Link N mRNA was used to generate the transfection complexes and Cy3 labelled Link N mRNA was successfully delivered into 71.08 ± 5.39 % SCP1 cells and 78.89 ± 4.22 % of primary chondrocytes.

The exogenous delivery of Link N mRNA does not affect the cell viability

To verify that Link N mRNA delivery into the cells is not detrimental, the cell viability was assessed. Human primary chondrocytes and SCP1 cells were transfected with 1 µg of Link N mRNA and 24 h post-transfection, the double staining using Acridine Orange and DAPI allowed the determination of the percentage of viable cells. For both cell types, a cell viability of > 96 % was detected (Figure 3e, f) and the cell viability was not significantly different from in the control cells.

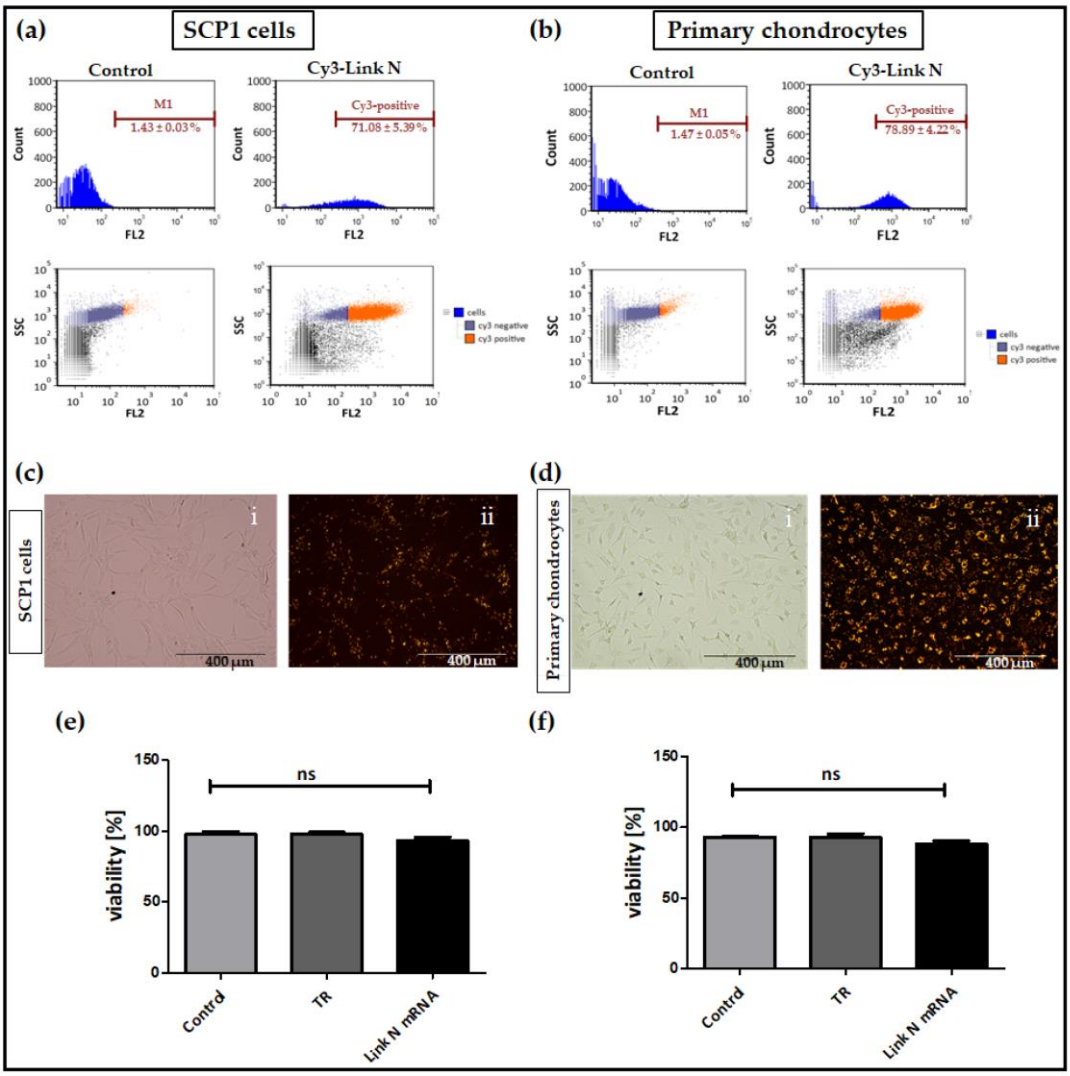

Figure 3: Analysis of Link N mRNA transfection efficiency in SCP1 cells and primary chondrocytes and the influence of Link N mRNA transfection on cell viability. (a) SCP1 cells and (b) human primary chondrocytes were analyzed 24 h post-transfection with 1 µg Cy3 labelled Link N mRNA using flow cytometry. Untransfected cells and cells treated with Lipofectamine 2000 were used as controls. Representative fluorescence microscopic images of Link N mRNA transfected (c) SCP1 cells (i- Untransfected control cells, ii- Cy3 labelled Link N mRNA transfected cells) and (d) human primary chondrocytes (i- Untransfected control cells, ii- Cy3 labelled Link N mRNA transfected cells). Scale bar = 400 µm. In vitro, the transfection of (e) SCP1 cells as well as (f) human primary chondrocytes with 1 µg unlabeled Link N mRNA had no adverse effect on the cell viability. Using NucleoCounter (NC-200), cell viability was assessed 24 h post-transfection. The Acridine Orange and DAPI double staining allowed the detection of the percentage of viable cells. Untransfected cells and cells transfected only with the transfection reagent (TR) Lipofectamine 2000 were used as controls. Data are represented as mean + SEM (N≥3) and were compared using one-way ANOVA with Bonferroni´s multiple comparison test. ns: not significant.

Link N mRNA transfection augments anabolic effects in human primary chondrocytes

The influence of delivered Link N mRNA on the chondrocyte anabolic markers was investigated by performing RT-PCR 24 h post-transfection of human primary chondrocytes with 1 μg Link N mRNA. Compared to untransfected cells and cells transfected with 1 μg eGFP mRNA, the transfection of cells with 1 μg Link N mRNA resulted in a significant increase in chondrocyte specific markers, Aggrecan (*ACAN*), *Sox 9*, and Col II (Figure 4a). The expression of *Sox 9* (***$p < 0.001$), a master transcription factor for the specification and maintenance of cartilage, and *ACAN* (***$p < 0.001$), which is an ECM specific marker for cartilage, was significantly increased up to 1.6 and 3.4-fold respectively, upon Link N mRNA transfection compared with the untransfected cells or cells transfected with eGFP mRNA. Similarly, the gene expression of type II collagen (*$p < 0.05$), which is a major cartilage ECM protein, was also increased by 1.4-fold in the Link N mRNA transfected group. On contrary, gene expression of type X collagen (**$p < 0.01$), a hypertrophic marker, was significantly downregulated to 0.6-fold in Link N mRNA transfected group compared with the untransfected cells or cells transfected with eGFP mRNA.

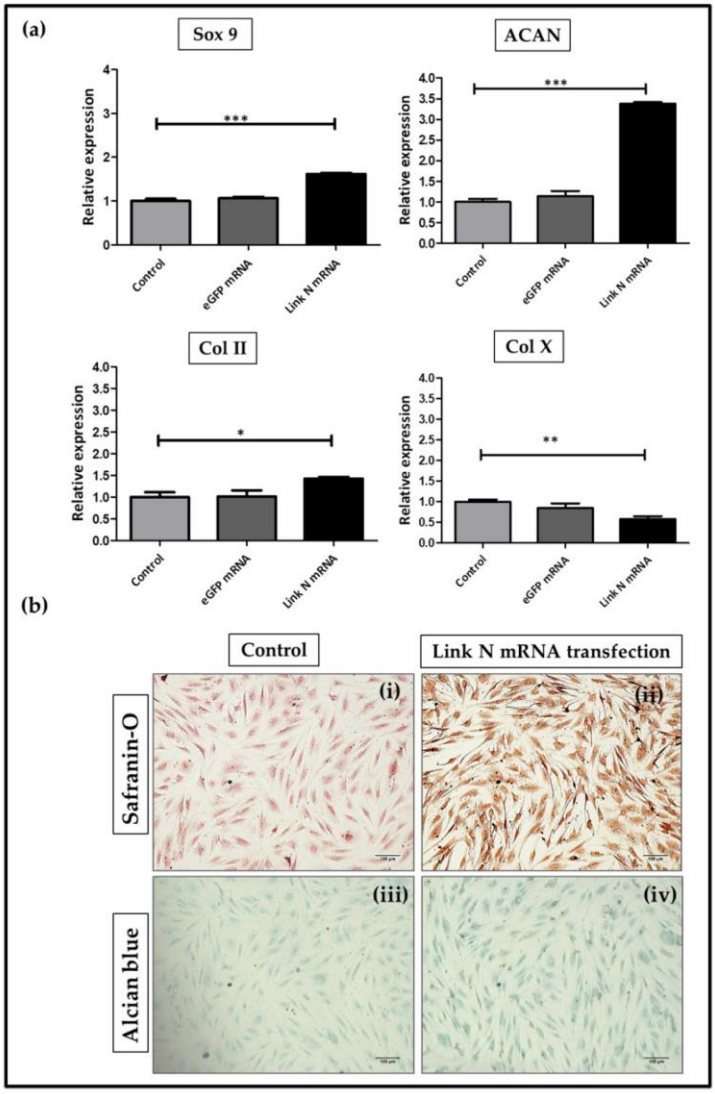

Figure 4: Influence of Link N mRNA delivery into primary chondrocytes on aggrecan (ACAN), Sox 9, type II and type X collagen gene expression and production of collagen and proteoglycan

matrix. 1 x 10^5 primary human chondrocytes were transfected with 1 μg Link N mRNA and the influence on the expression of chondrocyte anabolic markers was investigated. a) Changes in ACAN, Sox 9, type II collagen COL2A1 (Col II) and type X collagen COL10A1 (Col x) gene expression were examined 24 h after Link N mRNA transfection, using RT-PCR. Untransfected and eGFP mRNA transfected cells were used as controls. GAPDH was used as an internal control and served to normalize the expression. Densitometric analyses are represented as mean ± SEM (N≥3) and were compared using one-way ANOVA with Bonferroni´s multiple comparison test (***P < 0.001, **P < 0.01, *P < 0.05). b) The expression of collagen and proteoglycan matrix proteins was examined in non-transfected (i, ii) and Link N mRNA transfected (ii, iv) human primary chondrocytes using safranin O and alcian blue-staining 7 days post-transfection. In comparison with the control, the Link N mRNA transfected cells showed the presence of intensely stained matrix. Scale bar = 100 μm.

Furthermore, the accumulation of chondrocyte specific ECM upon Link N mRNA delivery was examined 7 days post-transfection. Alcian blue and safranin-O staining was used to investigate the expression of proteoglycans and collagen respectively. Safranin O staining showed an intense red color in Link N mRNA transfected cells compared to the cells treated with Lipofectamine 2000 and/or eGFP mRNA. The formation of GAGs was confirmed using alcian blue dye, which resulted in an intense blue color in Link N mRNA transfected cells compared to untransfected control cells (Figure 4b) and also with eGFP mRNA. Thus, these results confirmed a positive effect of Link N mRNA transfection on ECM metabolism of chondrocytes and showed accordance with the results of gene expression analyses.

Link N mRNA transfection upholds the expression of ECM-related genes in SCP1 cells

To investigate the response of MSCs to the synthetic Link N mRNA treatment, SCP1 cells were transfected with 1 μg Link N mRNA and RT-PCR was performed 24 h post transfection. A significantly higher expression of chondrocyte specific marker Sox 9 (*$p < 0.05$), ACAN (*$p < 0.05$) and collagen II (***$p < 0.001$) was observed in Link N mRNA transfected cells compared to untransfected cells or cells transfected with eGFP mRNA (Figure 5).

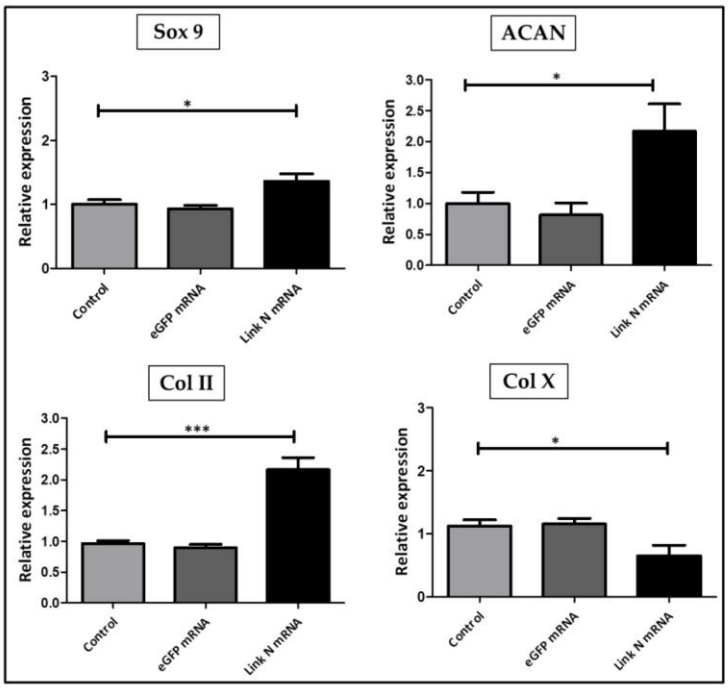

Figure 5: Influence of Link N mRNA delivery into SCP1 cells on aggrecan (ACAN), Sox 9, type II and type X collagen gene expression. 1 x 10^5 SCP1 cells were transfected with 1 µg Link N mRNA and the influence on the expression of chondrocyte specific markers was investigated. Changes in ACAN, Sox 9, type II collagen COL2A1 (col II) and type X collagen COL10A1 (col x) gene expression were examined 24 h after Link N mRNA transfection, using RT-PCR. Untransfected and eGFP mRNA transfected cells were used as controls. GAPDH was used as an internal control and served to normalize the expression. Densitometric analyses are represented as mean ± SEM (N=3) and were compared using one-way ANOVA with Bonferroni´s multiple comparison test (***P < 0.001, **P< 0.01, *P < 0.05).

Although, synthetic Link N mRNA delivery in SCP1 cells increased Sox 9 expression to 1.3-fold, a stronger effect was seen on collagen II and aggrecan with 2.2 -fold change increase for both compared to untransfected cells or cells transfected with eGFP mRNA. Additionally, the col X (*p < 0.05) gene expression was significantly downregulated to 0.6-fold upon Link N mRNA transfection. Overall, synthetic Link N mRNA delivery into SCP1 cells upholds the expression of ECM related genes.

Transfectability of cells seeded on knitted titanium scaffold with eGFP mRNA

Biocompatibility is a fundamental prerequisite for any biomaterial to be used in tissue engineering. Thus, a knitted titanium scaffold, which showed in our previous studies a high biocompatibility, was used as an example for the 3D cultivation of cells for a potential application in IVD treatment [24]. SCP1 cells and primary human chondrocytes were seeded on these biocompatible knitted titanium scaffolds and the transfectability of these cells was analyzed by using lipoplexes containing Lipofectamine 2000 and 1 µg eGFP mRNA. Figure 6a illustrates the overexpression of eGFP in cells (either SCP1 cells or human primary chondrocytes) seeded on the knitted titanium scaffold 24 h post-transfection. The successful eGFP mRNA transfection of SCP1 cells as well as human primary chondrocytes was demonstrated by detection of eGFP protein expression using fluorescence microscopy (Figure 6b).

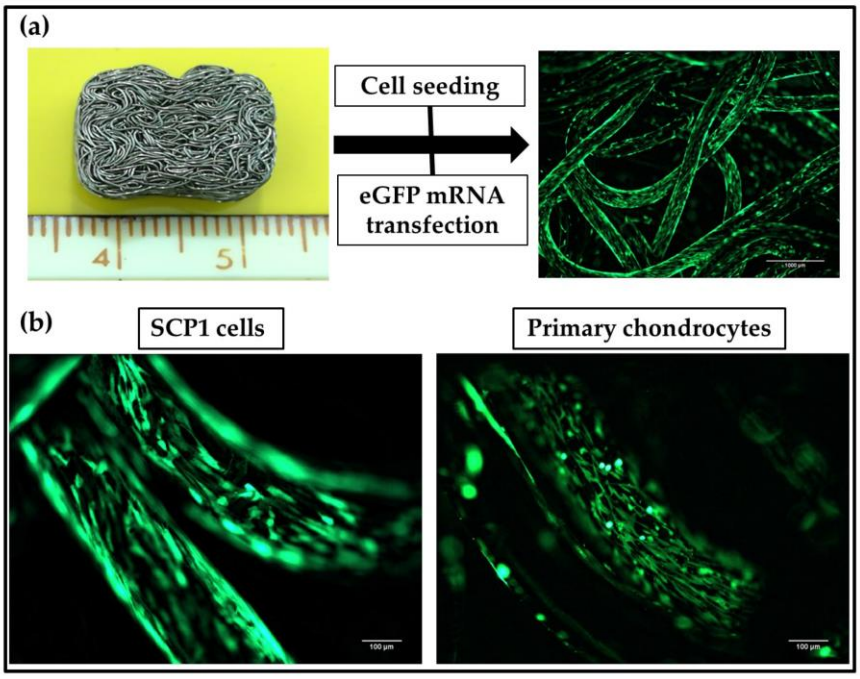

Figure 6: eGFP mRNA transfection of cells seeded on knitted titanium scaffolds. (a) Illustration of cell seeding on the knitted titanium scaffolds and the following eGFP mRNA transfection. (b) Positive eGFP expression of SCP1 cells and human primary chondrocytes adhered to knitted titanium scaffold confirmed the successful mRNA transfection. Scale bar = 100 µm.

Link N mRNA transfection of cells seeded on knitted titanium scaffold triggers the expression of chondrocyte specific and ECM related genes.

Transfection with 1 µg Link N mRNA was performed on SCP1 cells and human primary chondrocytes seeded on knitted titanium scaffolds. Functional potency was evaluated by analyzing the expression of aggrecan, *Sox 9*, and type II and type X collagen using RT-PCR 24 h post Link N mRNA transfection. 2 -fold change increase in *Sox 9* (**$p < 0.01$), 1.7-fold increase in *ACAN* (**$p < 0.01$), and 1.2-fold increase in collagen II (*$p < 0.05$) gene expression was detected, which confirmed that Link N mRNA transfection can augment the anabolic effect in chondrocytes in 3D culture (Figure 7a). Moreover, collagen X (***$p < 0.001$) gene expression was significantly downregulated 0.3-fold.

In SCP1 cells seeded on scaffolds, chondrocyte specific genes *Sox 9* (*$p < 0.05$) and *ACAN* (**$p < 0.01$) were also significantly upregulated to 1.6-fold and 1.8-fold respectively, 24 h post transfection (Figure 7b), compared to untransfected cells or cells transfected with eGFP mRNA. The expression of collagen II tended to be upregulated and collagen X was downregulated after the Link N mRNA transfection, but these differences were not significant.

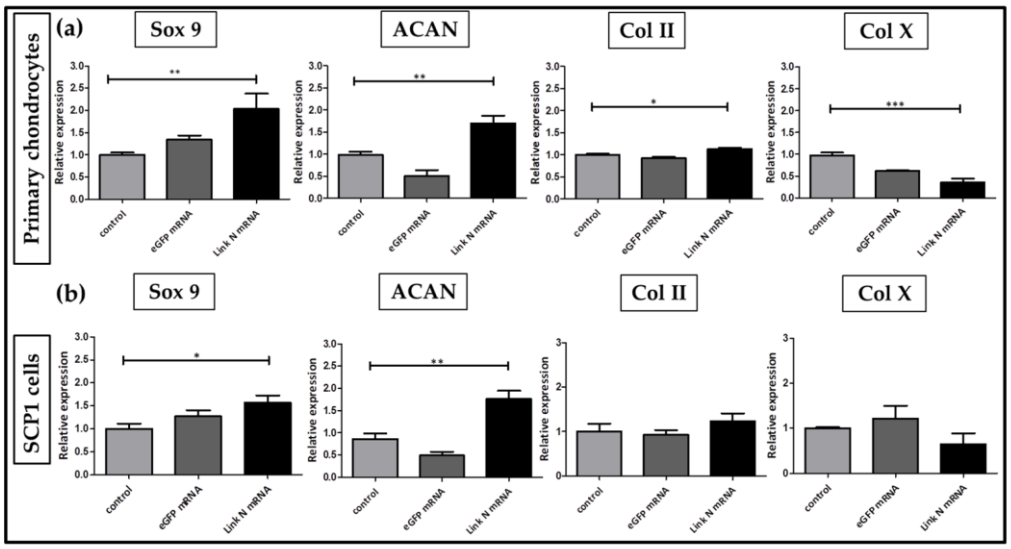

Figure 7: Effect of Link N mRNA transfection on cells seeded on knitted titanium scaffold-changes in aggrecan (ACAN), Sox 9, type II and type X collagen gene expression. 1 x 10^5 primary human chondrocytes or SCP1 cells were transfected with 1 µg Link N mRNA and the influence on ECM related genes and chondrocyte anabolic markers were investigated. Changes in ACAN, Sox 9, type II collagen COL2A1 (col II) and type X collagen COL10A1 (col x) gene expression were examined 24 h after Link N mRNA transfection in (a) human primary chondrocytes and (b) SCP1 cells seeded on knitted titanium scaffolds using RT-PCR. Untransfected and eGFP mRNA transfected cells were used as controls. GAPDH was used as an internal control and served to normalize the expression. Densitometric analyses are represented as mean ± SEM (N≥3) and were compared using one way ANOVA with Bonferroni´s multiple comparison test (***P < 0.001, **P < 0.01, *P < 0.05).

3. Discussion

In recent years, viral vectors and plasmid based gene therapy has drawn much attention as an alternative to the administration of growth factors or peptides. However, the major problem is still the safety concerns [25,26], thus the clinical application remains challenging [27]. In contrast, mRNA-based strategies have been shown to be a safer alternative to produce a protein of interest inside the cells without the integration into the host genome compared to viral and plasmid-based delivery methods [13,28,29]. In addition, the stability of synthetic mRNA as well as immune activation potential can be effectively reduced by chemical modifications [30]. In the present study, a functional synthetic mRNA encoding Link N was successfully generated to stimulate the ECM production. Using a cationic lipid, the chemically modified mRNA encoding Link N was efficiently delivered into chondrocytes and SCP1 cells without any adverse effect on the cell viability. As a result, the Link N mRNA transfection enhanced the expression of cartilage specific ECM components *ACAN* and Col II in human primary chondrocytes as well as in SCP1 cells and furthermore reduced the Col X synthesis. Thus, we assume that the transient genome integration free overexpression of Link N in chondrocytes and MSCs using synthetic mRNA may improve the joint repair.

While there is great similarities between the expression profile of collagen and aggrecan in articular cartilage and IVDs, their ratios are different respectively [31]. Moreover, there is a substantial difference regarding their distinct morphology and/or extracellular matrix expression profile between the articular cartilage from joints and IVD tissue [32]. The progressive loss of ECM components, Col II and *ACAN*, primarily due to the increase in catabolic pathophysiological events is the hallmark of articular cartilage and IVD degeneration [31,33]. Nonetheless, remarkable upregulation of collagen type X has also been reported to occur in articular cartilage and IVDs during osteoarthritis and low back pain respectively [34]. It ultimately leads to cartilage or IVD destruction and loss of function, therefore, the repair or replacement of these tissues is required. From the vast knowledge of cartilage anabolic factors, one of the anabolic agents *e.g.* RUNX1 are able to induce cartilage regeneration [14]. Although various strategies have been initiated to attempt cartilage repair [35], their clinical therapeutic efficacy remains major challenge in chronic joint diseases. Recently, the N terminal peptide of Link protein (Link N: DHLSDNYTLDHDRAIH) generated due to proteolytic cleavage has been identified as a potential growth factor that plays a pivotal role in stimulating anabolic effect during IVD repair [16]. Additionally, it has been demonstrated that Link N synthetic peptide treatment restores the proteoglycan content, which is a prerequisite for IVD repair [20]. Moreover, the injection of synthetic Link N into discs of a rabbit model of IVD degeneration resulted in partial restoration of disc height [22]. However, challenges associated with peptide drugs, such as interplay between the pharmacokinetics upon administration, immunogenicity and formulation conditions and in addition, the rapid clearance from the body and conformational flexibility limits their clinical use [36,37]. Moreover, concentration of peptide drugs and their local activity is often not sufficient to support the later stages of tissue repair due to low bioavailability. On contrary, nucleic acid therapy provides the steady release of the desired protein from cells [13].

In this study, for the first time, we analyzed the potential of the exogenous delivery of synthetic Link N mRNA to restore ECM content as a potential musculoskeletal therapeutic application. The influence of the synthetic Link N mRNA on the gene expression of chondrocyte specific markers was analyzed. The Link N mRNA delivery was accompanied by enhanced expression of *Sox 9* and its transcriptional target type II collagen. Furthermore, in addition to the upregulation of aggrecan and collagen II gene expression, the alcian blue and safranin O staining confirmed the increased production of collagen and proteoglycans. Although primary chondrocytes were used in our experiments, these findings were in accordance with the previous study by Mwale *et al.* [20], which demonstrated that Link N has the potential to be used in repairing degenerated IVD. Additionally, discernible downregulation of the hypertrophic chondrocyte marker collagen X in Link N mRNA

transfected cells was also observed compared to untreated cells. *Sox 9* as a cartilage anabolic transcription factor could suppress cooperatively with Link N the hypertrophy.

The present study also investigated the synergy between the MSCs and Link N mRNA delivery regarding the stimulation of ECM synthesis. Link N mRNA delivery in SCP1 cells upregulated chondrocyte specific marker expression as seen 24 h after the transfection. Previously, Antoniou *et al* showed that Link N alone cannot drive the chondrogenesis in MSCs, but it can boost the ongoing process [21]. Besides the potential to enhance the chondrogenic differentiation of MSCs, the negative impact of Link N on osteogenesis and hypertrophy was also demonstrated in previous studies [20,21], although the exact molecular mechanism of Link N is still not yet clear. Thus, we speculate that the exogenous delivery of Link N mRNA and the presence of unique ECM milieu containing growth factors at the defect site could strengthen the formation of either a disc-like or a cartilage-like matrix.

Due to lack of self-healing capability, cartilage and IVD injuries do not completely heal [38]. Most of the current cartilage and IVD treatments fail to fully restore the damaged tissue [38-41]. Thus, there is a huge need for alternative treatment strategies that can activate the repair and healing process upon and provide mechanical stability. Consequently, in this study, we analyzed a combined approach of synthetic Link N mRNA delivery together with knitted titanium scaffold as a promising strategy to improve and support the reparative processes for the treatment of joint tissues. Previously, our group demonstrated that knitted titanium scaffold, which was aimed for IVD nucleus pulposus replacement, supports cell attachment, growth of human primary chondrocytes as well as SCP1 cells *in vitro* [24]. Importantly, the 3D architecture of the porous knitted titanium scaffold is expected to play a role in maintaining space, which is necessary for tissue integration upon implantation *in vivo*. In this study, SCP1 cells and human primary chondrocytes seeded on titanium scaffolds were successfully transfected with the synthetic mRNA, which was demonstrated by using eGFP mRNA and the subsequent eGFP production in the cells. The consequence of combined use of knitted titanium and Link N mRNA was validated by analyzing the gene expression of chondrocyte specific markers in chondrocytes and SCP1 cells seeded on knitted titanium scaffold. The Link N mRNA transfection of cells seeded on knitted titanium scaffolds resulted in significant upregulation of chondrocyte specific genes, confirming the bioactivity of generated Link N mRNA. Cellular behavior in response to exogenous Link N mRNA delivery on titanium scaffold revealed unraveled that, the expression levels of chondrocyte specific genes in 2D and 3D environment were almost alike. However, the 3D structure of the knitted titanium scaffold can further improve the migration, spreading and proliferation of cells and thus influence the cell differentiation, organization and function [42]. Pore size and the porosity also further positively affect the cellular infiltration and diffusion rate of nutrients. Thus, the increased Link N production in combination with knitted titanium scaffolds can result in improved long term healing response and the integrity of the scaffold *in vivo* and thereby reduce aseptic loosening events. To advance this approach to clinical translation, the regeneration potential should be analyzed in animal models upon the delivery of Link N mRNA either unaided or together with scaffold.

4. Materials and Methods

Ethics Statement

All studies involving human participants were performed in accordance with the 1964 Helsinki declaration and its later revisions. Primary human chondrocytes were isolated from femoral condyle tissue explants of the patients that received total joint replacement. Tissue was harvested only after medical consulation and patient consent. Corresponding ethical vote (338/2015BO2) was approved by Ethik-Kommission an der Medizinischen Fakultät der Eberhard-Karls-Universität und am Universitätsklinikum Tübingen.

Generation of modified synthetic mRNA

Link N and enhanced green fluorescent protein (eGFP) mRNAs were generated as previously reported [43]. Briefly, pcDNA 3.3 plasmid (Aldevron, Fargo, North Dakota, USA) insert encoding eGFP and pEX-K4 plasmid insert encoding Link N (Eurofins Genomics GmbH, Ebersberg, Germany) were amplified using the HotStar HiFidelity Polymerase Kit (Qiagen, Hilden, Germany) according to manufacturer's instructions. Therefore, forward (TTGGACCCTCGTACAGAAGCTAATACG) and reverse (T_{120} CTTCCTACTCAGGCTTTATTCAAAGACCA) primer (Ella Biotech, Martinsried, Germany) were used to amplify the insert. PCR product was then purified using QIAquick PCR Purification Kit (Qiagen, Hilden, Germany) followed by elution in 2 x 10 µl nuclease-free water (Qiagen, Hilden, Germany) and processed for qualitative analysis. Subsequently, *in vitro* transcription (IVT) was performed to generate mRNA from the DNA product. IVT was conducted using MEGAscript T7 Kit (Ambion, Glasgow, Scotland) and the generated mRNA was modified using 2.5 mM 3´-0-Me-m7G(5')ppp(5')G RNA Cap Structure Analog (New England Biolabs, Frankfurt am Main, Germany). Furthermore, 7.5 mM ATP, 1.875 mM GTP (both from MEGAscript T7 Kit), 7.5 mM 5-methylcytidine (5mCTP), 7.5 mM pseudouridine (Ψ) (both from TriLink BioTechnologies, San Diego, CA, USA), and 40 U RiboLock RNase inhibitor (Thermo Scientific, Waltham, MA, USA) were added into the reaction tube. Finally, the product was purified with the RNeasy Kit (Qiagen, Hilden, Germany) and eluted in 2 x 15 µl nuclease-free water. Subsequently, dephosphorylation was performed using the Antarctic Phosphatase Kit (New England Biolabs, Frankfurt am Main, Germany) to remove 5'-triphosphates and the synthetic mRNA was purified again using the RNeasy Kit in 2 x 40 µl nuclease-free water. The quality of the obtained mRNA was analyzed using 1 % agarose gel electrophoresis and the concentration of the mRNA was measured using a spectrophotometer.

Cy3 labelling of Link N mRNA

During the IVT of synthetic Link N mRNA, 1.9 mM 5-azido-C3-UTP (Jena Bioscience, Jena, Germany) and 5.6 mM Ψ were used instead of 7.5 mM Ψ and the product was purified using RNeasy MinElute Cleanup Kit. To perform Cu(I)-free azide-(dibenzocyclooctyne [DBCO]) click reaction, 5-fold molar excess of DBCO-sulfo-Cy3 (Jena Bioscience, Jena, Germany) was used to conjugate Cy3 to 5-azido-C3-UTP-modified mRNA in a total amount of 40 µl nuclease-free water for 1 h at 37 °C. Then, the reaction mixture was purified using RNeasy MiniElute Cleanup Kit and the mRNA concentration was determined using a photometer. The mRNA was stored at -80 °C.

Analysis of transfection efficiency using Cy3 labelled Link N mRNA

SCP1 cells and primary chondrocytes were transfected with Cy3 labelled synthetic Link N mRNA. After 24 h, cells were washed with DPBS (w/o Ca^{2+}/Mg^{2+}) and the uptake of Cy3 labelled Link N mRNA was analyzed by using an epifluorescence microscope (Life technologies, Darmstadt, Germany). Furthermore, cells were trypsinized (Trypsin-EDTA; 0.05 % / 0.02 %, Merck, Darmstadt, Germany), centrifuged and resuspended to attain a cell suspension and 20,000 cells were analyzed by FACScan flow cytometer (Sysmex, Norderstedt, Germany). Cells expressing Cy3 were detected using the FL2 channel and fluorescence was measured (Ex/Em = 554/568 nm). FACS data were displayed in dot plots and respective histograms. For the evaluation, a marker M1 was set, which contained maximum of approximately ≤ 1.5 % of control cells (cells treated with transfection medium without mRNA). FCS5 express flow cytometer software (De novo software, US) was used to determine the percentage of Cy3 positive cells and thereby the transfection efficiency.

Analysis of cell viability

SCP1 cells and primary chondrocytes were transfected with synthetic Link N mRNA (1 µg/1 x 10^5 cells). After 24 h, the cells were detached, loaded into a Via1-Cassette™, which is coated with Acridine Orange and DAPI (ChemoMetec, Kaiserslautern, Germany). Using the NucleoCounter® NC-200™, the cell count and viability were determined. All cells stained with Acridine Orange appeared green and non-viable cells stained with DAPI appeared blue. The cell viability was calculated by the NucleoCounter software.

Cultivation of cells

Human immortalized bone marrow derived mesenchymal stromal cell line (SCP1 cells) [44] was a kind gift from Prof. Dr. Matthias Schieker. Cell were expanded in culture medium (α-MEM (minimal essential medium; GIBCO, Darmstadt, Germany)), 10 % FCS (GIBCO, Darmstadt, Germany) and 1 % penicillin/streptomycin (Merck, Darmstadt, Germany) 10,000 units/ml penicillin and 10 mg/ml streptomycin) in a cell incubator at 37 °C and 5 % CO_2 [45].
The isolation of primary human chondrocytes was performed as previously described [24]. Briefly, chondrocytes were isolated from donated femoral condyle tissues (N = 23; mean age, 74 years) (BG Klinik, Tübingen) by collagenase (1500 U/ml, GIBCO, Darmstadt, Germany) digestion and expanded in culture medium (DMEM/Ham's F12 (1:1), 10 % FCS, 1 % penicillin/streptomycin, 50 µM L-ascorbate-2-phosphate (Merck, Darmstadt, Germany) at 37 °C and 5 % CO_2. Passage number 2 was used further for all the experiments.

Transfection of cells with modified synthetic Link N mRNA in 2D cell culture

SCP1 cells and human primary chondrocytes were seeded onto 12-well plate (Corning Costar, Merck, Darmstadt, Germany) with a density of 1 x 10^5 cells per well and incubated in a cell incubator (Heraeus 6000 Thermo Fischer Scientific, Langenselbold, Germany) overnight at 37 °C and 5 % CO_2. Next day, cells reached a confluency of around 80- 90 % and the mRNA transfection was performed. Briefly, 1 µg of synthetic mRNA encoding Link N or eGFP was co-incubated with 2 µl Lipofectamine 2000 (Invitrogen, Carlsbad, CA, USA) in 500 µl Opti-MEM I (Invitrogen, Carlsbad, CA, USA) for 20 min at room temperature, allowing the formation of lipoplexes. After the incubation time, cell culture medium was aspirated and cells were washed with 1 ml DPBS (w/o Ca^{2+}/Mg^{2+}, Merck, Darmstadt, Germany) and then, transfection complexes were added to the cells and incubated initially for 4 h at 37 °C and 5 % CO_2. Subsequently, the transfection solution was replaced with 1 ml of fresh cell culture medium.

Semi-quantitative reverse-transcription polymerase chain reaction (RT-PCR)

To extract the total RNA, TriFAST reagent (Peqlab, Erlangen, Germany) was used according manufacturer´s instructions. RNA concentration was measured using spectrophotometer (Omega plate reader, BMG Labtech, Offenburg, Germany) and 1 µg of total RNA was reverse transcribed to generate the complementary DNA (cDNA) with the First Strand cDNA Synthesis Kit (Fermentas, St. Leon-Rot, Germany). RT-PCRs were performed using Biozym Ready Mix (Biozym, Hessisch Oldendorf, Germany). Primer sequences and PCR conditions are summarized in Table 1 whereas; GAPDH was used as an internal control for normalization. PCR products were separated by gel electrophoresis and visualized by ethidium bromide, where, pUC19/Msp1 marker (Carl Roth, Karlsruhe, Germany) was used as size reference. Densitometric analysis was performed to quantify signal intensities using the ImageJ software (NIH, Bethesda, USA).

Table 1. List of used primers, product lengths, annealing temperatures.

Gene	Accession number	Forward primer (5'-3')	Reverse primer (3'-5')	Product length (bp)	T_m (°C)
GAPDH	NM_002046.4	GTCAGTGGTGGACCTGACCT	AGGGGTCTACATGGCAACTG	420	56
SOX-9 (*SOX9*)	NM_000346.3	GAAGGACCACCCGGATTACA	GCCTTGAAGATGGCGTTGG	120	60
Aggrecan (*ACAN*)	NM_001135.3	CTTGGACTTGGGCAAACTGC	CACTAAAGTCAGGCAGGCCA	143	60
Collagen X (*COL10A1*)	NM_000493.3	AAACCTGGACAACAGGGACC	CGACCAGGAGCACCATATCC	125	60
Collagen II (*COL2A1*)	NM_001844.4	TGGATGCCACACTCAAGTCC	GCTGCTCCACCAGTTCTTCT	254	60

Histochemical analysis of ECM production

Glycosaminoglycans (GAGs) and collagen are the primary matrix constituents of articular cartilage and IVDs and confer tensile and compressive integrity to these joints [46]. Thus, to assess the influence of the exogenous delivery of synthetic Link N mRNA on GAGs and collagen synthesis, human primary chondrocytes were transfected with (1 µg/1 x 10^5 cells) Link N mRNA. After 7 days of cultivation post-transfection, alcian blue and safranin O stainings were performed. Briefly, after the removal of cell culture medium, cells were fixed in 4 % paraformaldehyde for 15 min and then washed twice with DPBS. Subsequently, 1 % alcian blue (in 3 % acetic acid) or 0.1 % safranin O (in distilled water) stain (Carl Roth, Karlsruhe, Germany) were added and incubated at room temperature for 30 min. Afterwards, dye solution was removed and cells were washed with distilled water. The stained cells were imaged using EVOS$_{fl}$ microscope (Life technologies, Darmstadt, Germany).

Preparation of knitted titanium scaffolds and cell seeding

Knitted titanium scaffolds (Buck GmbH & CO., Bondorf, Germany), which showed in our previous study [23,24] a high cytocompatibility, were used for the 3D cultivation of chondrocytes and SCP1 cells. Therefore, 2.0 x 10^5 cells were seeded per 50 µl cell culture medium per scaffold and incubated initially for 3 h at 37 °C to allow cell attachment. Afterwards, culture medium was added and seeded scaffolds were further incubated at 37 °C and 5 % CO_2. This seeding protocol was identified as the optimal way to facilitate cell attachment in our previous study [23,24].

Transfection of cells seeded on knitted titanium scaffold

The transfection of cells with synthetic Link N mRNA was performed 24 h after the seeding of the scaffolds with cells. Therefore, 1 µg of mRNA was co-incubated with 2 µl of Lipofectamine 2000 in 50 µl Opti-MEM for 20 min at room temperature, allowing the formation of lipoplexes. After the incubation time, cell culture medium was aspirated and cells seeded on the scaffold were washed with 1 ml DPBS (w/o Ca^{2+}/Mg^{2+}, Sigma, Munich, Germany). Transfection complexes were then added and incubated initially for 4 h at 37 °C and 5 % CO_2. Subsequently, 750 µl of fresh cell culture medium was added and scaffolds were incubated at 37 °C and 5 % CO_2. eGFP mRNA was used as a positive control to confirm the transfection. Functional potency of synthetic Link N mRNA was examined by evaluating chondrocyte specific gene expression, 24 h post transfection.

Statistical analysis

Analysis was performed using GraphPad Prism 5.0 software (El Camino Real, CA, USA) and PAST.exe (http://folk.uio.no/ohammer/past/index). All experiments were conducted at least thrice, independently (N≥3) and results are represented as mean ± standard error of mean (SEM). Statistical significance was compared using one-way ANOVA with Bonferroni´s multiple comparison test (***$p < 0.001$, **$p < 0.01$, *$p < 0.05$).

5. Conclusions

In this study, the synthetic modified Link N mRNA was successfully generated and the delivery of Link N mRNA into chondrocytes and SCP1 cells resulted in an anabolic response augmentation. In combination with a knitted titanium scaffold, Link N mRNA delivery also led to an increased expression of chondrocyte specific markers. Therefore, we suppose that the application of Link N mRNA therapeutics to the field of musculoskeletal tissue engineering either in combination with or without a scaffold offers a promising forthcoming direction for the repair of articular cartilage and IVD. The present study provides a first step toward mRNA-based approach to improve musculoskeletal regeneration.

Author Contributions: Conception, G.T., H.P.W. and A.K.N.; Methodology, G.T. and M.A.A.; Investigations, G.T., S.E., V.S., T.C., and S.G.; Formal Analysis, G.T. and M.A.A.; Resources, A.K.N., H.P.W. and H.P.K.; Writing-Original Draft Preparation, G.T. and M.A.A.; Writing-Review & Editing, S.E., V.S., T.C., H.P.W., A.K.N.; Visualization, G.T., M.A.A.; Supervision, M.A.A. and A.K.N.

Funding: The study was partially supported by Zentrales Innovationsprogramm Mittelstand (ZIM) des Bundesministeriums für Wirtschaft und Energie –KF3010902AJ4.

Acknowledgments: The authors gratefully acknowledge Ludmilla Hann for her technical assistance with a generation of *in vitro* transcribed mRNA. We also acknowledge support by Deutsche Forschungsgemeinschaft and Open Access Publishing Fund of University of Tübingen.

Conflicts of Interest: The authors declare no conflict of interest.

Abbreviations

IVD	Intervertebral disc
OA	Osteoarthritis
LBP	Low back pain
IVT	*In vitro* transcribed

References

1. Fontana, G.; See, E.; Pandit, A. Current trends in biologics delivery to restore intervertebral disc anabolism. *Adv Drug Deliv Rev* **2015**, *84*, 146-158, doi:10.1016/j.addr.2014.08.008.
2. Khan, A.; Jacobsen, H.; Khan, J.; Filippi, C.; Levine, M.; Lehman, R.; Riew, K.; Lenke, L.; Chahine, N. Inflammatory biomarkers of low back pain and disc degeneration: a review. *Annals of the New York Academy of Sciences* **2017**, *1410*, 68-84, doi:10.1111/nyas.13551.
3. Kawai, K.; Kawai, A.; Wollan, P.; Yawn, B. Adverse impacts of chronic pain on health-related quality of life, work productivity, depression and anxiety in a community-based study. *Family Practice* **2017**, *34*, 656-661, doi:10.1093/fampra/cmx034.
4. Hoy, D.; Bain, C.; Williams, G.; March, L.; Brooks, P.; Blyth, F.; Woolf, A.; Vos, T.; Buchbinder, R. A systematic review of the global prevalence of low back pain. *Arthritis and Rheumatism* **2012**, *64*, 2028-2037, doi:10.1002/art.34347.
5. Freemont, A. The cellular pathobiology of the degenerate intervertebral disc and discogenic back pain. *Rheumatology* **2009**, *48*, 5-10, doi:10.1093/rheumatology/ken396.

519 6. Richardson, S.; Mobasheri, A.; Freemont, A.; Hoyland, J. Intervertebral disc biology, degeneration
520 and novel tissue engineering and regenerative medicine therapies. *Histology and Histopathology* **2007**, *22*,
521 1033-1041.
522 7. Urban, J.; Roberts, S. Degeneration of the intervertebral disc. *Arthritis Research & Therapy* **2003**, *5*,
523 120-130, doi:10.1186/ar629.
524 8. Clouet, J.; Fusellier, M.; Camus, A.; Le Visage, C.; Guicheux, J. Intervertebral disc regeneration: From
525 cell therapy to the development of novel bioinspired endogenous repair strategies. *Adv Drug Deliv Rev*
526 **2018**, doi:10.1016/j.addr.2018.04.017.
527 9. Henry, N.; Clouet, J.; Le Bideau, J.; Le Visage, C.; Guioheux, J. Innovative strategies for intervertebral
528 disc regenerative medicine: From cell therapies to multiscale delivery systems. *Biotechnology Advances* **2018**,
529 *36*, 281-294, doi:10.1016/j.biotechadv.2017.11.009.
530 10. Rustenburg, C.M.E.; Emanuel, K.S.; Peeters, M.; Lems, W.F.; Vergroesen, P.P.A.; Smit, T.H.
531 Osteoarthritis and intervertebral disc degeneration: quite different, quite similar. *JOR Spine*, e1033 %@
532 2572-1143.
533 11. Lieberman, J.R.; Ghivizzani, S.C.; Evans, C.H. Gene transfer approaches to the healing of bone and
534 cartilage. *Mol Ther* **2002**, *6*, 141-147.
535 12. Katz, M.; Fargnoli, A.; Williams, R.; Bridges, C. Gene Therapy Delivery Systems for Enhancing Viral
536 and Nonviral Vectors for Cardiac Diseases: Current Concepts and Future Applications. *Human Gene*
537 *Therapy* **2013**, *24*, 914-927, doi:10.1089/hum.2013.2517.
538 13. Steinle, H.; Behring, A.; Schlensak, C.; Wendel, H.P.; Avci-Adali, M. Concise Review: Application of
539 In Vitro Transcribed Messenger RNA for Cellular Engineering and Reprogramming: Progress and
540 Challenges. *Stem Cells* **2017**, *35*, 68-79, doi:10.1002/stem.2402.
541 14. Aini, H.; Itaka, K.; Fujisawa, A.; Uchida, H.; Uchida, S.; Fukushima, S.; Kataoka, K.; Saito, T.; Chung,
542 U.I.; Ohba, S. Messenger RNA delivery of a cartilage-anabolic transcription factor as a disease-modifying
543 strategy for osteoarthritis treatment. *Sci Rep* **2016**, *6*, 18743, doi:10.1038/srep18743.
544 15. Bach, F.C.; Laagland, L.T.; Grant, M.P.; Creemers, L.B.; Ito, K.; Meij, B.P.; Mwale, F.; Tryfonidou, M.A.
545 Link-N: The missing link towards intervertebral disc repair is species-specific. *PLoS One* **2017**, *12*, e0187831,
546 doi:10.1371/journal.pone.0187831.
547 16. Gawri, R.; Antoniou, J.; Ouellet, J.; Awwad, W.; Steffen, T.; Roughley, P.; Haglund, L.; Mwale, F.
548 Link-N can stimulate proteoglycan synthesis in the degenerated human intervertebral discs. *European Cells*
549 *& Materials* **2013**, *26*, 107-119, doi:10.22203/eCM.v026a08.
550 17. Gawri, R.; Ouellet, J.; Onnerfjord, P.; Alkhatib, B.; Steffen, T.; Heinegard, D.; Roughley, P.; Antoniou,
551 J.; Mwale, F.; Haglund, L. Link N is Cleaved by Human Annulus Fibrosus Cells Generating a Fragment
552 With Retained Biological Activity. *Journal of Orthopaedic Research* **2014**, *32*, 1189-1197, doi:10.1002/jor.22653.
553 18. Wang, Z.; Hutton, W.C.; Yoon, S.T. ISSLS Prize winner: Effect of link protein peptide on human
554 intervertebral disc cells. *Spine (Phila Pa 1976)* **2013**, *38*, 1501-1507, doi:10.1097/BRS.0b013e31828976c1.
555 19. Gawri, R.; Antoniou, J.; Ouellet, J.; Awwad, W.; Steffen, T.; Roughley, P.; Haglund, L.; Mwale, F. Best
556 paper NASS 2013: link-N can stimulate proteoglycan synthesis in the degenerated human intervertebral
557 discs. *Eur Cell Mater* **2013**, *26*, 107-119; discussion 119.
558 20. Mwale, F.; Wang, H.; Roughley, P.; Antoniou, J.; Haglund, L. Link N and Mesenchymal Stem Cells
559 Can Induce Regeneration of the Early Degenerate Intervertebral Disc. *Tissue Engineering Part a* **2014**, *20*,
560 2942-2949, doi:10.1089/ten.tea.2013.0749.
561 21. Antoniou, J.; Wang, H.T.; Alaseem, A.M.; Haglund, L.; Roughley, P.J.; Mwale, F. The effect of Link N
562 on differentiation of human bone marrow-derived mesenchymal stem cells. *Arthritis research & therapy*
563 **2012**, *14*, R267 %@ 1478-6354.
564 22. Mwale, F.; Masuda, K.; Pichika, R.; Epure, L.M.; Yoshikawa, T.; Hemmad, A.; Roughley, P.J.;
565 Antoniou, J. The efficacy of Link N as a mediator of repair in a rabbit model of intervertebral disc
566 degeneration. *Arthritis research & therapy* **2011**, *13*, R120 %@ 1478-6354.
567 23. Tendulkar, G.; Grau, P.; Ziegler, P.; Buck, A.; Badke, A.; Kaps, H.P.; Ehnert, S.; Nussler, A.K. Imaging
568 Cell Viability on Non-transparent Scaffolds - Using the Example of a Novel Knitted Titanium Implant. *J Vis*
569 *Exp* **2016**, doi:10.3791/54537.
570 24. Tendulkar, G.; Sreekumar, V.; Rupp, F.; Teotia, A.K.; Athanasopulu, K.; Kemkemer, R.; Buck, A.;
571 Kaps, H.P.; Geis-Gerstorfer, J.; Kumar, A., et al. Characterisation of porous knitted titanium for
572 replacement of intervertebral disc nucleus pulposus. *Sci Rep* **2017**, *7*, 16611, doi:10.1038/s41598-017-16863-8.

25. Sampara, P.; Banala, R.R.; Vemuri, S.K.; Av, G.R.; Gpv, S. Understanding the molecular biology of intervertebral disc degeneration and potential gene therapy strategies for regeneration: a review. *Gene Ther* **2018**, *25*, 67-82, doi:10.1038/s41434-018-0004-0.
26. Shimer, A.L.; Chadderdon, R.C.; Gilbertson, L.G.; Kang, J.D. Gene therapy approaches for intervertebral disc degeneration. *Spine (Phila Pa 1976)* **2004**, *29*, 2770-2778.
27. Evans, C.H.; Huard, J. Gene therapy approaches to regenerating the musculoskeletal system. *Nat Rev Rheumatol* **2015**, *11*, 234-242, doi:10.1038/nrrheum.2015.28.
28. Subramanian, A.; Ranganathan, P.; Diamond, S.L. Nuclear targeting peptide scaffolds for lipofection of nondividing mammalian cells. *Nat Biotechnol* **1999**, *17*, 873-877, doi:10.1038/12860.
29. Goodrich, L.; Grieger, J.; Phillips, J.; Khan, N.; Gray, S.; McIlwraith, C.; Samulski, R. scAAVIL-1ra dosing trial in a large animal model and validation of long-term expression with repeat administration for osteoarthritis therapy. *Gene Therapy* **2015**, *22*, 536-545, doi:10.1038/gt.2015.21.
30. Avci-Adali, M.; Behring, A.; Keller, T.; Krajewski, S.; Schlensak, C.; Wendel, H.P. Optimized conditions for successful transfection of human endothelial cells with in vitro synthesized and modified mRNA for induction of protein expression. *J Biol Eng* **2014**, *8*, 8, doi:10.1186/1754-1611-8-8.
31. Mwale, F.; Roughley, P.; Antoniou, J. Distinction between the extracellular matrix of the nucleus pulposus and hyaline cartilage: a requisite for tissue engineering of intervertebral disc. *Eur Cell Mater* **2004**, *8*, 58-63; discussion 63-54.
32. Kim, A.J.; Adkisson, H.D.; Wendland, M.; Seyedin, M.; Berven, S.; Lotz, J.C. Juvenile chondrocytes may facilitate disc repair. *Open Tissue Eng Regen Med J* **2010**, *3*, 28.
33. Adams, M.A.; Dolan, P. Intervertebral disc degeneration: evidence for two distinct phenotypes. *J Anat* **2012**, *221*, 497-506, doi:10.1111/j.1469-7580.2012.01551.x.
34. Steck, E.; Bertram, H.; Abel, R.; Chen, B.; Winter, A.; Richter, W. Induction of intervertebral disc–like cells from adult mesenchymal stem cells. *Stem cells* **2005**, *23*, 403-411 %@ 1066-5099.
35. Bougioukli, S.; Evans, C.H.; Alluri, R.K.; Ghivizzani, S.C.; Lieberman, J.R. Gene Therapy to Enhance Bone and Cartilage Repair in Orthopaedic Surgery. *Curr Gene Ther* **2018**, *18*, 154-170, doi:10.2174/1566523218666180410152842.
36. Otvos, L.; Wade, J.D. Current challenges in peptide-based drug discovery. *Front Chem* **2014**, *2*, 62, doi:10.3389/fchem.2014.00062.
37. Fosgerau, K.; Hoffmann, T. Peptide therapeutics: current status and future directions. *Drug Discov Today* **2015**, *20*, 122-128, doi:10.1016/j.drudis.2014.10.003.
38. van Uden, S.; Silva-Correia, J.; Oliveira, J.M.; Reis, R.L. Current strategies for treatment of intervertebral disc degeneration: substitution and regeneration possibilities. *Biomater Res* **2017**, *21*, 22, doi:10.1186/s40824-017-0106-6.
39. Lewis, G. Nucleus pulposus replacement and regeneration/repair technologies: present status and future prospects. *J Biomed Mater Res B Appl Biomater* **2012**, *100*, 1702-1720, doi:10.1002/jbm.b.32712.
40. Nerurkar, N.L.; Elliott, D.M.; Mauck, R.L. Mechanical design criteria for intervertebral disc tissue engineering. *J Biomech* **2010**, *43*, 1017-1030, doi:10.1016/j.jbiomech.2009.12.001.
41. Zigler, J.E.; Delamarter, R.B. Five-year results of the prospective, randomized, multicenter, Food and Drug Administration investigational device exemption study of the ProDisc-L total disc replacement versus circumferential arthrodesis for the treatment of single-level degenerative disc disease. *J Neurosurg Spine* **2012**, *17*, 493-501, doi:10.3171/2012.9.SPINE11498.
42. Hutmacher, D.W. Scaffolds in tissue engineering bone and cartilage. *Biomaterials* **2000**, *21*, 2529-2543.
43. Avci-Adali, M.; Behring, A.; Steinle, H.; Keller, T.; Krajeweski, S.; Schlensak, C.; Wendel, H.P. In vitro synthesis of modified mRNA for induction of protein expression in human cells. *J Vis Exp* **2014**, e51943, doi:10.3791/51943.
44. Böcker, W.; Yin, Z.; Drosse, I.; Haasters, F.; Rossmann, O.; Wierer, M.; Popov, C.; Locher, M.; Mutschler, W.; Docheva, D., et al. Introducing a single-cell-derived human mesenchymal stem cell line expressing hTERT after lentiviral gene transfer. *J Cell Mol Med* **2008**, *12*, 1347-1359, doi:10.1111/j.1582-4934.2008.00299.x.
45. Ehnert, S.; Baur, J.; Schmitt, A.; Neumaier, M.; Lucke, M.; Dooley, S.; Vester, H.; Wildemann, B.; Stöckle, U.; Nussler, A.K. TGF-β1 as possible link between loss of bone mineral density and chronic inflammation. *PLoS One* **2010**, *5*, e14073, doi:10.1371/journal.pone.0014073.

626 46. Jeong, J.; Bae, K.; Kim, S.-G.; Kwak, D.; Moon, Y.-J.; Choi, C.-H.; Kim, Y.-R.; Na, C.-S.; Kim, S.-J.
627 Anti-osteoarthritic effects of ChondroT in a rat model of collagenase-induced osteoarthritis. *BMC*
628 *complementary and alternative medicine* **2018**, *18*, 131 %@ 1472-6882.
629


630
631

CHAPTER 5

3.4 Unpublished results

3.4.1 Cellular responses to knitted titanium wear debris particles

With respect to scaffold biomechanics, one of the most vital factors to be considered is wear and corrosion resistance. Generation of wear debris is unavoidable problem for any joint replacements, no matter what materials are being used (Chen and Thouas, 2015). Low wear resistance and high friction are two likely possibilities that mainly generate micro particles at the site of implant and consequently cause aseptic implant loosening (Schmiedberg *et al.*, 1994; Bobyn *et al.*, 1995; Chen and Thouas, 2015). Wear debris particles have been reported to have role to induce toxicity (Bitar and Parvizi, 2015; Hussein *et al.*, 2015), especially particle mediated inflammation triggers the granuloma cascade, necrosis and / or fibrosis all together causing the aseptic loosening and therefore the excessive amount of the wear debris particles within the host system can cause adverse cellular host reactions. Although the exact mechanism is not fully understood, accumulation of wear debris tends to activate the immune system (Schmiedberg *et al.*, 1994; Bobyn *et al.*, 1995; Chen and Thouas, 2015;).

As pain is the primary revision reasons for all the patients undergoing intervertebral disc replacement surgery, the contributions of wear debris particles and cell responses to the development of pain was the focus of the next investigation in our study. It was therefore hypothesized in this study that, biological reactions to wear debris in the spine are unique, where the production and interplay between key inflammatory mediators may be contributing to atypical or enhanced pain sensitization. Investigation of the immune responses to titanium wear debris particles revealed the involvement of inflammatory factors (**figure 14**) that might play both a direct and indirect role in inflammatory-mediated pain.

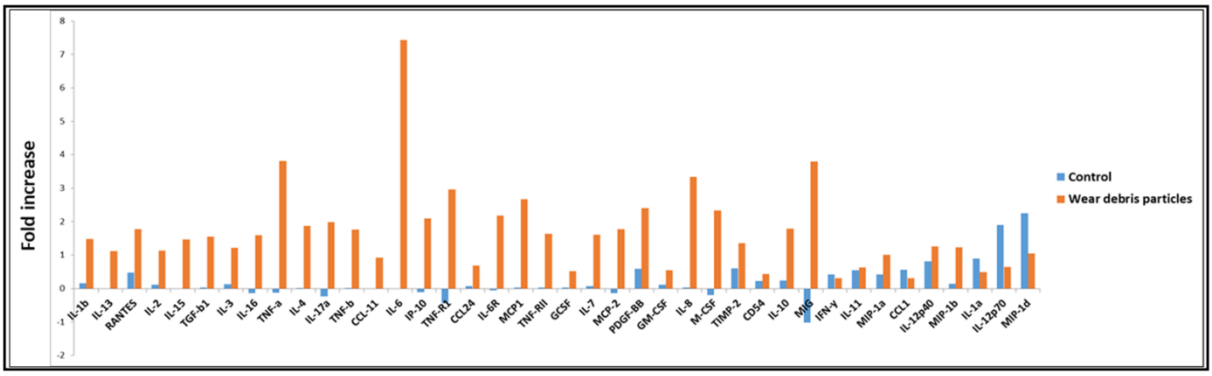

Figure 14. Human inflammatory cytokine array.
Total blood sample was exposed to wear debris particle and 24 h post treatment, cytokine profile was measured using human inflammatory cytokine array.

As a response to knitted titanium wear debris particles, upregulation of proinflammatory cytokines such as TNFα and IL-1β speculated to play direct and / or indirect role in inflammatory mediated pain as proposed in **figure 15**. Nonetheless, significant increased wear resistance (chapter 3.) upon electro-polishing treatment can ensure prolonged functional longevity of this scaffold *in vivo*.

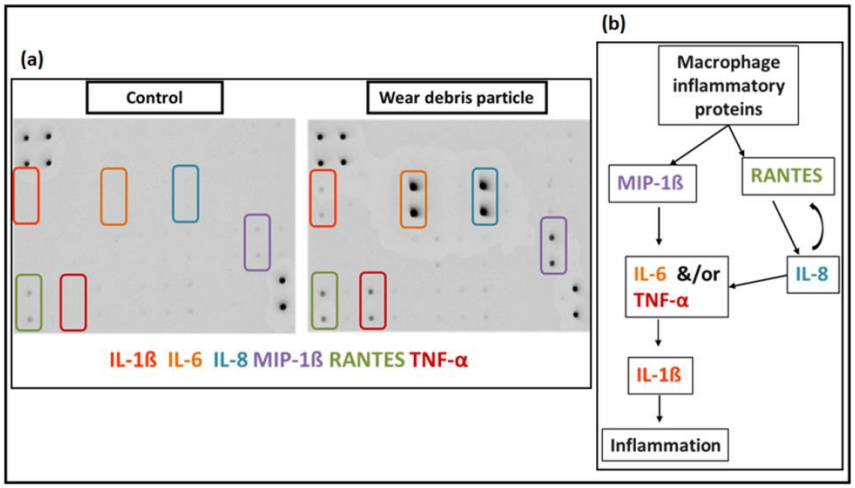

Figure 15. Proinflammatory marker analysis upon exposure to wear debris particles of knitted titanium. Total blood sample was exposed to wear debris particles and 24 h post treatment cytokine profile was measured using human inflammatory cytokine array. Proinflammatory markers: IL-1β IL-6 TNF-α MIP-1β and chemoattractants: IL-8 RANTES were compared to control (a) and Illustrated the probable mechanism of inflammation due to the wear debris particles (b).

3.4.2 Wear debris particle characterization:

According to the previous studies, osteolysis is not as prevalent in spinal arthroplasty due to it having a smaller range of motion than hip and knee replacements, which would indicate smaller wear tracks and fewer debris particles (Schmiedberg *et al.*, 1994; Cunningham, 2004). The intensity of local inflammation (wear debris prone) depends on several critical debris characteristics: chemical reactivity, aspect ratio and particle load (size and volume) (Hallab, 2009). Phagocytosable size to induce an inflammatory reaction (< 10 μm), with 0.24 - 7.2 μm size range is the most pro-inflammatory (Hallab, 2009; Reeks and Liang, 2015).

To determine whether there is any difference between the unpolished and electro-polished scaffold based wear debris particles; in terms of particle size, shape, number based distribution; characterization was performed (**figure 16**). Biomechanics was done by Buck GmbH & Co. and generated wear debris during the biomechanical testing was collected. Collected particles were further analyzed using G3ID microscope. Wear debris particles of knitted titanium varied from submicron range over 100 μm, although the average mean diameter mainly ranged from 1-10 μm. Nonetheless, wear particle analysis of unpolished and

electro-polished scaffold further showed that there is no significant difference in terms of the number and size based distribution of particles; however the overall concentration of wear debris particles were significantly reduced in electro-polished scaffold.

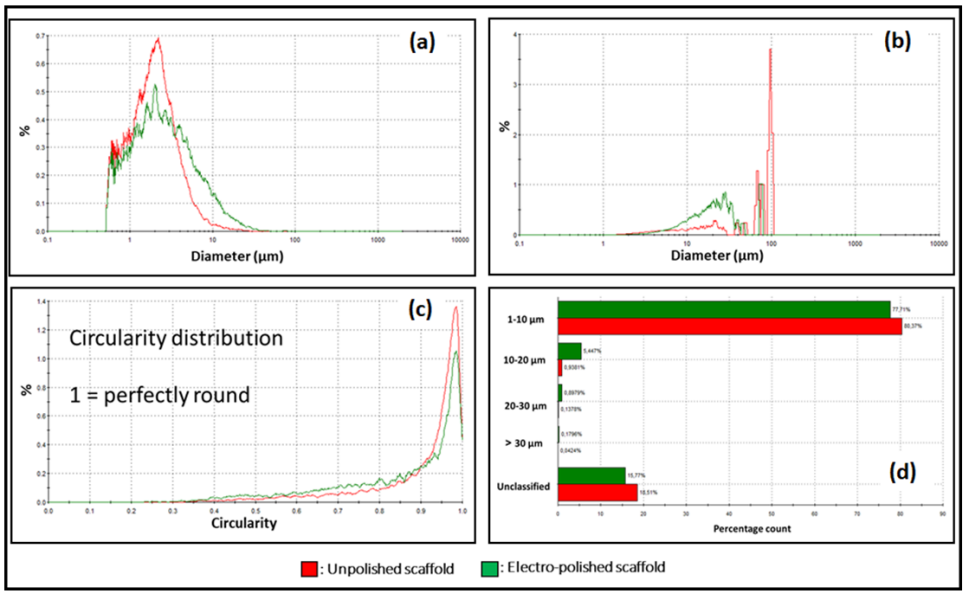

Figure 16. Wear particle size and shape analysis of knitted titanium scaffold.
The samples were measured on the Morphology G3-ID. The particle size and shape distributions were compared as number (a) and volume (b) based distributions. Circularity based distribution (c), and percentage of particles per size bands (d) between the groups were compared.

3.4.3 Hemocompatibility test:

The hemocompatibility of the knitted titanium scaffold will play a critical role for potential clinical translation and especially for the electro-polished scaffold; therefore, the influence of electro-polishing treatment on knitted titanium scaffold surface upon contact activation by whole human blood sample was tested (**figure 12**). Hemocompatibility testing of porous knitted titanium scaffolds was carried out according to ISO 10993-4. The model consists of a modified Chandler-Loop design with closed heparin-coated PVC Loops and a thermostated water bath.

The tests were performed with anticoagulated human whole blood. Human whole blood (n=6) exposed to either unpolished or electro-polished scaffold was circulated in a Chandler loop model for 90 minutes at 37°C. After incubation in the loop, blood was analyzed for blood cell count, coagulation and inflammatory activation markers (TAT, β-TG, SC5b-9 and PMN-elastase). The new Chandler-Loop model (**figure 17**) was used as an alternative to animal and current *in vitro* models, especially for the determination of early events after scaffold implantation.

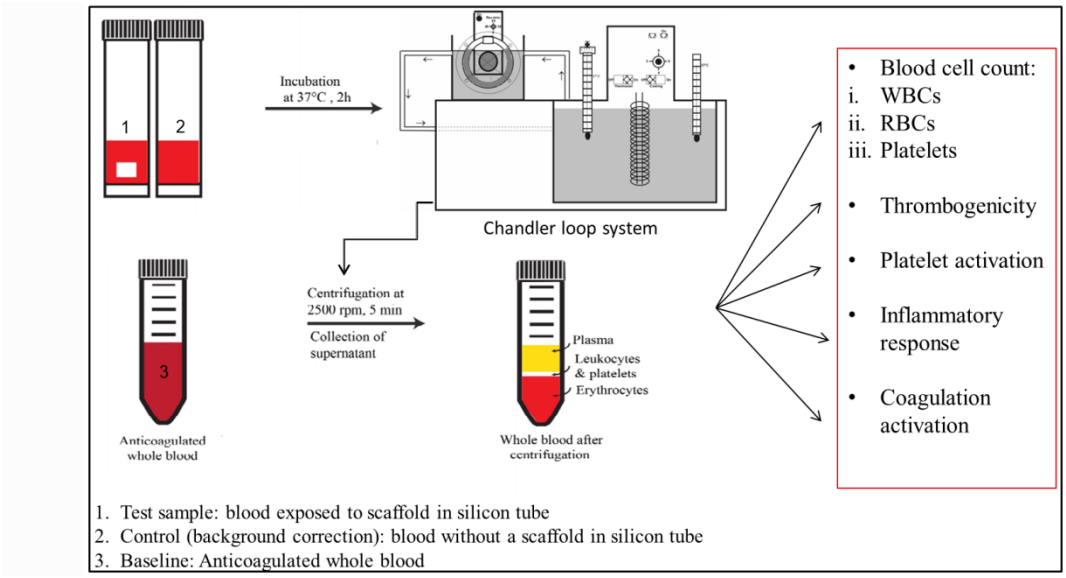

Figure 17: Experimental set up for knitted titanium scaffold hemocompatibility testing.

Platelet count red and white blood cell count as well as hemolysis was not significantly different between the unpolished and electro-polished knitted titanium scaffold (**figure 18**).

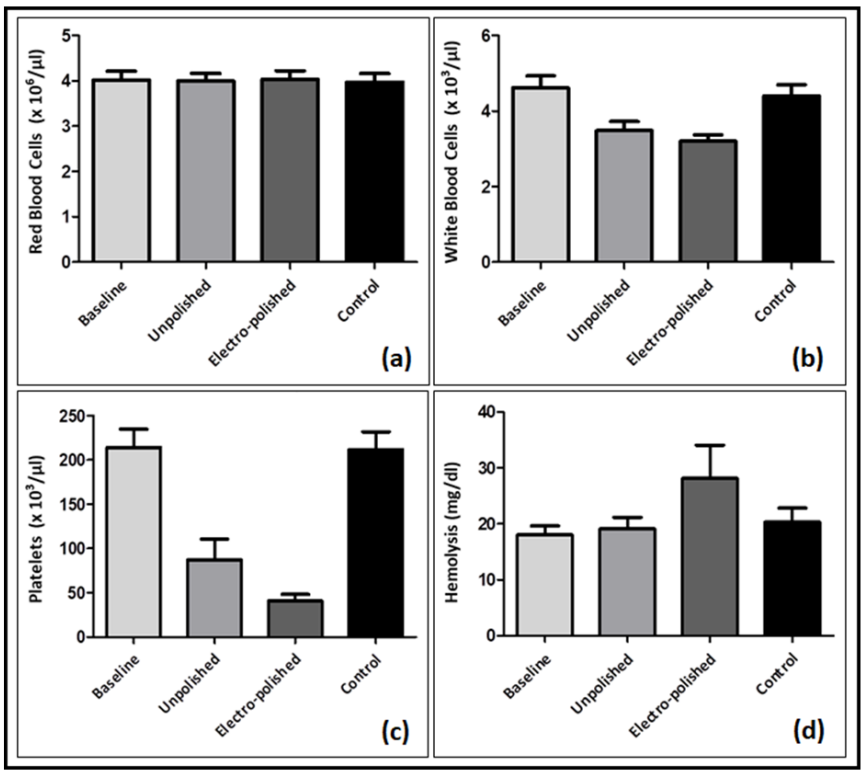

Figure 18: Blood cell counts in human whole blood before and after the knitted titanium scaffold incubation. Numbers of red blood cells (a), white blood cells (b), and platelets (c) per microliter of blood were measured. Additionally, hemoglobin (d) values were quantified. One way ANOVA was carried out and data are shown as mean ± SEM of N=6 independent experiments.

These early stage reactions after implantation are the result of blood material contact. Since metallic biomaterials especially titanium have inherent thrombogenic property (Hong *et al.*, 1999), contact of blood with metallic scaffolds tends to increase the platelet activation and intrinsic coagulation (represented by TAT complex formation) with subsequent upregulation of markers such as SP-selectin and β-thromboglobulin (Gemmell, 2001). In order to distinguish the potency of coagulation activation as a consequence of electro-polishing treatment on knitted titanium scaffold, we further tested coagulation and inflammatory activation markers (TAT, β-TG, SC5b-9 and PMN-elastase).

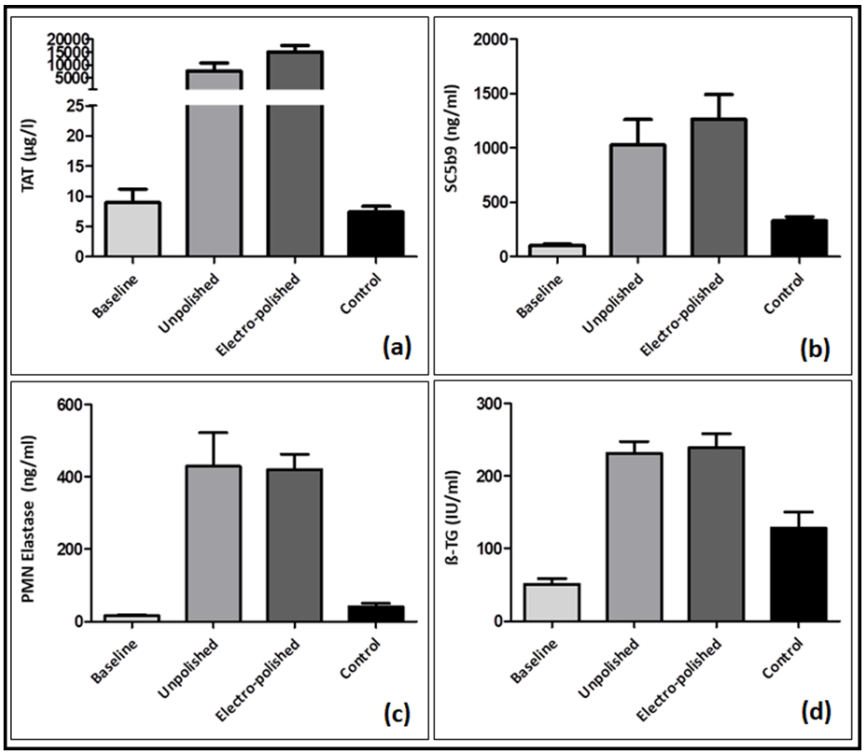

Figure 19: Hemocompatibility of knitted titanium scaffold incubated in human whole blood. Markers for the activation of blood coagulation (a;TAT) and the complement system (b;SC5b-9), as well as for neutrophils (c;PMN elastase) and platelets (d;β-thromboglobulin), were quantified using ELISA and compared to untreated human whole blood (baseline) or blood without scaffold (control) in a dynamic flow model. One way ANOVA was carried out and data are shown as mean ± SEM of N=6 independent experiments.

As expected, knitted titanium exposure was found to provoke a very strong response in coagulation activation measured by TAT generation; as a result of metal hyper-reactivity. Activation of platelets, represented by β-TG, complement activation (SC5b9) and neutrophil activation (PMN elastase) values was also found to be higher in the blood samples exposed to

knitted titanium (**figure 19**) than control. However electro-polishing treatment did not significantly affect the activation of analyzed protein markers.

3.4.4 Biological surface modification:

With respect to titanium and titanium alloy based scaffolds, various physical and chemical surface modifications have shown to improve the cell material interaction thereby obtaining a suitable biomechanics. In addition to gain the tissue inductive potential, many strategies such as biochemical methods are studied with the aim to induce the cell responses by immobilized biomolecules (Yamaguchi *et al.*, 2004; Morra, 2006). Bioactive molecules and extracellular proteins are frequently used to modify the scaffold surface aiming to facilitate the cell attachment on the bio-inert surfaces. The extracellular matrix mainly provides a cell survival environment, and regulates cell morphology, migration, proliferation, maturation and differentiation (Mao and Li, 2014). Complex and dynamic network of ECM provides physical cues that certainly direct mechanical properties of tissue. Collagen (Col) is one of the main components of cartilage / bone extracellular matrix which plays role in modulating the cellular behavior (Morra, 2006; Mao and Li, 2014). Hyaluronic acid (HA), is a form of glycosaminoglycan which contributes ubiquitously to form an extracellular matrix of many tissues. It primly involves in tissue support, lubrication and together with proteoglycans it modulates the viscoelasticity (Ao *et al.*, 2017). Fibronectin (FN) is one of the widely studied components of ECM for the scaffold surface modification, as it is thought to play a vital role in regulating cell adhesion, proliferation and also a differentiation. Moreover FN in tends to bind rapidly and efficiently to titanium oxide without the use of intervening chemical coupling agents (Rapuano *et al.*, 2012b). Therefore, the components of ECM especially Col, HA and FN have been widely used for the creation of novel scaffold and / or for surface modification of the biomaterial with the utility in tissue engineering.

Scaffold surface properties primarily modulate the cellular behavior at material interface (Boyan *et al.*, 1996; Schwartz *et al.*, 1996; Puleo and Nanci, 1999; Hutmacher, 2000; Kurella and Dahotre, 2005). Previously, various studies have explored the biomolecule coating of titanium to improve the tissue integration and conduction of titanium based scaffold. It has also been reported that, the biomolecule immobilization on the scaffold certainly stimulate the cell proliferation while promoting the cell ingrowth of chondrocytes *in vitro* and reducing the foreign body response *in vivo* (Chang and Wang, 2011; Murphy *et al.*, 2013). Moreover, in this study we investigated the effect of collagen, hyaluronic acid, fibronectin and synergy of

collagen: hyaluronic acid coating on the electro-polished scaffold on the ability to influence the cell adhesion, proliferation and cell spreading.

Biological scaffold surface modification demonstrated that, the initial cell adhesion after 24 h was not stimulated by coating the knitted titanium scaffold either with Col, HA, FN or the combination of Col:HA using SCP1 cells. In our experimental set up, this effect was observed only with respect to Col:HA combination (**figure 20**), although there were no significant difference between them in later time points. Day 3 onwards, no significant increase in cell proliferation was observed. On contrary, cell adhesion of primary chondrocytes on the modified scaffolds was significantly higher compare to control. We also observed that biomolecule covalently immobilized on knitted scaffold possessed excellent biological properties and significantly improved cell attachment as well as cell proliferation of primary chondrocytes.

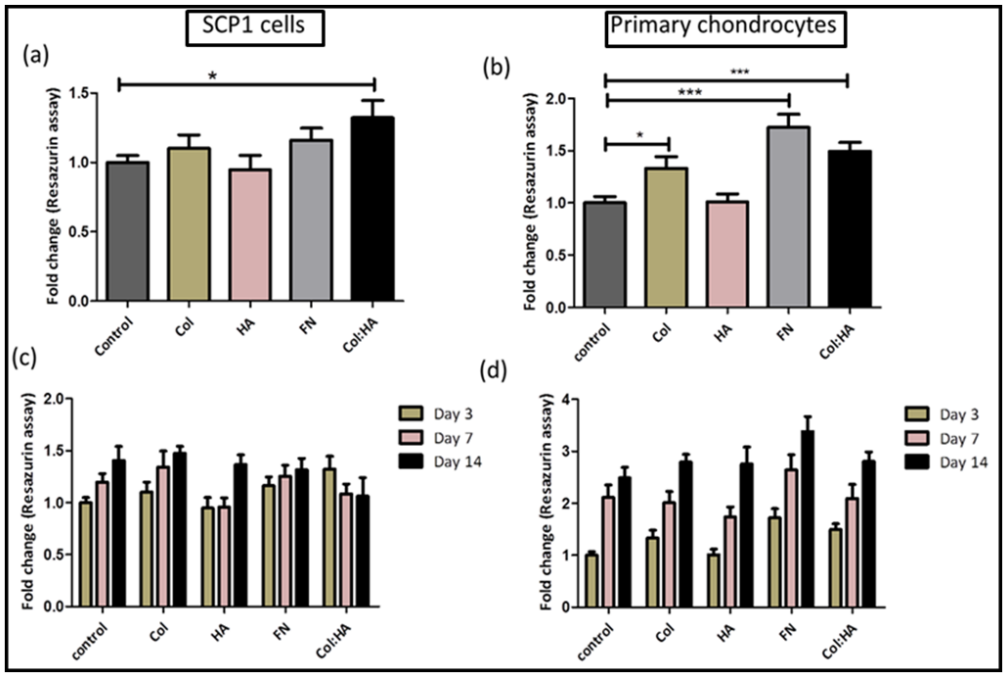

Figure 20. Cell adhesion and proliferation on coated knitted titanium scaffolds.
Resazurin conversion – indirect assay for cell adhesion at day 3 (a);(b) and cell proliferation (c);(d) of SCP1 cells and human primary chondrocytes respectively was carried out. Data represented as mean + SEM; analyzed by Mann Whitney test. $P \leq 0.05$ was considered to be minimum level of significance. * $p \leq 0.05$, ** $p \leq 0.01$, *** $p \leq 0.001$.

CHAPTER 6

4 Discussion

Replacement or regeneration / repair of intervertebral disc nucleus pulposus has been attracting much attention recently as a suitable surgical option for chronic back pain treatment. Moreover, this approach holds a theoretical prospect of minimal invasive technique which does not compromise structural mobility or additionally cause post-surgical complications such as adjacent intervertebral degeneration. Although several biomaterials has been tested for their biocompatibility, biodegradability and biomechanical properties and moreover the cytocomptibility, not all the biomaterials are suitable for every application (Hutmacher, 2000; Raghunath *et al.*, 2007; El-Ayoubi *et al.*, 2011). Therefore, many factors needs to be considered while selecting an appropriate material for the intervertebral disc nucleus pulposus (Goins *et al.*, 2005; Lewis, 2012b). With respect to intervertebral disc nucleus pulposus replacement, ideally, scaffold should be fatigue resistant and biologically compatible; wherein it should support function of cartilage matrix, and maintain their differentiated function and its architecture should define the ultimate shape of the new cartilage (Hutmacher, 2000; Stock and Vacanti, 2001). Moreover, scaffold should adequately fit into the defect site or require certain properties that offer minimal invasive implantation or injection with appropriate biocompatibility and biodegradability (Stock and Vacanti, 2001). Additionally, it does not have the potential to elicit an immunological or clinically detectable primary or secondary foreign body reactions (Hutmacher, 2000).

Currently considered nucleus pulposus implants made of hydrogels, polymers although have shown promising results, many issues such as viscoelastic properties, lack of tissue integration, implant expulsion etc. remain unreciprocated (Di Martino *et al.*, 2005; Goins *et al.*, 2005; Lewis, 2012b). In order to overcome these demerits, Buck GmbH & Co (Buck and Kaps, 2014) proposed a porous knitted titanium scaffold as an substitute mechanical scaffold. In this thesis, we have determined the effectiveness and cytocompatibility of knitted titanium scaffold mainly by investigating the cell material interactions. Although titanium alloy Ti-6Al-4V commonly used for pivot joint replacements (Lütjering and Williams, 2007), high stiffness often results in stress shielding, leading to implant resorption and ultimately failure. Thus, porous structure of titanium (Wang *et al.*, 2016) was then widely explored to facilitate vascularization and moreover the tissue integration.

The results described above highlight three main important issues in the emerging field of intervertebral disc nucleus pulposus replacement; in this thesis. First one is porous knitted titanium where we have shown the reproducible conditions with novel and defined physicochemical properties of knitted titanium can be done. Second is how electrochemical properties of the scaffold surface improve the wear resistance and controls the cellular behavior. Moreover, how the surface modification of the scaffold either by biochemical modification or by oxygen plasma treatment affects the cell material interactions. Thirdly, we demonstrated *in vitro* transcribed messenger RNA encoding Link N either unaided or together with knitted titanium scaffold as a promising strategy for repair while replacement.

Role of knitted titanium scaffold physicochemical properties and wear performance on the expression of cell behavior

In this thesis, we report a characterization of porous knitted titanium scaffold and a new approach to enhance cell material interaction. Spatial architecture of the knitted scaffold represents that pores are roughly heterogeneous with a porosity of roughly around 67.67 ± 10% and the average pore size of the scaffold was found to be 300 ± 159 μm. The results suggest that the pore size, porosity and moreover the bulk properties of the porous knitted titanium scaffold could be certainly, specifically and individually controlled. Axial compression testing revealed material elastic properties that were calculated from stress-strain relationship was approximately 20.85 MPa. The test results revealed that the values were comparable to cancellous bone (0.01–3.0 GPa) (Geetha *et al.*, 2009). Besides, the compressive strength of the knitted titanium scaffold could be tailored by regulating the orientation and distribution of the knitted titanium mesh, which thus likely to acquire the adequate biomechanics and the essential porous structure. Therefore, this method of production speculated to have significant advantage to overcome stress shielding effects and subsequent scaffold resorption which otherwise could cause scaffold failure.

The wear behavior of the scaffold was also investigated in this work. Based on the wear debris, generated after the biomechanical compression test of knitted titanium, cytokine profiling showed the production and interplay between key inflammatory mediators such as IL8, IL-1β, IL-6, TNF-α, MIP-1β, RANTES which may be attributed to the initial inflammatory action, contributing to atypical or enhanced pain sensitization (Ingham and Fisher, 2000). Wear debris that primarily generated at the bearing interface is one of the key

factors, which may shortens the longevity of the implant by causing mechanical instability, joint mobility restriction and increase in pain and consequently leads to revision of surgery (Schmiedberg *et al.*, 1994; Bobyn *et al.*, 1995; Kostuik, 1997; Cunningham, 2004; Park and Ryu, 2018). Previously, various studies have also demonstrated the correlation between wear particles and bone resorption (Schmiedberg *et al.*, 1994; Ingham and Fisher, 2000; Cunningham, 2004). At molecular level, interaction between the tumor necrosis factor (TNF-α) and the receptor activator of nuclear factor kappa-B ligand (RANKL) has been shown to promotes osteoclast activity, which is associated with wear debris (Cunningham, 2004). Such wear rate, however, were even lower upon electro-polishing treatment compare to unpolished knitted titanium scaffold. One possible reason for the difference was due to the change in surface roughness which led to cause the low friction. Song *et al*. have also demonstrated that the wear rate of the electro-polished titanium is low (Song *et al.*, 2007).

On the other hand, it has been reported that the wear particle characterization of unpolished and electro-polished scaffolds showed no subtle difference in terms of the number, volume and size based distribution, which otherwise has correlated in predicting wear rate and understanding the wear mechanism which plays a role in the progression of aseptic loosening (Sundfeldt *et al.*, 2006). Moreover, clearly visible wear debris accumulation is usually considered as a sign of too fast implant degradation and several studies have also documented wear debris prone scaffold failure *in vivo* (Ingham and Fisher, 2000). Whereas low burden of wear debris particles were observed in this study after electro-polishing treatment and based on our wear particles characterization results, indicating that the electro-polishing treatment reduced the wear rate of knitted titanium scaffold. The changing trends of surface roughness after the electro-polishing treatment did not affect the wettability of the scaffold and moreover the cellular behavior as well remained unaffected. These observations are consistent with a previous study which demonstrated that the surface energy than the surface roughness possess the more ability to modulate the cellular behavior (Hallab *et al.*, 2001). Electro-polishing the scaffold surface however did not change the compressive modulus and other physicochemical parameters such as pore size, wettability, surface chemistry. Titanium alloy based scaffold depicted weak hydrophilic surfaces; exhibiting the contact angle between 80-90°. An observed lowest wettability of knitted titanium scaffold is a result of a higher surface energy.

Hemocompatibility of the knitted titanium scaffold

The influence of electro-polishing treatment on knitted titanium scaffold surface on contact activation by whole human blood sample was tested. Specifically, the extent of activation of the common pathway of blood coagulation, of platelet activation and of the complement system were monitored by ELISA against specific marker proteins; namely thrombin-anti thrombin III (TAT) complexes, PMN elastase (platelet activation), and SC5b-9, respectively. In all cases, protein concentrations in partially-heparinized whole human blood before and after 90 min incubation with unpolished and electro-polished Ti scaffold were compared. Both types of scaffolds showed strong increase in SC5b-9, PMN elastase, β thromboglobulin, TAT concentrations with time; as a result of metal hyper-reactivity. Generally, blood clot formation and activation of blood coagulation factors are strongly time dependent (Milleret *et al.*, 2012), indicating potential amplification of initial contact activation by autocrine and paracrine mechanisms. Additionally, Gorbet and Sefton (Gorbet and Sefton, 2004) have recently proposed a model of time dependent biomaterial-associated thrombogenicity with a sequential change from contact activation of the blood clotting cascade, to platelet activation and later to leukocyte mediated activation of the tissue factor pathway as the primary source of thrombin activation and thrombogenicity. However, electro-polishing treatment did not significantly affect the activation of analyzed protein markers. Besides, there was no impact on the hemolysis and the destruction of blood cells, confirming the hemocompatibility of the knitted titanium scaffold.

Influence of electro-polishing treatment of knitted titanium scaffold on SCP1 cells and chondrocytes behavior *in vitro*

The *in vitro* biocompatibility of knitted titanium scaffold with respect to its ability to support mesenchymal stromal cells as well as human primary chondrocytes was determined by direct cell attachment and indirect cytotoxicity tests. The better cell attachment, growth as well as higher cell viability over the period of time on the unpolished knitted titanium scaffold resulted in no toxic effects of the scaffold. The results validated the positive implication of the titanium as a biomaterial (Tendulkar *et al.*, 2016; Tendulkar *et al.*, 2017). Moreover the porous knitted structure observed to support the functionality of both mesenchymal stromal cells as well as human primary chondrocytes with respect to cell adhesion, spreading, and proliferation. Further cyto-compatibility study illustrated the promise of electro-polished

knitted titanium scaffold held in replacing intervertebral disc nucleus pulposus. Electro-polishing treatment although change the surface roughness of knitted titanium scaffold (Tendulkar *et al.,* 2017), change in the wettability and calculated surface energy were remained in weak hydrophilic range. Initial events of cell material interaction *i.e.* cell adhesion and cytoskeleton organization with respect to cell spreading upon adherent cells were well spread on both type of scaffold surface. Although, the cell morphology on the scaffold surface is topography driven phenomenon (Ross *et al.,* 2012), submicron scale variation between the electro-polished and unpolished knitted titanium scaffold surface roughness did not marked any differences with respect to the cell morphology. We observed that focal contacts were well formed even on the electro-polished scaffold and cells were well spread oriented in the parallel direction on the surface grooves. Our results differ from that reported by Ross *et al.* (Ross *et al.,* 2012) who did observe the relationship between the cell adhesion and the surface roughness. Cell adhesion later directs the cellular events such as cell proliferation and differentiation which is as well influenced by the surface properties such as surface roughness, wettability and the surface energy (Boyan *et al.,* 1996). With respect to knitted titanium, we noticed insignificant differences with regards to cell proliferation of SCP1 cells and human primary chondrocytes on unpolished and electro-polished scaffold surface. A parallel to observation by Castellani *et al.* (Castellani *et al.,* 1999), who did not observe any difference with respect to cell proliferation on surface with different surface roughness, we certainly observed insignificant changed in the cell proliferation on the two different material surfaces of knitted titanium scaffold. Results are unlike to the previous studies on the effect of surface roughness on cell proliferation. Based on our results, the role of minor differences in the surface roughness of the material surface with knitted design doesn't seemed regulating the adherent cell percentage, cytoskeleton organization and ultimately the cell proliferation. *In vitro* results indeed indicated that electro-polished knitted titanium scaffold has a better biological profile, with respect to increased wear resistance and the initial cellular behavior on the scaffold surface. The influence of the subtle variation in the surface roughness did not change these characteristics. This offers the potential for further improvement in their biological performance by introducing surface modifications. Biomechanical performance of electro-polished knitted titanium scaffold further enhanced its mechanical properties. Additionally, cytoskeleton organization and percent cell adhesion did not change with the degree of the surface roughness of the knitted titanium surface, speculating wettability and not the surface roughness plays role determining the cellular behavior at the cell material interface. Besides, the role of surface energy and hydrophilicity

in directing the initial cellular events at the material interface has been studied by several groups, demonstrating that wettability is the most important than the surface roughness (Ranella *et al.*, 2010).

Role of scaffold wettability on the expression of cell behavior *in vitro*

Previously it has been reported that, modification of surface wettability effectively enhances the biological response (Gittens *et al.*, 2014; Rupp *et al.*, 2014). Scaffold surface properties such as composition, surface roughness, topography, surface energy and wettability synergistically or individually influence the cell response towards the material surface. The next aim of this study was therefore to elucidate the surface hydrophilisation effect, where oxygen plasma treatment was performed *in vitro*. The surface hydrophilisation has the advantage of generating super hydrophilic scaffold surface which thus increase the bioactivity of the metal surface as has been reported by others (Gittens *et al.*, 2014; Rupp *et al.*, 2014). Many different ways of surface hydrophilisation have been reported using titanium (Rupp *et al.*, 2014). Oxygen plasma treatment has shown the condition in which scaffold surface hydrophilisation can be achieved, thereby modulating physicochemical properties of electro-polished knitted titanium. With respect to knitted titanium scaffold, oxygen plasma treatment certainly achieved scaffold surface hydrophilisation thereby increase in the surface energy. Since surface energy is dominant property of a surface, the cell adhesion of SCP1 cells and human primary chondrocytes was higher on hydrophilised scaffold surface. The same reasoning can be given with regard to cell proliferation, where the percent cell adhesion was higher. Moreover with respect to knitted titanium scaffold, the cytoskeleton organization upon cell seeding of SCP1 cells as well as human primary chondrocytes on the surface was observed different where cells were fully spread and exhibited filopodial extensions from their surface on super-hydrophilised scaffold surface compare to control. Actin fibers arrangement thus illustrated a strong attachment on hydrophilised surface (Tendulkar *et al.*, 2017). Wei *et al.* observed similar kind of results with fully spread cell behavior (Wei *et al.*, 2009a). Furthermore, we could observe higher percent rate of cell attachment and consequently, cell proliferation was also higher on hydrophilised scaffold surface. Both these observations could be due to the increased surface wettability on oxygen plasma treated scaffold which subsequently increased the surface energy and thereby defined the strength of the cell material interactions. As surface wettability and cell proliferation is directly correlated, we indeed noticed a higher percent cell adhesion as well as cell proliferation on oxygen

plasma treated scaffold surface. Studies done by Wei *et al.* (Wei *et al.*, 2009b) and Oh *et al.* (Oh and Lee, 2013) have also shown similar behavior with regards to cell adhesion and cell proliferation on the hydrophilised surface. In agreement with these observations, we certainly achieved a super-hydrophilic scaffold surface which reacted better for cellular behavior compared to the untreated control electro-polished scaffold surface. Improved hydrophilised surface showed a positive influence on cell behavior in terms of cell viability, proliferation and the morphology; thus indicating a crucial role in mediating the cell response towards the scaffold surface.

Cell biological responses of SCP1 cells and chondrocytes upon covalent immobilization of ECM proteins on knitted titanium scaffold

Biomaterial surfaces modified with ECM proteins and cell binding motifs have been shown to improve the cell material interactions (Rapuano *et al.*, 2012a; Heller *et al.*, 2015), which subsequently leads to higher success rate of the scaffold. While, immobilized biomolecules interaction with scaffold surface is completely dependent on the scaffold physicochemical properties (Ducheyne, 2017). RGD (tripeptide consists of Arginine, Glycine, and Aspartate) motifs in fibronectin, collagen and hyaluronic acid have been shown to induce integrin mediated cell adhesion at cell material interface (Hersel *et al.*, 2003). The study demonstrates that, there was a significant effect of adsorbed collagen, hyaluronic acid and fibronectin on the chondrocytes attachment and proliferation on knitted titanium scaffold compared to uncoated control. On contrary, the study demonstrates that the cell attachment and moreover the proliferation of the SCP1 cells does not stimulated by coating the knitted titanium scaffold either with collagen, hyaluronic acid or fibronectin. However, in this study this effect was observed only during initial cell attachment upon coating the scaffold with collagen:hyaluronic acid. After one day of incubation no significant effect on cell proliferation could be observed. The competitive adsorption-desorption of fetal bovine serum (FCS) proteins (Tamaddon *et al.*, 2017) on coated and uncoated knitted titanium scaffold may have resulted in a continuously decreasing surface concentration of biomolecules with time, which subsequently limiting their favorable influence on the SCP1 cells. These results show that a collagen, hyaluronic acid or fibronectin coating does not stimulate the cell attachment or proliferation of mesenchymal stromal cells seeded on knitted titanium scaffold. However, the interaction between the biomolecules and the substratum may be important during the initial cell material interactions in the knitted titanium surface (Wilson *et al.*, 2005). It might

be possible that low concentration of biomolecules that was used for the immobilization was not sufficient to stimulate SCP1 cells but was enough to slightly enhance chondrocytes adhesion and proliferation.

Synthetically modified Link N mRNA and its combination with scaffold

Recently, messenger RNA (mRNA) has emerged as an alternative to viral vectors and plasmid based gene therapy. The advantage of mRNA delivery is that, cell cytoplasm entry followed by mRNA translation yields a production of a therapeutic protein, and therefore avoids the risk of insertional mutagenesis (Steinle *et al.*, 2017). Several approaches have been optimized and /or implemented in regards to mRNA stability and its translation (Karikó *et al.*, 2008; Kormann *et al.*, 2011; Avci-Adali *et al.*, 2014). Inclusion of chemically modified nucleotides, prolonging the poly (A) tail and the insertion of untranslated regions (UTRs) during *in vitro* transcription of mRNA plays a pivotal role in stability of resulting mRNA and protein translation (Avci-Adali *et al.*, 2014). On parallel, a transition of new therapeutic approach of mRNA therapy (Steinle *et al.*, 2017) in combination with biomaterial has gained substantial attention where the exogenous delivery of synthetic modified mRNA into cells, induces over expression of desired protein which they normally cannot produce or would naturally not need.

During musculoskeletal therapeutics, lack of intrinsic self-repair capacity in articular cartilage of joint tissue and IVDs (Richardson *et al.*, 2007), often prolongs or delays the healing. This is typically seen even after the implantation which frequently involves complications with delayed or nonunion defect (Panteli *et al.*, 2015). Despite some success with tissue engineering approach, these scaffolds often require a further stimulus to promote complete healing of cartilage and/or intervertebral disc defects (Vinatier and Guicheux, 2016). A well-known stimulus of cartilage formation is TGF-ß, bone morphogenetic protein (BMPs), which has already been extensively used in clinical applications (Badlani *et al.*, 2009; Yu and Hunter, 2016). Recently, Link protein N terminal short peptide (Link N), is gaining attention as a promising candidate for IVD repair (Gawri *et al.*, 2013a). Link N (DHLSDNYTLDHDRAIH) mainly stabilizes the proteoglycan aggregates. Previous reports have shown that Link N stimulates synthesis of proteoglycans and collagens in IVD (Mwale *et al.*, 2003). Also there are several parallel studies that have shown, Link N has a stronger chondrogenic potential (Mwale *et al.*, 2011a; Gawri *et al.*, 2013b; Mwale *et al.*, 2014; Bach *et al.*, 2017). Although

previous studies have applied the concept of Link N peptide delivery to establish IVD regeneration, in this study, we investigated a delivery of synthetically modified mRNA encoding Link N in primary human chondrocytes. An attempt to transcribed synthetically modified mRNA encoding Link N *in vitro* has been made by investigating the transfection efficiency and, the detrimental effect of mRNA transfection on the cell viability. 2D *in vitro* cell culture studies showed that the Link N mRNA delivery into the human primary chondrocytes and in SCP1 cells augmented the anabolic response. Taking the example of knitted titanium scaffold, we further aimed to generate a promising tool (Steinle *et al.*, 2017) to stimulate anabolic response in 3D cells culture.

While considering scaffold free approach, it may be necessary to use scaffold since it can serve as a load bearing structure to support biomechanical forces and thus provide stable microenvironment for tissue regeneration (Vinatier and Guicheux, 2016). Although biomaterials have been routinely used in musculoskeletal system, various strategies including surgeries and / or tissue engineering has been developed to improve articular cartilage and IVD repair for the treatment of severe fractures (Benneker *et al.*, 2014; Clouet *et al.*, 2018; Henry *et al.*, 2018). In order to improve the biomaterial's effectiveness, they can be commonly used as cell carriers and / or together with bioactive agents such as; growth factors. Encapsulation of bioactive agent in a biomaterial also increases their systemic and local delivery with increased bioavailability and stability thereby alleviating side effects over a longer period of time (Lee *et al.*, 2011). Therefore, The uses of growth factors, peptides, are one of the most successful approaches that have shown great efficacy into the clinic (Craik *et al.*, 2013). However, it is associated with many challenges like short half-life, rapid degradation *in vivo* due to oral administration, their hydrophilic nature prevents them to a large extent from getting past physiological obstacles.

Taking the advantage of mRNA therapeutics, our study showed that Link N mRNA delivery into the chondrocytes as well as in SCP1 cells seeded on the scaffolds, augmented chondrocyte specific gene expression. Moreover, together with knitted titanium scaffold we speculate that the phenotype of cells can be affected by the physical architecture of the scaffold and co-stimulation of Link N mRNA may functionally support the extracellular matrix production. The results were consistent with previous findings that Link N peptide supplements improved intervertebral disc regeneration (Mwale *et al.*, 2003; Mwale *et al.*, 2011a; Gawri *et al.*, 2013a; Gawri *et al.*, 2013b; Mwale *et al.*, 2014). Taking together, Link N

mRNA delivery speculated to be a potential candidate for further *in vivo* studies to enhance translation in musculoskeletal therapeutics.

In **conclusion**, the porous knitted titanium scaffold was successfully characterized. Their physicochemical properties such as porosity, pore size and subsequent mechanical properties can be precisely and individually controlled by changing the orientation of knitting structure of the titanium mesh without forgoing porous structure. Meanwhile, electro-polishing treatment functioned as a barrier for wear rate, helped increase the wear resistance. Cell adhesion, spreading and cell proliferation on the knitted titanium indicated the better cytocompatibility. Functional immobilization of ECM molecule on the knitted titanium scaffold, demonstrated the slight enhancement of cell adhesion and proliferation of chondrocytes but no significant impact on SCP1 cells compare to uncoated control. Therefore, further *in vivo* and *in vitro* investigations are needed to establish the ideal biochemical coating for the knitted titanium scaffold. Enhanced scaffold surface hydrophilicity attributed better cell material interaction, speculating surface energy and not the surface roughness plays important role directing cellular behavior. Biochemical scaffold surface modification using collagen, hyaluronic acid and fibronectin, did not stimulate initial cellular events at material interface. However, chondrocytes proliferation was moderately enhanced on coated scaffolds than control. Our discussion thus far has been limited to intervertebral disc nucleus pulposus replacement; however annulus fibrosis, endplate and vertebral body do play an important role being a part of disparate intervertebral disc tissue. The study as well investigated the strategy aimed at regenerating or repairing during the replacement of intervertebral disc nucleus pulposus that has mainly relied on the classical approach of using biomaterial, either unaided or in combination with growth factors at the site of injury. The synthetic modified Link N mRNA was successfully generated and the delivery of Link N mRNA into chondrocytes and SCP1 cells resulted in an anabolic response augmentation. In combination with a knitted titanium scaffold, Link N mRNA delivery also led to an increased expression of chondrocyte specific markers. Thereby, it was demonstrated that the Link N mRNA therapy could be combined for tissue engineering applications. Using this approach, the structural support, 3D environment, as well as the increased production of chondrocyte specific ECM proteins by Link N mRNA delivery can effectively stimulate the reparative events at the site of cartilage damage. The present study provides a first step toward mRNA-based approach to improve intervertebral disc regeneration.

Future directions:

Despite the fact that substantial progress has clearly been made toward engineering a functional replacement for the intervertebral disc nucleus pulposus, there are numerous challenges that certainly remained unaddressed if the knitted titanium scaffold is to be implemented clinically.

- We have used predefined scaffold for the cytocompatibility study. By varying the knitting pattern; effect of pore size and the porosity can further be evaluated to understand the better performance of the scaffold. The variation in the dimensions and moreover in the pore size and porosity could give useful insights by mimicking the *in vivo* environment as encountered by the cells upon scaffold implantation.
- The ability of the knitted titanium scaffold to support tissue growth could be further investigated by studying *in vivo*, where sheep / baboons could be used as an animal model. The scaffolds could be inserted in the region of the intervertebral disc nucleus pulposus and carefully monitoring the progress of the tissue formation around the scaffold by histochemical studies. Additionally, biomechanics as well could be investigated which is the at most criteria that scaffold has to fulfill.
- *In vivo* cytotoxicity of the scaffold could also be evaluated by investigating the wear rate and consequent release of metal ion into the blood stream and its possible effects if any.
- More detail *in vitro* investigation of messenger RNA encoding Link N needs to be done, in order to achieve sustain delivery either unaided or together with the scaffold to improve the functional potential.
- *In vivo* delivery of Link N messenger RNA into degenerated disc model could be attempted to investigate the therapeutic efficacy.

CHAPTER 7

5 Summary

Intervertebral disc degeneration is one of the many causative factors of chronic back pain. Severe trauma and / or aging can often induce irreversible structural damage of intervertebral disc leading to degeneration. This leads to functional deficit and consequently affects the quality of the life of patients. An effective treatment of intervertebral disc injuries is presently an utmost clinical need. In the cases where annular fibrosis is intact, a therapeutic invention such as intervertebral disc nucleus pulposus replacement can be beneficial.

This thesis demonstrates the cytocompatibility of knitted titanium scaffold as a replacement for the intervertebral disc nucleus pulposus thereby promoting it as a potential intervention to combat chronic back pain. Porous knitted titanium nucleus scaffold showed to support cellular behavior of bone marrow derived MSCs and human primary chondrocytes thereby promoting cell adhesion and cell spreading. It also exerted a strong effect on cell proliferation. Physicochemical properties of the scaffold which influence the biological function of cells can be enhanced by suitable surface modification treatments. In this way, the cell material interaction can be coupled to stimulate the cellular function leading to tissue integration. Furthermore, the scaffold surface modification results showed that electro-polishing treatment enhanced the propensity of scaffold to generate wear debris particles in low rate. Interestingly, wear particle characterization of unpolished and electro-polished scaffold showed no difference in terms of number, volume and size based distribution. Although, electro-polishing treatment significantly enhanced the surface roughness, its effective wettability remained unchanged. In response to change in surface roughness, bone marrow derived MSCs and human primary chondrocytes displayed negligible difference in cell adhesion, spreading and proliferation behavior. Consequences supported the possibility that, the surface energy is a dominating factor in promoting cell growth. Further outcome of the hemocompatibility tests demonstrated that, unpolished and electro-polished scaffold had negligible effect on hemolysis. Moreover, there was no significant difference between the unpolished and electro-polished scaffold. Thus, the study showed that the electro-polished knitted titanium scaffold based microstructure could hold good potential in positively regulating tissue replacement with respect to both biomechanics and cytocompatibility.

In order to further enhance the cell material interactions, scaffold surface modification using oxygen plasma treatment was eventually carried out. The effect of wettability on cellular behavior was investigated by generating super-hydrophilic scaffold surface, which was further confirmed by static and dynamic contact angle measurements. Based on *in vitro* results, super-hydrophilicity achieved upon oxygen plasma treatment was further evidenced by static and dynamic contact angle measurements. Super-hydrophilic surface based knitted titanium scaffold was then utilized to investigate the cell material interactions. MSCs and human primary chondrocytes seeded on the oxygen plasma treated scaffold elucidated significantly enhanced cellular response in terms of cell adhesion, spreading and proliferation. When compared to biological modification of the scaffold using collagen, hyaluronic acid and fibronectin, cellular response was seen to be much weaker. Thus super-hydrophilic scaffold surface constituted optimal microenvironment that could increase the ability of MSCs and human primary chondrocytes to induce tissue integration.

In order to enhance the reparative process in intervertebral disc tissue injuries by increasing the ECM synthesis and activating the biological cues, we further investigated the combined approach of synthetic Link N mRNA delivery together with the use of knitted titanium scaffold as a promising musculoskeletal therapeutics. Delivery of Link N mRNA unaided or together with a porous knitted titanium scaffold could provide local release of stimulatory factors. Link N mRNA delivery augmented anabolic response in human primary chondrocytes as well as in SCP1 cells thereby promoting matrix synthesis related gene expression. Together with the use of knitted titanium scaffold, we speculate that it may structurally support and functionally stimulate the reparative events. Furthermore, increased synthesis of specific extracellular matrix proteins could significantly improve the regenerative potential of tissue-engineered constructs.

Overall, we have shown for the first time the cytocompatibility of porous knitted titanium scaffold. Physicochemical characterization and cell material interactions gave us an insight into the cellular response upon a surface modification. While proposing a regenerative potential, a delivery of Link N mRNA together with the use of knitted titanium scaffold could be used as a likely therapeutic intervention in treating intervertebral disc degeneration.

6 Zusammenfassung

Die Bandscheibendegeneration ist eine von vielen Ursachen für chronische Rückenschmerzen. Schwere Traumata und / oder Alterung verursachen oft bleibende Strukturschäden an den Bandscheiben und führen somit zu deren Degeneration. Dies führt zum Verlust der Funktionalität der Bandscheiben und beeinflusst folglich negativ die Lebensqualität der Betroffenen. Eine effektive Behandlung der beschädigten Bandscheiben gehört heutzutage zu einer der größten klinischen Herausforderungen. Bei einem intakten Bandscheibenring (oder *anulus fibrosus*) könnte die Entwicklung eines therapeutischen einsetzbaren Bandscheibenersatzes von Vorteil sein.

Die vorliegende Arbeit untersuchte die Zytokompatibilität eines aus Titan gestrickten Scaffolds, welches als Ersatz für den Nucleus Pulposus einer Bandscheibe und somit als eine potenzielle Behandlung gegen chronische Rückenschmerzen dienen soll. Es konnte gezeigt werden, dass das poröse Titangestrick die zelluläre Aktivität humaner primärer Chondrozyten sowie mesenchymaler Stammzellen (MSCs), aus dem Knochenmark, unterstützt und die Zelladhäsion und Zellausbreitung fördert. Darüber hinaus, konnte eine starke Auswirkung auf Zellproliferation beobachtet werden. Die physikochemischen Eigenschaften des Titangestricks, welche die biologischen Funktionen der Zellen beeinflussen, können außerdem durch die entsprechenden Oberflächenmodifizierenden Behandlungen verbessert werden. Auf diese Weise kann, durch Zell – Material Interaktion, die zelluläre Funktion stimuliert werden, was zu einer möglichen Gewebeintegration führt. Die Ergebnisse der Oberflächenmodifikationen des Scaffolds zeigten darüber hinaus, dass sich durch die Elektropolitur die Menge an unerwünschten Abriebpartikel deutlich reduzieren lässt. Interessanterweise zeigten die Charakteristika der Abriebpartikeln von unpoliertem sowie elektropoliertem Titangestrick keine Unterschiede bezüglich der Anzahl, des Volumens und der größenbasierenden Verteilung. Obwohl die Behandlung mit Elektropolitur die Oberflächenbeschaffenheit signifikant verbesserte, blieb die effektive Benetzbarkeit der Oberfläche unverändert. In ihrer Reaktion auf die Veränderung in der Oberflächenkörnung, wiesen die mesenchymalen Stammzellen aus dem Knochenmark sowie die humane primären Chondrozyten nur geringere Unterschiede bezüglich der Zelladhäsion, -ausbreitung und Proliferation auf. Die Ergebnisse unterstützten die Annahme, dass die Oberflächenenergie ein dominierender Faktor in der Förderung des Zellwachstums sein kann. Weitere Ergebnisse der Hämokompatibilitätstests zeigten, dass nicht-polierte sowie elektropolierte Gestricke eher einen geringeren Einfluss auf die Hämolyse haben. Ferner, gab es keinen signifikanten

Unterschied zwischen den nicht-polierten und elektropolierten titangestrickten Scaffolds. Die Untersuchungen zeigten, dass die Mikrostruktur eines elektropolierten Titangestricks in Bezug auf Biomechanik und Zytokompatibilität ein großes Potenzial besitzt, um den Gewebeersatz positiv zu beeinflussen.

Um die Zell – Material Interaktion zu verbessern, wurde die Oberfläche im Folgenden mithilfe der Sauerstoffplasmabehandlung weiter modifiziert. Der Einfluss der Benetzbarkeit auf das zelluläre Verhalten wurde untersucht, indem eine superhydrophile Gerüstoberfläche erzeugt wurde, welche durch statische und dynamische Kontaktwinkelmessungen bestätigt wurde. Basierend auf In-vitro-Ergebnissen wurde die durch Sauerstoffplasmabehandlung erzielte Superhydrophilie durch statische und dynamische Kontaktwinkelmessungen bestätigt. Ein superhydrophiles oberflächenbasiertes gestricktes Titangerüst wurde daraufhin verwendet, um die Zellmaterialwechselwirkungen zu untersuchen. Es konnte gezeigt werden, dass mesenchymalen Stammzellen sowie humane primäre Chondrozyten eine verbesserte zelluläre Reaktion auf der mit dem Sauerstoff behandelten Oberfläche bezüglich der Zelladhäsion, Ausbreitung und Proliferation aufwiesen. Im Vergleich dazu fiel die Reaktion der Zellen nach biologischen Oberflächenmodifikationen mit Kollagen, Hyaluronsäure und Fibronectin deutlich schwächer aus. Somit stellt die superhydrophile Oberfläche des Scafflolds die optimale Mikroumgebung dar, welche die Fähigkeit der MSCs und humanen primären Chondrozyten verbessert, die Gewebeintegration zu induzieren.

Um die Wiederherstellungsprozesse in einem verletzten Knorpelgewebe durch Steigerung der ECM Synthese und Aktivierung der biologischen Signale zu verbessern, untersuchten wir des Weiteren den kombinierten Ansatz aus Zugabe des synthetischen Link N mRNA und Anwendung des Titangestricks als vielversprechende Behandlungsstrategie. Die Zugabe von Link N mRNA alleine oder zusammen mit dem Titangestrick wäre in der Lage stimulierende Faktoren lokal freizusetzten. Außerdem verstärkte die Zugabe von Link N mRNA die anabolische Antwort der humanen primären Chondrozyten sowie in SCP1 Zellen und unterstützt somit die mit der Matrixsynthese-verbundene Genexpression. Wir behaupten, dies könnte in Kombination mit dem Titangestrick die Wiederherstellungsprozesse strukturell unterstützen und funktionell stimulieren. Darüber hinaus könnte die gesteigerte Synthese der Chondrozyten-spezifischen extrazellulären Matrixproteine das regenerative Potenzial der Scaffolds signifikant verbessern.

Zusammenfassend konnten wir zum ersten Mal die Zytokompatibilität eines porösen titangestrickten Scaffolds zeigen. Die physikochemische Charakterisierung und die

Untersuchung der Zellmaterialwechselwirkungen gaben uns einen Einblick in die zelluläre Antwort auf die getesteten Oberflächenmodifikationen. Während ein regeneratives Potential vorgeschlagen wird, könnte eine Verabreichung von Link N mRNA zusammen mit der Verwendung von gestricktem Titangerüst als wahrscheinliche therapeutische Intervention bei der Behandlung von Bandscheibendegenerationen eingesetzt werden.

CHAPTER 8

7 References

Adams MA, Dolan P (2012) Intervertebral disc degeneration: evidence for two distinct phenotypes. J Anat **221**: 497-506.

Ahsan R, Tajima N, Chosa E, Sugamata M, Sumida M, Hamada M (2001) Biochemical and morphological changes in herniated human intervertebral disc. J Orthop Sci **6**: 510-518.

Aini H, Itaka K, Fujisawa A, Uchida H, Uchida S, Fukushima S, Kataoka K, Saito T, Chung UI, Ohba S (2016) Messenger RNA delivery of a cartilage-anabolic transcription factor as a disease-modifying strategy for osteoarthritis treatment. Sci Rep **6**: 18743.

Alghazali KM, Nima ZA, Hamzah RN, Dhar MS, Anderson DE, Biris AS (2015) Bone-tissue engineering: complex tunable structural and biological responses to injury, drug delivery, and cell-based therapies. Drug Metab Rev **47**: 431-454.

Alla RK, Ginjupalli K, Upadhya N, Shammas M, Ravi RK, Sekhar R (2011) Surface roughness of implants: a review. Trends in Biomaterials and Artificial Organs **25**: 112-118.

Allen MJ, Schoonmaker JE, Bauer TW, Williams PF, Higham PA, Yuan HA (2004) Preclinical evaluation of a poly (vinyl alcohol) hydrogel implant as a replacement for the nucleus pulposus. Spine (Phila Pa 1976) **29**: 515-523.

Antoniou J, Wang H, Alaseem A, Haglund L, Roughley P, Mwale F (2012a) The effect of Link N on differentiation of human bone marrow-derived mesenchymal stem cells. Arthritis Research & Therapy **14**.

Antoniou J, Wang HT, Alaseem AM, Haglund L, Roughley PJ, Mwale F (2012b) The effect of Link N on differentiation of human bone marrow-derived mesenchymal stem cells. Arthritis Research & Therapy **14**: R267 %@ 1478-6354.

Ao H, Lin C, Nie B, Yang S, Xie Y, Wan Y, Zheng X (2017) The synergistic effect of type I collagen and hyaluronic acid on the biological properties of Col/HA-multilayer-modified titanium coatings: an in vitro and in vivo study. RSC Advances **7**: 25828-25837.

Arnau JM, Vallano A, Lopez A, Pellisé F, Delgado MJ, Prat N (2006) A critical review of guidelines for low back pain treatment. Eur Spine J **15**: 543-553.

Assendelft WJ, Morton SC, Yu EI, Suttorp MJ, Shekelle PG (2004) Spinal manipulative therapy for low back pain. Cochrane Database Syst Rev: CD000447.

Att W, Hori N, Takeuchi M, Ouyang J, Yang Y, Anpo M, Ogawa T (2009) Time-dependent degradation of titanium osteoconductivity: an implication of biological aging of implant materials. Biomaterials **30**: 5352-5363.

Avci-Adali M, Behring A, Steinle H, Keller T, Krajeweski S, Schlensak C, Wendel HP (2014) In vitro synthesis of modified mRNA for induction of protein expression in human cells. J Vis Exp: e51943.

Bach F, Laagland L, Grant M, Creemers L, Ito K, Meij B, Mwale F, Tryfonidou M (2017) Link-N: The missing link towards intervertebral disc repair is species-specific. PLoS One **12**.

Bach FC, Willems N, Penning LC, Ito K, Meij BP, Tryfonidou MA (2014) Potential regenerative treatment strategies for intervertebral disc degeneration in dogs. BMC Vet Res **10**: 3.

Bachmeier BE, Nerlich A, Mittermaier N, Weiler C, Lumenta C, Wuertz K, Boos N (2009) Matrix metalloproteinase expression levels suggest distinct enzyme roles during lumbar disc herniation and degeneration. Eur Spine J **18**: 1573-1586.

Badlani N, Oshima Y, Healey R, Coutts R, Amiel D (2009) Use of bone morphogenic protein-7 as a treatment for osteoarthritis. Clin Orthop Relat Res **467**: 3221-3229.

Bain AC, Sherman T, Norton BK, Hutton WC (2000) A comparison of the viscoelastic behavior of the lumbar intervertebral disc before and after the implantation of a prosthetic disc nucleus. Asme-publications-BED **48**: 203-204.

Bao Q-B, Higham PA (1991)Hydrogel intervertebral disc nucleus. Google Patents.

Bao Q-B, Higham PA (1993)Hydrogel bead intervertebral disc nucleus. Google Patents.

Bao Q-B, Higham PA (1996)Hydrogel intervertebral disc nucleus with diminished lateral bulging. Google Patents.

Bao Q-B, Higham PA (2001)Hydrogel intervertebral disc nucleus implantation method. Google Patents.

Bao Q-B, Higham PA, Bagga CS, Yuan HA (1998)Method and apparatus for injecting an elastic spinal implant. Google Patents.

Bao Q-B, Yuan HA (2001)Implantable tissue repair device. Google Patents.

Bao QB, McCullen GM, Higham PA, Dumbleton JH, Yuan HA (1996) The artificial disc: theory, design and materials. Biomaterials **17**: 1157-1167.

Bao QB, Yuan HA (2000) Artificial disc technology. Neurosurg Focus **9**: e14.

Benneker LM, Andersson G, Iatridis JC, Sakai D, Härtl R, Ito K, Grad S (2014) Cell therapy for intervertebral disc repair: advancing cell therapy from bench to clinics. Eur Cell Mater **27**: 5-11.

Bertagnoli R, Sabatino CT, Edwards JT, Gontarz GA, Prewett A, Parsons JR (2005) Mechanical testing of a novel hydrogel nucleus replacement implant. Spine J **5**: 672-681.

Bettinger T, Carlisle RC, Read ML, Ogris M, Seymour LW (2001) Peptide-mediated RNA delivery: a novel approach for enhanced transfection of primary and post-mitotic cells. Nucleic acids research **29**: 3882-3891 %@ 1362-4962.

Bitar D, Parvizi J (2015) Biological response to prosthetic debris. World journal of orthopedics **6**: 172.

Bobyn JD, Jacobs JJ, Tanzer M, Urban RM, Aribindi R, Sumner DR, Turner TM, Brooks CE (1995) The susceptibility of smooth implant surfaces to periimplant fibrosis and migration of polyethylene wear debris. Clinical orthopaedics and related research: 21-39 %@ 0009-0921X.

Boyan BD, Hummert TW, Dean DD, Schwartz Z (1996) Role of material surfaces in regulating bone and cartilage cell response. Biomaterials **17**: 137-146.

Brånemark PI, Breine U, Johansson B, Roylance PJ, Röckert H, Yoffey JM (1964) Regeneration of bone marrow. Cells Tissues Organs **59**: 1-46 %@ 1422-6405.

Bridwell KH, Anderson PA, Boden SD, Vaccaro AR, Wang JC (2013) What's new in spine surgery. J Bone Joint Surg Am **95**: 1144-1150.

Brinjikji W, Luetmer PH, Comstock B, Bresnahan BW, Chen LE, Deyo RA, Halabi S, Turner JA, Avins AL, James K, Wald JT, Kallmes DF, Jarvik JG (2015) Systematic literature review of imaging features of spinal degeneration in asymptomatic populations. AJNR Am J Neuroradiol **36**: 811-816.

Buck AE, Kaps H-P (2014)Implant for surgical use in humans or vertebrates. Google Patents.

Buckwalter JA (1995) Aging and degeneration of the human intervertebral disc. Spine (Phila Pa 1976) **20**: 1307-1314.

Buric J, Pulidori M (2011) Long-term reduction in pain and disability after surgery with the interspinous device for intervertebral assisted motion (DIAM) spinal stabilization system in patients with low back pain: 4-year follow-up from a longitudinal prospective case series. Eur Spine J **20**: 1304-1311.

Burns K, Yao C, Webster TJ (2009) Increased chondrocyte adhesion on nanotubular anodized titanium. J Biomed Mater Res A **88**: 561-568.

Büttner-Janz K, Schellnack K, Zippel H (1989) Biomechanics of the SB Charite lumbar intervertebral disc endoprosthesis. International orthopaedics **13**: 173-176 %@ 0341-2695.

Cassinelli EH, Kang JD (2000) Current understanding of lumbar disc degeneration. Operative techniques in orthopaedics **10**: 254-262 %@ 1048-6666.

Castellani R, de Ruijter A, Renggli H, Jansen J (1999) Response of rat bone marrow cells to differently roughened titanium discs. Clinical oral implants research **10**: 369-378 %@ 0905-7161.

Chan BP, Leong KW (2008) Scaffolding in tissue engineering: general approaches and tissue-specific considerations. Eur Spine J **17 Suppl 4**: 467-479.

Chang H-I, Wang Y (2011)Cell responses to surface and architecture of tissue engineering scaffolds. In: Regenerative medicine and tissue engineering-cells and biomaterials, InTech.

Chen Q, Thouas GA (2015) Metallic implant biomaterials. Materials Science and Engineering: R: Reports **87**: 1-57 %@ 0927-0796X.

Cinotti G, David T, Postacchini F (1996) Results of Disc Prosthesis After a Minimum Follow-Up Period of 2 Years. Spine **21**: 995-1000 %@ 0362-2436.

Cleveland DA (1955) The use of methylacrylic for spinal stabilization after disc operations. Marquette Med Rev **20**: 62-64.

Clouet J, Fusellier M, Camus A, Le Visage C, Guicheux J (2018) Intervertebral disc regeneration: From cell therapy to the development of novel bioinspired endogenous repair strategies. Adv Drug Deliv Rev.

Colombier P, Clouet J, Hamel O, Lescaudron L, Guicheux J (2014) The lumbar intervertebral disc: from embryonic development to degeneration. Joint Bone Spine **81**: 125-129.

Coric D, Mummaneni PV (2008) Nucleus replacement technologies.

Costa Martínez E, Escobar Ivirico JL, Muñoz Criado I, Gómez Ribelles JL, Monleón Pradas M, Salmerón Sánchez M (2007) Effect of poly(L-lactide) surface topography on the morphology of in vitro cultured human articular chondrocytes. J Mater Sci Mater Med **18**: 1627-1632.

Craik DJ, Fairlie DP, Liras S, Price D (2013) The future of peptide-based drugs. Chemical biology & drug design **81**: 136-147 %@ 1747-0277.

Cramer Gregory, Darby, Susan (2014) Clinical Anatomy of the Spine, Spinal Cord, and ANS.

Cunningham BW (2004) Basic scientific considerations in total disc arthroplasty. Spine J **4**: 219S-230S.

De Bari C, Pitzalis C, Dell'Accio F (2006) Reparative medicine: from tissue engineering to joint surface regeneration. Regen Med **1**: 59-69.

de Kleuver M, Oner F, Jacobs W (2003) Total disc replacement for chronic low back pain: background and a systematic review of the literature. European Spine Journal **12**: 108-116.

de Schepper E, Damen J, van Meurs J, Ginai A, Popham M, Hofman A, Koes B, Bierma-Zeinstra S (2010) The Association Between Lumbar Disc Degeneration and Low Back Pain The Influence of Age, Gender, and Individual Radiographic Features. Spine **35**: 531-536.

Delamarter RB, Fribourg DM, Kanim LEA, Bae H (2003) ProDisc artificial total lumbar disc replacement: introduction and early results from the United States clinical trial. Spine **28**: S167-S175 %@ 0362-2436.

DePalma MJ, Ketchum JM, Saullo T (2011) What is the source of chronic low back pain and does age play a role? Pain Med **12**: 224-233.

Di Martino A, Vaccaro AR, Lee JY, Denaro V, Lim MR (2005) Nucleus pulposus replacement: basic science and indications for clinical use. Spine (Phila Pa 1976) **30**: S16-22.

Ding F, Shao ZW, Xiong LM (2013) Cell death in intervertebral disc degeneration. Apoptosis **18**: 777-785.

Dowling DP, Miller IS, Ardhaoui M, Gallagher WM (2011) Effect of surface wettability and topography on the adhesion of osteosarcoma cells on plasma-modified polystyrene. J Biomater Appl **26**: 327-347.

Ducheyne P (2017) Comprehensive Biomaterials II. Elsevier.

El-Ayoubi R, DeGrandpré C, DiRaddo R, Yousefi AM, Lavigne P (2011) Design and dynamic culture of 3D-scaffolds for cartilage tissue engineering. J Biomater Appl **25**: 429-444.

Eskola PJ, Lemmelä S, Kjaer P, Solovieva S, Männikkö M, Tommerup N, Lind-Thomsen A, Husgafvel-Pursiainen K, Cheung KM, Chan D, Samartzis D, Karppinen J (2012) Genetic association studies in lumbar disc degeneration: a systematic review. PLoS One **7**: e49995.

Fernstrom ULF (1966) Arthroplasty with intercorporal endoprothesis in herniated disc and in painful disc. Acta Chir Scand Suppl **357**: 154-159.

Fontana G, See E, Pandit A (2015) Current trends in biologics delivery to restore intervertebral disc anabolism. Adv Drug Deliv Rev **84**: 146-158.

Fosgerau K, Hoffmann T (2015) Peptide therapeutics: current status and future directions. Drug Discov Today **20**: 122-128.

Freemont A (2009a) The cellular pathobiology of the degenerate intervertebral disc and discogenic back pain. Rheumatology **48**: 5-10.

Freemont AJ (2009b) The cellular pathobiology of the degenerate intervertebral disc and discogenic back pain. Rheumatology (Oxford) **48**: 5-10.

Gawri R, Antoniou J, Ouellet J, Awwad W, Steffen T, Roughley P, Haglund L, Mwale F (2013a) Best paper NASS 2013: link-N can stimulate proteoglycan synthesis in the degenerated human intervertebral discs. Eur Cell Mater **26**: 107-119; discussion 119.

Gawri R, Antoniou J, Ouellet J, Awwad W, Steffen T, Roughley P, Haglund L, Mwale F (2013b) Link-N can stimulate proteoglycan synthesis in the degenerated human intervertebral discs. European Cells & Materials **26**: 107-119.

Gawri R, Ouellet J, Onnerfjord P, Alkhatib B, Steffen T, Heinegard D, Roughley P, Antoniou J, Mwale F, Haglund L (2014) Link N is Cleaved by Human Annulus Fibrosus Cells Generating a Fragment With Retained Biological Activity. Journal of Orthopaedic Research **32**: 1189-1197.

Geetha M, Singh AK, Asokamani R, Gogia AK (2009) Ti based biomaterials, the ultimate choice for orthopaedic implants–a review. Progress in materials science **54**: 397-425 %@ 0079-6425.

Gemmell CH (2001) Activation of platelets by in vitro whole blood contact with materials: increases in microparticle, procoagulant activity, and soluble P-selectin blood levels. Journal of Biomaterials Science, Polymer Edition **12**: 933-943 %@ 0920-5063.

Gittens RA, Scheideler L, Rupp F, Hyzy SL, Geis-Gerstorfer J, Schwartz Z, Boyan BD (2014) A review on the wettability of dental implant surfaces II: Biological and clinical aspects. Acta Biomater **10**: 2907-2918.

Goins ML, Wimberley DW, Yuan PS, Fitzhenry LN, Vaccaro AR (2005) Nucleus pulposus replacement: an emerging technology. Spine J **5**: 317S-324S.

Gorbet MB, Sefton MV (2004) Biomaterial-associated thrombosis: roles of coagulation factors, complement, platelets and leukocytes. Biomaterials **25**: 5681-5703 %@ 0142-9612.

Griffith LG, Naughton G (2002) Tissue engineering--current challenges and expanding opportunities. Science **295**: 1009-1014.

Guterl CC, See EY, Blanquer SB, Pandit A, Ferguson SJ, Benneker LM, Grijpma DW, Sakai D, Eglin D, Alini M, Iatridis JC, Grad S (2013) Challenges and strategies in the repair of ruptured annulus fibrosus. Eur Cell Mater **25**: 1-21.

Haldorsen EM, Kronholm K, Skouen JS, Ursin H (1998) Multimodal cognitive behavioral treatment of patients sicklisted for musculoskeletal pain: a randomized controlled study. Scand J Rheumatol **27**: 16-25.

Hallab NJ (2009) A review of the biologic effects of spine implant debris: Fact from fiction. SAS J **3**: 143-160 %@ 1935-9810.

Hallab NJ, Bundy KJ, O'Connor K, Moses RL, Jacobs JJ (2001) Evaluation of metallic and polymeric biomaterial surface energy and surface roughness characteristics for directed cell adhesion. Tissue engineering **7**: 55-71 %@ 1076-3279.

Hallab NJ, Singh V (2014)Intervertebral disc joint replacement technology. In: Joint Replacement Technology, Elsevier, pp 531-570.

Heller M, Kämmerer PW, Al-Nawas B, Luszpinski MA, Förch R, Brieger J (2015) The effect of extracellular matrix proteins on the cellular response of HUVECS and HOBS after covalent immobilization onto titanium. J Biomed Mater Res A **103**: 2035-2044.

Henry N, Clouet J, Le Bideau J, Le Visage C, Guioheux J (2018) Innovative strategies for intervertebral disc regenerative medicine: From cell therapies to multiscale delivery systems. Biotechnology Advances **36**: 281-294.

Hersel U, Dahmen C, Kessler H (2003) RGD modified polymers: biomaterials for stimulated cell adhesion and beyond. Biomaterials **24**: 4385-4415.

Hong J, Andersson J, Ekdahl KN, Elgue G, Axen N, Larsson R, Nilsson B (1999) Titanium is a highly thrombogenic biomaterial: possible implications for osteogenesis. Thrombosis and haemostasis **82**: 58-64 %@ 0340-6245.

Hoy D, Bain C, Williams G, March L, Brooks P, Blyth F, Woolf A, Vos T, Buchbinder R (2012) A systematic review of the global prevalence of low back pain. Arthritis Rheum **64**: 2028-2037.

Hsieh AH, Twomey JD (2010) Cellular mechanobiology of the intervertebral disc: new directions and approaches. J Biomech **43**: 137-145.

Huang YC, Hu Y, Li Z, Luk KDK (2018) Biomaterials for intervertebral disc regeneration: current status and looming challenges. J Tissue Eng Regen Med.

Hunter CJ, Matyas JR, Duncan NA (2004) Cytomorphology of notochordal and chondrocytic cells from the nucleus pulposus: a species comparison. J Anat **205**: 357-362.

Hussein MA, Mohammed AS, Al-Aqeeli N (2015) Wear characteristics of metallic biomaterials: a review. Materials **8**: 2749-2768.

Hutmacher DW (2000) Scaffolds in tissue engineering bone and cartilage. Biomaterials **21**: 2529-2543.

Iatridis JC, Weidenbaum M, Setton LA, Mow VC (1996) Is the nucleus pulposus a solid or a fluid? Mechanical behaviors of the nucleus pulposus of the human intervertebral disc. Spine **21**: 1174-1184 %@ 0362-2436.

Ingham E, Fisher J (2000) Biological reactions to wear debris in total joint replacement. Proc Inst Mech Eng H **214**: 21-37.

Ishihara H, Urban JP (1999) Effects of low oxygen concentrations and metabolic inhibitors on proteoglycan and protein synthesis rates in the intervertebral disc. J Orthop Res **17**: 829-835.

Jäger M, Zilkens C, Zanger K, Krauspe R (2007) Significance of nano-and microtopography for cell-surface interactions in orthopaedic implants. BioMed Research International 2007 %@ 1110-7243.

Javedan SP, Dickman CA (1999) Cause of adjacent-segment disease after spinal fusion. Lancet **354**: 530-531.

Jayaraman M, Meyer U, Bühner M, Joos U, Wiesmann HP (2004) Influence of titanium surfaces on attachment of osteoblast-like cells in vitro. Biomaterials **25**: 625-631.

Jiang L, Yuan F, Yin X, Dong J (2014) Responses and adaptations of intervertebral disc cells to microenvironmental stress: a possible central role of autophagy in the adaptive mechanism. Connect Tissue Res **55**: 311-321.

Jin D, Qu D, Zhao L, Chen J, Jiang J (2003) Prosthetic disc nucleus (PDN) replacement for lumbar disc herniation - Preliminary report with six months' follow-up. Journal of Spinal Disorders & Techniques **16**: 331-337.

Joshi A, Mehta S, Vresilovic E, Karduna A, Marcolongo M (2005) Nucleus implant parameters significantly change the compressive stiffness of the human lumbar intervertebral disc. J Biomech Eng **127**: 536-540.

Kang JD, Georgescu HI, McIntyre-Larkin L, Stefanovic-Racic M, Evans CH (1995) Herniated cervical intervertebral discs spontaneously produce matrix metalloproteinases, nitric oxide, interleukin-6, and prostaglandin E2. Spine (Phila Pa 1976) **20**: 2373-2378.

Kang JD, Stefanovic-Racic M, McIntyre LA, Georgescu HI, Evans CH (1997) Toward a biochemical understanding of human intervertebral disc degeneration and herniation:

contributions of nitric oxide, interleukins, prostaglandin E2, and matrix metalloproteinases. Spine **22**: 1065-1073 %@ 0362-2436.

Karikó K, Buckstein M, Ni H, Weissman D (2005) Suppression of RNA recognition by Toll-like receptors: the impact of nucleoside modification and the evolutionary origin of RNA. Immunity **23**: 165-175 %@ 1074-7613.

Karikó K, Muramatsu H, Welsh FA, Ludwig J, Kato H, Akira S, Weissman D (2008) Incorporation of pseudouridine into mRNA yields superior nonimmunogenic vector with increased translational capacity and biological stability. Molecular therapy **16**: 1833-1840 %@ 1525-0016.

Katti KS (2004) Biomaterials in total joint replacement. Colloids Surf B Biointerfaces **39**: 133-142.

Katz M, Fargnoli A, Williams R, Bridges C (2013) Gene Therapy Delivery Systems for Enhancing Viral and Nonviral Vectors for Cardiac Diseases: Current Concepts and Future Applications. Human Gene Therapy **24**: 914-927.

Kepler CK, Ponnappan RK, Tannoury CA, Risbud MV, Anderson DG (2013) The molecular basis of intervertebral disc degeneration. Spine J **13**: 318-330.

Kettler A, Kaps HP, Haegele B, Wilke HJ (2007) Biomechanical behavior of a new nucleus prosthesis made of knitted titanium filaments. SAS J **1**: 125-130.

Koes BW, van Tulder M, Lin CW, Macedo LG, McAuley J, Maher C (2010) An updated overview of clinical guidelines for the management of non-specific low back pain in primary care. Eur Spine J **19**: 2075-2094.

Kormann MSD, Hasenpusch G, Aneja MK, Nica G, Flemmer AW, Herber-Jonat S, Huppmann M, Mays LE, Illenyi M, Schams A (2011) Expression of therapeutic proteins after delivery of chemically modified mRNA in mice. Nature biotechnology **29**: 154 %@ 1546-1696.

Kostuik JP (1997) Intervertebral disc replacement. Experimental study. Clin Orthop Relat Res: 27-41.

Kurella A, Dahotre NB (2005) Review paper: surface modification for bioimplants: the role of laser surface engineering. J Biomater Appl **20**: 5-50.

Langrana N, Parsons J, Lee C, Vuonohawkins M, Yang S, Alexander H (1994) Materials and design concepts for an intervertebral disc spacer .I. fiber-reinforced composite design. Journal of Applied Biomaterials **5**: 125-132.

Le H, Sandhu FA, Fessler RG (2003) Clinical outcomes after minimal-access surgery for recurrent lumbar disc herniation. Neurosurg Focus **15**: E12.

Lee CK, Langrana NA, Parsons JR, Zimmerman MC (1991) Development of a prosthetic intervertebral disc. Spine (Phila Pa 1976) **16**: S253-255.

Lee K, Silva EA, Mooney DJ (2011) Growth factor delivery-based tissue engineering: general approaches and a review of recent developments. Journal of the Royal Society Interface **8**: 153-170 %@ 1742-5689.

Lewis G (2012a) Nucleus pulposus replacement and regeneration/repair technologies: Present status and future prospects. Journal of Biomedical Materials Research Part B-Applied Biomaterials **100B**: 1702-1720.

Lewis G (2012b) Nucleus pulposus replacement and regeneration/repair technologies: present status and future prospects. J Biomed Mater Res B Appl Biomater **100**: 1702-1720.

Lieberman JR, Ghivizzani SC, Evans CH (2002) Gene transfer approaches to the healing of bone and cartilage. Mol Ther **6**: 141-147.

Lim TKY, Anderson KM, Hari P, Di Falco M, Reihsen TE, Wilcox GL, Belani KG, LaBoissiere S, Pinto MR, Beebe DS, Kehl LJ, Stone LS (2017) Evidence for a Role of Nerve Injury in Painful Intervertebral Disc Degeneration: A Cross-Sectional Proteomic Analysis of Human Cerebrospinal Fluid. J Pain **18**: 1253-1269.

Liu M, Zeng X, Ma C, Yi H, Ali Z, Mou X, Li S, Deng Y, He N (2017) Injectable hydrogels for cartilage and bone tissue engineering. Bone Res **5**: 17014.

Lord MS, Foss M, Besenbacher F (2010) Influence of nanoscale surface topography on protein adsorption and cellular response. Nano Today **5**: 66-78 %@ 1748-0132.

Luoma K, Riihimäki H, Luukkonen R, Raininko R, Viikari-Juntura E, Lamminen A (2000) Low back pain in relation to lumbar disc degeneration. Spine (Phila Pa 1976) **25**: 487-492.

Lütjering G, Williams JC (2007) Beta Alloys. Springer.

MacGregor AJ, Andrew T, Sambrook PN, Spector TD (2004) Structural, psychological, and genetic influences on low back and neck pain: a study of adult female twins. Arthritis Rheum **51**: 160-167.

Malda J, Frondoza CG (2006) Microcarriers in the engineering of cartilage and bone. Trends in biotechnology **24**: 299-304 %@ 0167-7799.

Mallapragada S, Peppas N (1996) Dissolution mechanism of semicrystalline poly(vinyl alcohol) in water. Journal of Polymer Science Part B-Polymer Physics **34**: 1339-1346.

Mallapragada SK, Peppas NA, Colombo P (1997) Crystal dissolution-controlled release systems. II. Metronidazole release from semicrystalline poly(vinyl alcohol) systems. J Biomed Mater Res **36**: 125-130.

Mao Y, Li X (2014) Research Progress on the Biochemical Modification of Titanium Implant Surface. Medicinal Chemistry **4**: 742-747.

Masuda K, Lotz JC (2010) New challenges for intervertebral disc treatment using regenerative medicine. Tissue Eng Part B Rev **16**: 147-158.

McKenzie AH (1995) Fernstrom intervertebral disc arthroplasty: a long-term evaluation. Orthop Int **3**: 313-324.

McNally DS, Adams MA (1992) Internal intervertebral disc mechanics as revealed by stress profilometry. Spine (Phila Pa 1976) **17**: 66-73.

Melrose J (2016) Strategies in regenerative medicine for intervertebral disc repair using mesenchymal stem cells and bioscaffolds. Regenerative Medicine **11**: 705-724.

Milleret V, Hefti T, Hall H, Vogel V, Eberli D (2012) Influence of the fiber diameter and surface roughness of electrospun vascular grafts on blood activation. Acta biomaterialia **8**: 4349-4356 %@ 1742-7061.

Milner R, Arrowsmith P, Millan EJ (2001)Intervertebral disc implant. Google Patents.

Mitchell DA, Nair SK (2000) RNA-transfected dendritic cells in cancer immunotherapy. The Journal of clinical investigation **106**: 1065-1069 %@ 0021-9738.

Monteiro N, Martins A, Reis RL, Neves NM (2015) Nanoparticle-based bioactive agent release systems for bone and cartilage tissue engineering. Regenerative Therapy **1**: 109-118 %@ 2352-3204.

Moore RJ (2000) The vertebral end-plate: what do we know? Eur Spine J **9**: 92-96.

Morra M (2006) Biochemical modification of titanium surfaces: peptides and ECM proteins. Eur Cell Mater **12**: 15.

Murakami T, Sawae Y, Nakashima K, Fisher J (2000)Tribological behaviour of artificial cartilage in thin film lubrication. In: Tribology Series, Elsevier, pp 317-327 %@ 0167-8922.

Murphy CM, O'Brien FJ, Little DG, Schindeler A (2013) Cell-scaffold interactions in the bone tissue engineering triad.

Murray C, Vos T, Lozano R (2014) Disability-adjusted life years (DALYs) for 291 diseases and injuries in 21 regions, 1990-2010: a systematic analysis for the Global Burden of Disease Study 2010 (vol 380, pg 2197, 2012). Lancet **384**: 582-582.

Murray CJ, Vos T, Lozano R, Naghavi M, Flaxman AD, Michaud C, Ezzati M, Shibuya K, Salomon JA, Abdalla S, Aboyans V, Abraham J, Ackerman I, Aggarwal R, Ahn SY, Ali MK, Alvarado M, Anderson HR, Anderson LM, Andrews KG, Atkinson C, Baddour LM, Bahalim AN, Barker-Collo S, Barrero LH, Bartels DH, Basáñez MG, Baxter A, Bell ML, Benjamin EJ, Bennett D, Bernabé E, Bhalla K, Bhandari B, Bikbov B, Bin Abdulhak A, Birbeck G, Black JA, Blencowe H, Blore JD, Blyth F, Bolliger I, Bonaventure A, Boufous S, Bourne R, Boussinesq M, Braithwaite T, Brayne C, Bridgett L, Brooker S, Brooks P, Brugha TS, Bryan-Hancock C, Bucello C, Buchbinder R, Buckle G, Budke CM, Burch M, Burney P, Burstein R, Calabria B, Campbell B, Canter CE, Carabin H, Carapetis J, Carmona L, Cella C, Charlson F, Chen H, Cheng AT, Chou D, Chugh SS, Coffeng LE, Colan SD, Colquhoun S, Colson KE, Condon J, Connor MD, Cooper LT, Corriere M, Cortinovis M, de Vaccaro KC, Couser W, Cowie BC, Criqui MH, Cross M, Dabhadkar KC, Dahiya M, Dahodwala N, Damsere-Derry J, Danaei G, Davis A, De Leo D, Degenhardt L, Dellavalle R, Delossantos A, Denenberg J, Derrett S, Des Jarlais DC, Dharmaratne SD, Dherani M, Diaz-Torne C, Dolk H, Dorsey ER, Driscoll T, Duber H, Ebel B, Edmond K, Elbaz A, Ali SE, Erskine H, Erwin PJ, Espindola P, Ewoigbokhan SE, Farzadfar F, Feigin V, Felson DT, Ferrari A, Ferri CP, Fèvre EM, Finucane MM, Flaxman S, Flood L, Foreman K, Forouzanfar MH, Fowkes FG, Fransen M, Freeman MK, Gabbe BJ, Gabriel SE, Gakidou E, Ganatra HA, Garcia B, Gaspari F, Gillum RF, Gmel G, Gonzalez-Medina D, Gosselin R, Grainger R, Grant B, Groeger J, Guillemin F, Gunnell D, Gupta R, Haagsma J, Hagan H, Halasa YA, Hall W, Haring D, Haro JM, Harrison JE, Havmoeller R, Hay RJ, Higashi H, Hill C, Hoen B, Hoffman H, Hotez PJ, Hoy D, Huang JJ, Ibeanusi SE, Jacobsen KH, James SL, Jarvis D, Jasrasaria R, Jayaraman S, Johns N, Jonas JB, Karthikeyan G, Kassebaum N, Kawakami N, Keren A, Khoo JP, King CH, Knowlton LM, Kobusingye O, Koranteng A, Krishnamurthi R, Laden F, Lalloo R, Laslett LL, Lathlean T, Leasher JL, Lee YY, Leigh J, Levinson D, Lim SS, Limb E, Lin JK, Lipnick M, Lipshultz SE, Liu W, Loane M, Ohno SL, Lyons R, Mabweijano J, MacIntyre MF, Malekzadeh R, Mallinger L, Manivannan S, Marcenes W, March L, Margolis DJ, Marks GB, Marks R, Matsumori A, Matzopoulos R, Mayosi BM, McAnulty JH, McDermott MM, McGill N, McGrath J, Medina-Mora ME, Meltzer M, Mensah GA, Merriman TR, Meyer AC, Miglioli V, Miller M, Miller TR, Mitchell PB, Mock C, Mocumbi AO, Moffitt TE, Mokdad AA, Monasta L, Montico M, Moradi-Lakeh M, Moran A, Morawska L, Mori R, Murdoch ME, Mwaniki MK, Naidoo K, Nair MN, Naldi L, Narayan KM, Nelson PK, Nelson RG, Nevitt MC, Newton CR, Nolte S, Norman P, Norman R, O'Donnell M, O'Hanlon S, Olives C, Omer SB, Ortblad K, Osborne R, Ozgediz D, Page A, Pahari B, Pandian JD, Rivero AP, Patten SB,

Pearce N, Padilla RP, Perez-Ruiz F, Perico N, Pesudovs K, Phillips D, Phillips MR, Pierce K, Pion S, Polanczyk GV, Polinder S, Pope CA, Popova S, Porrini E, Pourmalek F, Prince M, Pullan RL, Ramaiah KD, Ranganathan D, Razavi H, Regan M, Rehm JT, Rein DB, Remuzzi G, Richardson K, Rivara FP, Roberts T, Robinson C, De Leòn FR, Ronfani L, Room R, Rosenfeld LC, Rushton L, Sacco RL, Saha S, Sampson U, Sanchez-Riera L, Sanman E, Schwebel DC, Scott JG, Segui-Gomez M, Shahraz S, Shepard DS, Shin H, Shivakoti R, Singh D, Singh GM, Singh JA, Singleton J, Sleet DA, Sliwa K, Smith E, Smith JL, Stapelberg NJ, Steer A, Steiner T, Stolk WA, Stovner LJ, Sudfeld C, Syed S, Tamburlini G, Tavakkoli M, Taylor HR, Taylor JA, Taylor WJ, Thomas B, Thomson WM, Thurston GD, Tleyjeh IM, Tonelli M, Towbin JA, Truelsen T, Tsilimbaris MK, Ubeda C, Undurraga EA, van der Werf MJ, van Os J, Vavilala MS, Venketasubramanian N, Wang M, Wang W, Watt K, Weatherall DJ, Weinstock MA, Weintraub R, Weisskopf MG, Weissman MM, White RA, Whiteford H, Wiebe N, Wiersma ST, Wilkinson JD, Williams HC, Williams SR, Witt E, Wolfe F, Woolf AD, Wulf S, Yeh PH, Zaidi AK, Zheng ZJ, Zonies D, Lopez AD, AlMazroa MA, Memish ZA (2012) Disability-adjusted life years (DALYs) for 291 diseases and injuries in 21 regions, 1990-2010: a systematic analysis for the Global Burden of Disease Study 2010. Lancet **380**: 2197-2223.

Mwale F, Demers CN, Petit A, Roughley P, Poole AR, Steffen T, Aebi M, Antoniou J (2003) A synthetic peptide of link protein stimulates the biosynthesis of collagens II, IX and proteoglycan by cells of the intervertebral disc. J Cell Biochem **88**: 1202-1213.

Mwale F, Masuda K, Pichika R, Epure L, Yoshikawa T, Hemmad A, Roughley P, Antoniou J (2011a) The efficacy of Link N as a mediator of repair in a rabbit model of intervertebral disc degeneration. Arthritis Research & Therapy **13**.

Mwale F, Masuda K, Pichika R, Epure LM, Yoshikawa T, Hemmad A, Roughley PJ, Antoniou J (2011b) The efficacy of Link N as a mediator of repair in a rabbit model of intervertebral disc degeneration. Arthritis Research & Therapy **13**: R120 %@ 1478-6354.

Mwale F, Roughley P, Antoniou J (2004) Distinction between the extracellular matrix of the nucleus pulposus and hyaline cartilage: a requisite for tissue engineering of intervertebral disc. Eur Cell Mater **8**: 58-63; discussion 63-54.

Mwale F, Wang H, Roughley P, Antoniou J, Haglund L (2014) Link N and Mesenchymal Stem Cells Can Induce Regeneration of the Early Degenerate Intervertebral Disc. Tissue Engineering Part a **20**: 2942-2949.

Nallagatla SR, Bevilacqua PC (2008) Nucleoside modifications modulate activation of the protein kinase PKR in an RNA structure-specific manner. Rna **14**: 1201-1213 %@ 1355-8382.

Nerurkar NL, Elliott DM, Mauck RL (2010) Mechanical design criteria for intervertebral disc tissue engineering. J Biomech **43**: 1017-1030.

Neves SC, Teixeira LSM, Moroni L, Reis RL, Van Blitterswijk CA, Alves NM, Karperien M, Mano JF (2011) Chitosan/Poly (ε-caprolactone) blend scaffolds for cartilage repair. Biomaterials **32**: 1068-1079 %@ 0142-9612.

Niinomi M (2007) Fatigue characteristics of metallic biomaterials. International Journal of Fatigue **29**: 992-1000 %@ 0142-1123.

Nishimura T, Ogino Y, Ayukawa Y, Koyano K (2018) Influence of the wettability of different titanium surface topographies on initial cellular behavior. Dent Mater J **37**: 650-658.

Noble PW (2002) Hyaluronan and its catabolic products in tissue injury and repair. Matrix Biol **21**: 25-29.

Oh SH, Lee JH (2013) Hydrophilization of synthetic biodegradable polymer scaffolds for improved cell/tissue compatibility. Biomedical Materials **8**: 014101 %@ 011748-014605X.

Ohnishi T, Sudo H, Tsujimoto T, Iwasaki N (2018) Age-related spontaneous lumbar intervertebral disc degeneration in a mouse model. J Orthop Res **36**: 224-232.

Olivares-Navarrete R, Lee EM, Smith K, Hyzy SL, Doroudi M, Williams JK, Gall K, Boyan BD, Schwartz Z (2017) Substrate Stiffness Controls Osteoblastic and Chondrocytic Differentiation of Mesenchymal Stem Cells without Exogenous Stimuli. PLoS One **12**: e0170312.

Osti OL, Vernon-Roberts B, Moore R, Fraser RD (1992) Annular tears and disc degeneration in the lumbar spine. A post-mortem study of 135 discs. J Bone Joint Surg Br **74**: 678-682.

Panteli M, Pountos I, Jones E, Giannoudis PV (2015) Biological and molecular profile of fracture non-union tissue: current insights. J Cell Mol Med **19**: 685-713.

Park CK, Ryu KS (2018) Are Controversial Issues in Cervical Total Disc Replacement Resolved or Unresolved?: A Review of Literature and Recent Updates. Asian Spine J **12**: 178-192.

Patel S, Caldwell JM, Doty SB, Levine WN, Rodeo S, Soslowsky LJ, Thomopoulos S, Lu HH (2018) Integrating soft and hard tissues via interface tissue engineering. J Orthop Res **36**: 1069-1077.

Pattappa G, Li Z, Peroglio M, Wismer N, Alini M, Grad S (2012) Diversity of intervertebral disc cells: phenotype and function. J Anat **221**: 480-496.

Pohler OE (2000) Unalloyed titanium for implants in bone surgery. Injury **31 Suppl 4**: 7-13.

Puleo DA, Nanci A (1999) Understanding and controlling the bone-implant interface. Biomaterials **20**: 2311-2321.

Putz RL, Müller-Gerbl M (1996) The vertebral column--a phylogenetic failure? A theory explaining the function and vulnerability of the human spine. Clin Anat **9**: 205-212.

Raghunath J, Rollo J, Sales KM, Butler PE, Seifalian AM (2007) Biomaterials and scaffold design: key to tissue-engineering cartilage. Biotechnol Appl Biochem **46**: 73-84.

Raj PP (2008) Intervertebral disc: anatomy-physiology-pathophysiology-treatment. Pain Pract **8**: 18-44.

Ranella A, Barberoglou M, Bakogianni S, Fotakis C, Stratakis E (2010) Tuning cell adhesion by controlling the roughness and wettability of 3D micro/nano silicon structures. Acta biomaterialia **6**: 2711-2720 %@ 1742-7061.

Rapuano BE, Hackshaw KM, Schniepp HC, MacDonald DE (2012a) Effects of coating a titanium alloy with fibronectin on the expression of osteoblast gene markers in the MC3T3 osteoprogenitor cell line. Int J Oral Maxillofac Implants **27**: 1081-1090.

Rapuano BE, Hackshaw KM, Schniepp HC, MacDonald DE (2012b) Effects of coating a titanium alloy with fibronectin on the expression of osteoblast gene markers in the MC3T3 osteoprogenitor cell line. The International journal of oral & maxillofacial implants **27**: 1081.

Ray CD (2002) The PDN prosthetic disc-nucleus device. Eur Spine J **11 Suppl 2**: S137-142.

Ray CD, Brock M, Mayer HM, Weigel K (1991) Lumbar Interbody Threaded Prostheses. Springer Berlin Heidelberg, Berlin, Heidelberg.

Ray CD, Dickhudt EA, Assell RL (1998)Prosthetic spinal disc nucleus. Google Patents.

Ray CD, Dickhudt EA, Ledoux PJ, Frutiger BA (1997)Prosthetic spinal disc nucleus. Google Patents.

Ray CDaC, T.P. (1988)Prosthetic disc and method of implanting.

Ray CDaC, T.P. (1990)Prosthetic disc containing therapeutic material. US.

Reeks J, Liang H (2015) Materials and their failure mechanisms in total disc replacement. Lubricants **3**: 346-364.

Richardson S, Mobasheri A, Freemont A, Hoyland J (2007) Intervertebral disc biology, degeneration and novel tissue engineering and regenerative medicine therapies. Histology and Histopathology **22**: 1033-1041.

Risbud MV, Shapiro IM (2011) Notochordal cells in the adult intervertebral disc: new perspective on an old question. Crit Rev Eukaryot Gene Expr **21**: 29-41.

Roberts S, Evans H, Trivedi J, Menage J (2006) Histology and pathology of the human intervertebral disc. J Bone Joint Surg Am **88 Suppl 2**: 10-14.

Ross AM, Jiang Z, Bastmeyer M, Lahann J (2012) Physical aspects of cell culture substrates: topography, roughness, and elasticity. Small **8**: 336-355.

Roughley PJ (2004) Biology of intervertebral disc aging and degeneration: involvement of the extracellular matrix. Spine (Phila Pa 1976) **29**: 2691-2699.

Rupp F, Gittens RA, Scheideler L, Marmur A, Boyan BD, Schwartz Z, Geis-Gerstorfer J (2014) A review on the wettability of dental implant surfaces I: theoretical and experimental aspects. Acta Biomater **10**: 2894-2906.

Rutges JP, Duit RA, Kummer JA, Bekkers JE, Oner FC, Castelein RM, Dhert WJ, Creemers LB (2013) A validated new histological classification for intervertebral disc degeneration. Osteoarthritis Cartilage **21**: 2039-2047.

Sakai D, Schol J (2017) Cell therapy for intervertebral disc repair: Clinical perspective. J Orthop Translat **9**: 8-18.

Schizas C, Kulik G, Kosmopoulos V (2010) Disc degeneration: current surgical options. Eur Cell Mater **20**: 306-315.

Schmiedberg SK, Chang DH, Frondoza CG, Valdevit AD, Kostuik JP (1994) Isolation and characterization of metallic wear debris from a dynamic intervertebral disc prosthesis. J Biomed Mater Res **28**: 1277-1288.

Schnitzer TJ (2006) Update on guidelines for the treatment of chronic musculoskeletal pain. Clin Rheumatol **25 Suppl 1**: S22-29.

Schwartz Z, Martin JY, Dean DD, Simpson J, Cochran DL, Boyan BD (1996) Effect of titanium surface roughness on chondrocyte proliferation, matrix production, and differentiation depends on the state of cell maturation. Journal of Biomedical Materials Research: An Official Journal of The Society for Biomaterials and The Japanese Society for Biomaterials **30**: 145-155 %@ 0021-9304.

Setton LA, Chen J (2006) Mechanobiology of the intervertebral disc and relevance to disc degeneration. J Bone Joint Surg Am **88 Suppl 2**: 52-57.

Shamji MF, Setton LA, Jarvis W, So S, Chen J, Jing L, Bullock R, Isaacs RE, Brown C, Richardson WJ (2010) Proinflammatory cytokine expression profile in degenerated and herniated human intervertebral disc tissues. Arthritis Rheum **62**: 1974-1982.

Shim CS, Lee SH, Park CW, Choi WC, Choi G, Choi WG, Lim SR, Lee HY (2003) Partial disc replacement with the PDN prosthetic disc nucleus device: early clinical results. J Spinal Disord Tech **16**: 324-330.

Shiri R, Karppinen J, Leino-Arjas P, Solovieva S, Viikari-Juntura E (2010) The association between smoking and low back pain: a meta-analysis. Am J Med **123**: 87.e87-35.

Silva TSN, Machado DC, Viezzer C, Júnior S, Novaes A, Oliveira MGd (2009) Effect of titanium surface roughness on human bone marrow cell proliferation and differentiation: an experimental study. Acta cirurgica brasileira **24**: 200-205 %@ 0102-8650.

Singh AV, Patil R, Thombre DK, Gade WN (2013) Micro-nanopatterning as tool to study the role of physicochemical properties on cell–surface interactions. Journal of Biomedical Materials Research Part A **101**: 3019-3032 %@ 1549-3296.

Singh K, Masuda K, Thonar EJ, An HS, Cs-Szabo G (2009) Age-related changes in the extracellular matrix of nucleus pulposus and anulus fibrosus of human intervertebral disc. Spine (Phila Pa 1976) **34**: 10-16.

Smith LJ, Fazzalari NL (2009) The elastic fibre network of the human lumbar anulus fibrosus: architecture, mechanical function and potential role in the progression of intervertebral disc degeneration. Eur Spine J **18**: 439-448.

Song H-J, Kim M-K, Jung G-C, Vang M-S, Park Y-J (2007) The effects of spark anodizing treatment of pure titanium metals and titanium alloys on corrosion characteristics. Surface and Coatings Technology **201**: 8738-8745 %@ 0257-8972.

Stammen JA, Williams S, Ku DN, Guldberg RE (2001) Mechanical properties of a novel PVA hydrogel in shear and unconfined compression. Biomaterials **22**: 799-806.

Steinle H, Behring A, Schlensak C, Wendel HP, Avci-Adali M (2017) Concise Review: Application of In Vitro Transcribed Messenger RNA for Cellular Engineering and Reprogramming: Progress and Challenges. Stem Cells **35**: 68-79.

Stock UA, Vacanti JP (2001) Tissue engineering: current state and prospects. Annu Rev Med **52**: 443-451.

Stratton S, Shelke NB, Hoshino K, Rudraiah S, Kumbar SG (2016) Bioactive polymeric scaffolds for tissue engineering. Bioact Mater **1**: 93-108.

Sundfeldt M, V Carlsson L, B Johansson C, Thomsen P, Gretzer C (2006) Aseptic loosening, not only a question of wear: a review of different theories. Acta orthopaedica **77**: 177-197 %@ 1745-3674.

Suri P, Pearson AM, Scherer EA, Zhao W, Lurie JD, Morgan TS, Weinstein JN (2016) Recurrence of pain after usual nonoperative care for symptomatic lumbar disk herniation: analysis of data from the Spine Patient Outcomes Research Trial. PM&R **8**: 405-414 %@ 1934-1482.

Szpalski M, Gunzburg R, Mayer M (2002) Spine arthroplasty: a historical review. Eur Spine J **11 Suppl 2**: S65-84.

Tallawi M, Rosellini E, Barbani N, Cascone MG, Rai R, Saint-Pierre G, Boccaccini AR (2015) Strategies for the chemical and biological functionalization of scaffolds for cardiac tissue engineering: a review. J R Soc Interface **12**: 20150254.

Tamaddon M, Samizadeh S, Wang L, Blunn G, Liu C (2017) Intrinsic Osteoinductivity of Porous Titanium Scaffold for Bone Tissue Engineering. Int J Biomater **2017**: 5093063.

Tavernier G, Andries O, Demeester J, Sanders NN, De Smedt SC, Rejman J (2011) mRNA as gene therapeutic: how to control protein expression. Journal of controlled release **150**: 238-247 %@ 0168-3659.

Tendulkar G, Grau P, Ziegler P, Buck A, Badke A, Kaps HP, Ehnert S, Nussler AK (2016) Imaging Cell Viability on Non-transparent Scaffolds - Using the Example of a Novel Knitted Titanium Implant. J Vis Exp.

Tendulkar G, Sreekumar V, Rupp F, Teotia AK, Athanasopulu K, Kemkemer R, Buck A, Kaps HP, Geis-Gerstorfer J, Kumar A, Nussler AK (2017) Characterisation of porous knitted titanium for replacement of intervertebral disc nucleus pulposus. Sci Rep **7**: 16611.

Thomas J, Lowman A, Marcolongo M (2003) Novel associated hydrogels for nucleus pulposus replacement. J Biomed Mater Res A **67**: 1329-1337.

Urban J, Roberts S (2003) Degeneration of the intervertebral disc. Arthritis Research & Therapy **5**: 120-130.

Urban JP, Smith S, Fairbank JC (2004) Nutrition of the intervertebral disc. Spine (Phila Pa 1976) **29**: 2700-2709.

Vadalà G, Mozetic P, Rainer A, Centola M, Loppini M, Trombetta M, Denaro V (2012) Bioactive electrospun scaffold for annulus fibrosus repair and regeneration. Eur Spine J **21 Suppl 1**: S20-26.

Vaday GG, Lider O (2000) Extracellular matrix moieties, cytokines, and enzymes: dynamic effects on immune cell behavior and inflammation. J Leukoc Biol **67**: 149-159.

van den Eerenbeemt KD, Ostelo RW, van Royen BJ, Peul WC, van Tulder MW (2010) Total disc replacement surgery for symptomatic degenerative lumbar disc disease: a systematic review of the literature. Eur Spine J **19**: 1262-1280.

van Tulder M, Koes B, Malmivaara A (2006) Outcome of non-invasive treatment modalities on back pain: an evidence-based review. European Spine Journal **15**: S64-S81.

van Uden S, Silva-Correia J, Oliveira JM, Reis RL (2017) Current strategies for treatment of intervertebral disc degeneration: substitution and regeneration possibilities. Biomater Res **21**: 22.

Vinatier C, Guicheux J (2016) Cartilage tissue engineering: From biomaterials and stem cells to osteoarthritis treatments. Ann Phys Rehabil Med **59**: 139-144.

Vlieghe P, Lisowski V, Martinez J, Khrestchatisky M (2010) Synthetic therapeutic peptides: science and market. Drug Discovery Today **15**: 40-56.

Waldrop R, Cheng J, Devin C, McGirt M, Fehlings M, Berven S (2015) The Burden of Spinal Disorders in the Elderly. Neurosurgery **77 Suppl 4**: S46-50.

Walker MH, Anderson DG (2004) Molecular basis of intervertebral disc degeneration. Spine J **4**: 158S-166S.

Walter BA, Torre OM, Laudier D, Naidich TP, Hecht AC, Iatridis JC (2015) Form and function of the intervertebral disc in health and disease: a morphological and stain comparison study. J Anat **227**: 707-716.

Wang X, Xu S, Zhou S, Xu W, Leary M, Choong P, Qian M, Brandt M, Xie YM (2016) Topological design and additive manufacturing of porous metals for bone scaffolds and orthopaedic implants: A review. Biomaterials **83**: 127-141.

Wang Y, Yi X-D (2017) The influence of artificial nucleus pulposus replacement on stress distribution in the cartilaginous endplate in a 3-dimensional finite element model of the lumbar intervertebral disc. Medicine **96**.

Wang Z, Hutton WC, Yoon ST (2013) ISSLS Prize winner: Effect of link protein peptide on human intervertebral disc cells. Spine (Phila Pa 1976) **38**: 1501-1507.

Wei J, Igarashi T, Okumori N, Igarashi T, Maetani T, Liu B, Yoshinari M (2009a) Influence of surface wettability on competitive protein adsorption and initial attachment of osteoblasts. Biomedical Materials **4**: 045002 %@ 041748-045605X.

Wei J, Igarashi T, Okumori N, Maetani T, Liu B, Yoshinari M (2009b) Influence of surface wettability on competitive protein adsorption and initial attachment of osteoblasts. Biomed Mater **4**: 045002.

Wennerberg A, Galli S, Albrektsson T (2011) Current knowledge about the hydrophilic and nanostructured SLActive surface. Clin Cosmet Investig Dent **3**: 59-67.

Werber A, Schiltenwolf M (2016) Treatment of Lower Back Pain-The Gap between Guideline-Based Treatment and Medical Care Reality. Healthcare (Basel) **4**.

Wilson CJ, Clegg RE, Leavesley DI, Pearcy MJ (2005) Mediation of biomaterial-cell interactions by adsorbed proteins: a review. Tissue Eng **11**: 1-18.

Wong CN-C, Yu JM-K, Law S-W, Lau HM-C, Chan CK-M (2010) Bilateral transtibial amputation with concomitant thoracolumbar vertebral collapse in a Sichuan earthquake survivor. Journal of orthopaedic surgery and research **5**: 43 %@ 1749-1799X.

Yamaguchi M, Shinbo T, Kanamori T, Wang PC, Niwa M, Kawakami H, Nagaoka S, Hirakawa K, Kamiya M (2004) Surface modification of poly(L: -lactic acid) affects initial cell attachment, cell morphology, and cell growth. J Artif Organs **7**: 187-193.

Yamamura K, Miura T, Kou I, Muramatsu T, Furusawa M, Yoshinari M (2015) Influence of various superhydrophilic treatments of titanium on the initial attachment, proliferation, and differentiation of osteoblast-like cells. Dent Mater J **34**: 120-127.

Yu SP, Hunter DJ (2016) Intra-articular therapies for osteoarthritis. Expert Opin Pharmacother **17**: 2057-2071.

Yue JJ, Bertagnoli R, McAfee PC, An HS (2008) Motion preservation surgery of the spine: advanced techniques and controversies. Elsevier Health Sciences.

Yuksel U, Walsh S, Curd D, Black K (2002) Fatigue durabiity of a novel disc nucleus repair system: in vitro studies in a calf spine model. The Spine Journal **2**: 103-104 %@ 1529-9430.

Zhang C, Berven SH, Fortin M, Weber MH (2016) Adjacent Segment Degeneration Versus Disease After Lumbar Spine Fusion for Degenerative Pathology: A Systematic Review With Meta-Analysis of the Literature. Clin Spine Surg **29**: 21-29.

Zhu X, Chen J, Scheideler L, Reichl R, Geis-Gerstorfer J (2004) Effects of topography and composition of titanium surface oxides on osteoblast responses. Biomaterials **25**: 4087-4103.

Zigler JE, Delamarter RB (2012) Five-year results of the prospective, randomized, multicenter, Food and Drug Administration investigational device exemption study of the

ProDisc-L total disc replacement versus circumferential arthrodesis for the treatment of single-level degenerative disc disease. J Neurosurg Spine **17**: 493-501.

8 List of abbreviations

µg	microgram
µl	microliter
µM	micromolar
µm	micro meter
2D	two- dimensional
3D	three-dimensional
ACAN	aggrecan
AF	annulus fibrosus
ANOVA	analysis of variance
BMP	bone morphogenic protein
bp	base pair
BSA	bovine serum albumin
cDNA	complementary DNA
Col	collagen
Col II	collagen type II
Col X	collagen type X
DDD	degenerated disc disease
DEPC	diethylpyrocarbonate
DMEM	dulbecco's modified eagle medium
DNA	deoxyribonucleic acid
dNTP	deoxynucleotidetriphosphate
DPBS	dulbecco’s phosphate buffered saline
ECM	extracellular matrix
FACS	fluorescent activated cell sorting
FBS	fetal bovine serum
FC	flow cytometry
FN	fibronectin
GAG	glycosaminoglycan
GAPDH	glyceraldehyde 3-phosphate dehydrogenase
HA	hyaluronic acid
IVD	intervertebral disc
MMP	matrix metalloprotease

mRNA	messenger RNA
MSC	mesenchymal stem/stromal cell
NP	nucleus pulposus
PCR	polymerase chain reaction
Pen/Strep	penicillin/streptomycin
RANKL	receptor activator of nuclear factor κ-B ligand
RNA	ribonucleic Acid
rpm	revolution per minute
RT	room temperature
RT-PCR	reverse transcription polymerase chain reaction
TGF-β	transforming growth factor beta
Tm	melting temperature

9 Appendix

Ethics Statement

All studies involving human participants were performed in accordance with the 1964 Helsinki declaration and its later revisions. Primary human chondrocytes were isolated from femoral condyle tissue explants of the patients that received total joint replacement. Tissue was harvested only after medical consulation and patient consent. Corresponding ethical vote (338/2015BO2) was approved by Ethik-Kommission an der Medizinischen Fakultät der Eberhard-Karls-Universität und am Universitätsklinikum Tübingen.

10 Declaration

I hereby declare that the submitted doctoral dissertation entitled: "*In vitro* characterization of porous knitted titanium scaffold for the replacement of intervertebral disc nucleus pulposus" was written independently using only the stated sources and aids and that quotes and excerpts, literal or otherwise, are marked correspondingly. I declare on oath that these statements are true and that I have concealed nothing. I am aware that false declarations or affirmations in lieu of an oath can be punished with a jail sentence of up to three years or with a fine.

Gauri Tendulkar

Authors contribution

Publication 1: Imaging cell viability on non-transparent scaffolds—using the example of a novel knitted titanium implant (*Journal of Visualized Experiments*, 2016)

Gauri Tendulkar (GT), Phillip Grau (PG), Patrick Ziegler (PZ), Alfred Buck Sr (ABS), Alfred Buck Jr (ABJ), Andreas Badke (AB), Hans-Peter Kaps (HPK), Sabrina Ehnert (SE), Andreas K. Nüssler (AKN)

ABS, ABJ, HPK, AKN conceived and designed the project. GT and PG carried out the experiments and created the figures. GT and SE carried out the analysis and interpretation. PZ and AB gave the clinical inputs. GT, SE and AKN wrote the manuscript. I consider my contribution to this study to be approximately 70% of total work.

Publication 2: Characterisation of porous knitted titanium for replacement of intervertebral disc nucleus replacement (*Scientific Reports*, 2017)

Gauri Tendulkar (GT), Vrinda Sreekumar (VS), Frank Rupp (FR), Arun K Teotia (AKT), Kiriaki Athanasopulu (KA), Ralf Kemkemer, Alfred Buck Sr (ABS), Alfred Buck jr (ABJ), Hans-Peter Kaps (HPK), Jürgen Geis-Gerstorfer (JG), Ashok Kumar (AK), Andreas K. Nüssler (AKN)

GT, ABS, ABJ, HPK and AKN conceived and designed the project. GT, KA and AKT carried out the experiments and created the figures. GT and FR carried out the analysis and interpretation oxygen plasma treatment data. RK, JG and AK supervised wear particle characterization, oxygen plasma treatment and optical profilometry experiments respectively and gave intellectual inputs. GT, VS, FR and AKN wrote the manuscript. I consider my contribution to this study to be approximately 80% of total work.

Publication 3: Exogenous delivery of Link N mRNA into chondrocytes and MSCs – the potential role in increasing anabolic response (*International Journal of Molecular Sciences*, 2018, submitted)

Gauri Tendulkar (GT), Sabrina Ehnert (SE), Vrinda Sreekumar (VS), Tao chen (TC), Hans-Peter Kaps (HPK), Sonia Golombek (SG), Hans-Peter Wendel (HPW), Andreas K Nüssler (AKN) and Meltem Avci-Adali (MAA).

GT, HPW and AKN conceived and designed the project. GT carried out the experiments and created the figures. SG performed cy3 nucleic acid labelling of Link N mRNA. GT and MAA carried out the analysis and interpretation. VS and AKN supervised the study. TC and SE gave intellectual inputs. GT, MAA and AKN wrote the manuscript. I consider my contribution to this study to be approximately 90% of total work.

11 Acknowledgements

First and foremost, I am grateful to my advisor Prof. Andreas K. Nüssler for giving me this opportunity and to work on this project, as well as introducing me to the field of tissue engineering. Thank you for believing in me at every stage of my doctoral study and extending full support in good and bad days. Without your constructive criticism, contagious optimism, work ethic, prefect amount of freedom and guidance which have been rewarding and invigorating, this dissertation would not have been possible. I further express my gratitude to my committee members, Prof. Hans-Peter Wendel and Prof. Dorothea Alexander-Friedrich for agreeing to supervise my thesis, and for providing constant support throughout.

Likewise, I wish to thank is Buck GmbH & Co., particularly for providing knitted titanium scaffolds which led to majority of the work presented in this thesis. Over the years, I have had a chance to interact with a number of people who contributed in some way to my scientific growth; I therefore thank Prof. Hans-Peter Kaps for providing insights into clinical scenarios and for fruitful discussions regarding nucleus replacements, Prof. Hans-Peter Wendel, PD. Dr. Meltem Avaci-Adali, Prof. Jürgen Geis-Gerstorfer, PD. Dr. Frank Rupp, Prof. Ralf Kemkemer and Prof. Ashok Kumar for their profitable collaborations. It has helped me to learn more about diverse areas of biomaterial and provided me with valuable insights during my research stay.

I have always enjoyed the brainstorming session during lab meetings and journal clubs with my lab mates and colleagues from Siegfried Weller Institute. Many thanks to all the lab members: Romina, Victor, Marc, Caren and Sabrina for creating an enjoyable atmosphere. Special thanks to Dr. Vrinda Sreekumar whose mentoring, unwavering support (including the thesis proof read!!) and encouragement has greatly helped me. I have thoroughly enjoyed our companionship. I also would like to appreciate discussions with Dr. Marie Reumann. Her optimism and positive attitude continues to amaze me. Big thanks to Dr. Sahar Sajadian and Dr. Tripura Chaturvedula who was my go-to person when I newly joined the lab, and who helped me with various personal, administrative, and scientific matters in the very beginning days. I also would like to thank Svetlana for constant personal (also for editing the translation of my German thesis summary!!) and administrative support and also, personnel from the Experimental medicine graduate program coordination office, especially Dr. Inka Montero and Pia for their assistance. I am thankful to the numerous bachelor/master/medical students

whom I have worked with, and some of whom I have had the pleasure of mentoring, especially Jacqueline, Tatjana and Mei-Li.

I would like to acknowledge financial support from the Zentrales Innovationsprogramm Mittelstand des Bundesministeriums für Wirtschaft und Energie –KF3010902AJ4.

I felt instantly at home in Tübingen because of Haveli people (Neel, Suryesh!!) and their endless backing. I like to address special thanks to Nidhi for introducing me to Haveli, and also, making my life in Tübingen more wonderful and enjoyable. Finally, and most importantly, I thank my parents (aai, baba) whose never ending support and encouragement has proved to be the greatest source of inspiration and confidence. Needless to say, this dissertation would not have been possible without their dedicated efforts. Additionally, I like to cherish countless memories with Chinmay, Siddhi and Samruddhi and would like to thank for all their love, care, encouragement, and support during my studies.